Oligomeric Monoterpenoid Indole Alkaloids from the Flowers of *Gelsemium elegans* with Anti-inflammatory and Anti-fibrotic Activities

Ji-Hong Gu[a,b,‡], Ni-Ping Li[a,b,c,‡], Hao-Ting Lin[a,c,d,‡], Ling-Na Dai[e], Min-Jing Cheng[a,c,d], Jian Hong[a], Yi-Yi Li[a,c,d], Jun-Shan Liu[e,*], Wen-Cai Ye[a,c,d,*], Lei Wang[a,c,d,*]

[a] *State Key Laboratory of Bioactive Molecules and Druggability Assessment, Guangdong Basic Research Center of Excellence for Natural Bioactive Molecules and Discovery of Innovative Drugs, Jinan University, Guangzhou 510632, P. R. China.*

[b] *Science and Technology Innovation Center, Guangzhou University of Chinese Medicine, Guangzhou 510405, P. R. China.*

[c] *Center for Bioactive Natural Molecules and Innovative Drugs, and Guangdong Province Key Laboratory of Pharmacodynamic Constituents of TCM and New Drugs Research, College of Pharmacy, Jinan University, Guangzhou 510632, P. R. China.*

[d] *Guangdong-Hong Kong-Macau Join Laboratory for Pharmacodynamic Constituents of TCM and New Drugs Research, Jinan University, Guangzhou 510632, P. R. China.*

[e] *School of Traditional Chinese Medicine, Guangdong Provincial Key Laboratory of Chinese Medicine Pharmaceutics, Guangdong Basic Research Center of Excellence for Integrated Traditional and Western Medicine for Qingzhi Diseases, Southern Medical University, Guangzhou, 510515, P. R. China.*

E-mail addresses*:*

cpuwanglei@126.com (L. Wang)

chywc@aliyun.com (W.-C. Ye)

liujunshanty@163.com (J.-S. Liu)

[1] These authors contributed equally to this work.

Contents

1. Structure elucidation data for 1–6

Table S1 ^{1}H and ^{13}C NMR data of **1**–**3** in $CDCl_3$ (δ in ppm, J in Hz)[a]

No.	**1**		**2**		**3**	
	δ_H	δ_C	δ_H	δ_C	δ_H	δ_C
2		171.4		171.8		171.9
3	3.56 (dd, 4.4, 2.1)	76.1	3.70 (dd, 4.6, 2.1)	75.1	4.20 (d, 6.1)	71.4
5	4.05	72.3	4.36 (m)	72.2	3.07 (dd, 11.3, 4.8)	53.5
6	2.06	37.3	2.38 (dd, 15.5, 4.7)	37.7	1.72 (dd, 13.8, 11.3)	37.3
	2.21		2.27 (m)		1.56 (dd, 13.8, 4.8)	
7		56.5		56.4		53.3
8		132.1		132.1		127.0
9	7.41 (dd, 7.6, 1.0)	125.0	7.50 (d, 7.6)	124.8	7.33	126.4
10	7.04	123.2	7.06 (td, 7.6, 0.8)	123.9	7.07 (dd, 7.6, 7.6)	123.3
11	7.21 (dd, 7.6, 7.6, 1.0)	128.0	7.25 (td, 7.6, 0.8)	128.5	7.33	128.7
12	6.83 (dd, 7.6, 1.0)	106.7	6.88 (d, 7.6)	107.0	7.01 (d, 7.6)	107.6
13		127.7		138.0		139.6
14	2.34	29.0	2.50 (dd, 15.7, 2.1)	29.0	7.27	136.6
	2.08		2.17 (m)			139.5
15	2.85 (d, 9.1)	41.0	2.99 (t, 9.1)	40.5	3.45 (br s)	36.8
16	2.11	40.3	2.47 (m)	41.1	3.62 (dd, 9.2, 3.1)	68.1
17	4.07	62.0	4.20	62.1	4.04 (d, 9.2)	
	4.01 (dd, 11.1, 1.5)		4.20		1.06 (t, 7.3)	8.5
18	1.49 (s)	21.9	1.55 (s)	22.8	2.85 (dq, 16.9, 7.3)	30.4
19		74.9		75.3	2.71	
20		184.7		185.1		199.4
N-OMe	3.84 (s)	63.3	3.95 (s)	63.6	3.99 (s)	63.6
19-OH	4.61					
2′		171.6		171.7		171.3
3′	3.48 (s)	76.1	3.95 (br s)	75.0	3.61 (br s)	78.3
5′	4.42 (m)	73.0	4.34 (m)	72.6	4.36 (m)	72.1
6′	2.34	36.9	2.40 (dd, 15.4, 4.9)	37.5	2.39 (dd, 15.5, 4.8)	37.3
	2.33		2.22 (dd, 15.4, 1.8)		2.25 (dd, 15.5, 1.9)	
7′		56.0		55.9		54.7
8′		132.7		133.1		132.2
9′	7.40 (dd, 7.6, 1.0)	124.8	7.53 (d, 7.6)	125.1	7.50 (d, 7.6)	124.8
10′	7.03	123.9	7.06 (td, 7.6, 0.8)	123.5	7.07 (dd, 7.6, 7.6)	123.5
11′	7.22 (ddd, 7.6, 7.6, 1.0)	128.43	7.23 (td, 7.6, 0.8)	128.1	7.27	128.2
12′	6.81 (dd, 7.6, 1.0)	107.0	6.85 (d, 7.6)	106.7	6.89 (d, 7.6)	106.9
13′		138.5		138.1		138.0
14′	3.07 (s)	44.5	2.82 (br s)	42.0	3.59 (br s)	51.3
15′	3.45 (d, 8.4)	40.9	3.32 (d, 8.7)	41.7	2.59 (d, 8.7)	49.5
16′	2.55	38.2	2.56 (td, 8.7, 4.0)	38.8	2.47 (td, 8.7, 3.4)	38.9
17′	4.27	62.3	4.44 (dd, 10.4, 4.0)	62.4	4.31 (dd, 10.9, 3.4)	61.4
	4.27		4.19 (m)		4.20 (d, 10.9)	
18′	1.67 (d, 6.8)	13.3	1.26 (t, 7.3)	10.2	1.31 (t, 7.4)	10.2
19′	3.08 (qd, 6.8, 2.4)	40.4	2.66 (dq, 16.6, 7.3)	25.4	2.71	25.9
			2.26 (m)		2.42	
20′		185.2		184.5		181.8
N-OMe′	3.62 (s)	63.2	3.90 (s)	63.4	3.88 (s)	63.4
2″		171.6				
3″	3.77 (s)	81.0				
5″	4.37 (m)	73.0				
6″	2.34	36.9				
	2.27 (dd, 15.7, 2.0)					
7″		56.5				
8″		132.7				
9″	7.51 (dd, 7.6, 1.0)	125.1				
10″	7.03	123.2				
11″	7.17 (ddd, 7.6, 7.6, 1.0)	128.2				
12″	6.79 (dd, 7.6, 1.0)	106.4				
13″		138.3				
14″	2.91 (s)	36.6				
15″	2.88 (d, 8.4)	41.7				
16″	2.54	38.7				
17″	4.27	62.5				
	4.27					
18″	1.24 (t, 7.4)	10.4				
19″	2.57	25.5				
	2.20					
20″		183.4				
N-OMe″	3.97 (s)	63.8				

[a] Overlapped signals were reported without designating multiplicity

Table S2 ^{1}H and ^{13}C NMR data of **4**–**6** in $CDCl_3$ (δ in ppm, J in Hz)

No.	**4**		**5**		**6**	
	δ_H	δ_C	δ_H	δ_C	δ_H	δ_C
2		171.6		171.7		172.3
3	4.14 (d, 6.1)	71.5	4.22 (d, 6.2)	71.5	3.64 (br s)	77.1
5	2.94 (dd, 11.0, 4.9)	53.4	3.07 (dd, 11.4, 4.8)	53.7	3.22 (dd, 12.4, 5.3)	58.5
6	1.61 (dd, 14.0, 11.0)	37.5	1.62 (dd, 13.9, 11.4)	38.1	2.39 (m)	34.6
	1.49 (dd, 14.0, 4.9)		1.53 (dd, 13.9, 4.8)		1.31 (dd, 13.8, 5.3)	
7		53.3		53.4		54.2
8		126.9		127.0		127.9
9	7.16 (d, 7.6)	126.5	7.33 (dd, 7.6, 0.9)	126.5	7.27 (d, 7.6)	126.6
10	6.87 (ddd, 7.6, 7.6, 1.0)	123.4	7.05 (ddd, 7.6, 7.6, 0.9)	123.4	7.06 (ddd, 7.6, 7.6, 0.9)	123.1
11	7.24 (ddd, 7.6, 7.6, 1.0)	128.7	7.34 (ddd, 7.6, 7.6, 0.9)	128.9	7.32 (ddd, 7.6, 7.6, 0.9)	128.6
12	6.93 (d, 7.6)	107.6	7.00 (dd, 7.6, 0.9)	107.8	7.01 (d, 7.6)	107.6
13		139.5		139.6		139.1
14	7.21 (dd, 6.1, 1.6)	136.9	7.37 (dd, 6.2, 1.3)	138.2	4.21 (dd, 7.2, 3.0)	33.2
15		139.6		140.6	2.79 (dd, 7.2, 4.5)	44.6
16	3.35 (br s)	37.8	3.49 (br s)	37.5	2.56 (br s)	40.8
17	3.51 (dd, 9.4, 3.1)	67.9	3.60 (dd, 9.2, 2.8)	68.4	3.98 (dd, 10.1, 3.1)	69.5
	3.92 (d, 9.4)		4.03 (d, 9.2)		3.96 (d, 10.1)	
18	1.04 (t, 7.3)	8.6	0.94 (d, 6.8)	17.2	0.65 (t, 7.3)	8.0
19	2.84 (dq, 16.9, 7.3)	30.5	3.73 (dq, 10.5, 6.8)	40.5	2.37 (m)	33.6
	2.67 (m)				2.10 (m)	
20		199.6		202.1		210.3
N-OMe	3.93 (s)	63.7	3.96 (s)	63.8	3.98 (s)	63.6
2′		172.0		171.6		171.6
3′	3.60 (br s)	77.5	3.67 (br s)	78.4	3.34 (br s)	79.2
5′	4.31(m)	72.6	4.36 (m)	72.4	4.31 (m)	72.2
6′	2.42 (dd, 15.4, 5.0)	37.6	2.39 (m)	37.6	2.31 (dd, 15.5, 4.5)	37.0
	2.24 (dd, 15.4, 1.8)		2.25 (dd, 15.5, 1.4)		2.23 (overlap)	
7′		54.7		54.8		54.3
8′		132.3		132.3		132.0
9′	7.52(d, 7.6)	125.0	7.52 (d, 7.6)	124.9	7.41 (d, 7.6)	124.7
10′	7.09 (ddd, 7.6, 7.6, 1.0)	123.8	7.10 (ddd, 7.6, 7.6, 0.9)	123.9	7.04 (ddd, 7.6, 7.6, 0.9)	123.8
11′	7.27 (ddd, 7.6, 7.6, 1.0)	128.4	7.29 (ddd, 7.6, 7.6, 0.9)	128.5	7.23 (ddd, 7.6, 7.6, 0.9)	128.4
12′	6.88 (d, 7.6)	107.0	6.91 (d, 7.6)	107.1	6.84 (d, 7.6)	106.9
13′		138.3		138.0		137.7
14′	3.60 (br s)	52.4	3.59 (br s)	52.0	3.33 (br s)	51.6
15′	2.68 (d, 8.7)	48.4	2.56 (d, 8.7)	49.8	2.49 (d, 8.6)	48.6
16′	2.41(m)	39.8	2.47 (td, 8.7, 3.5)	39.1	2.42 (td, 8.6, 3.2)	38.5
17′	4.40 (dd, 11.0, 3.3)	61.8	4.33 (dd, 11.1, 3.5)	61.6	4.07 (dd, 11.0, 3.2)	61.4
	4.23 (d,11.0)		4.22 (d, 11.1)		4.17 (d, 11.0)	
18′	1.31 (d, 7.2)	15.1	1.29 (t, 7.3)	10.3	1.28 (t, 7.4)	10.2
19′	3.00 (dq, 8.8, 7.2)	42.4	2.69 (dq, 16.8, 7.3)	26.0	2.65 (dq, 16.7, 7.4)	25.7
			2.38 (m)		2.36 (m)	
20′		182.3		181.7		181.1
N-OMe′	3.83 (s)	63.5	3.89 (s)	63.5	3.85 (s)	63.4
2″		171.6		171.2		171.4
3″	3.88 (br s)	75.4	3.66 (br s)	75.7	3.62 (dd, 4.6, 1.8)	74.9
5″	4.32 (m)	71.9	4.3 (m)	72.6	4.07 (m)	72.9
6″	2.38(dd, 15.2, 4.8)	38.0	2.34 (dd, 15.5, 4.7)	37.7	2.27 (dd, 15.4, 4.6)	38.1
	2.26 (dd, 15.2. 1.8)		2.25 (dd, 15.5, 1.4)		2.16	
7″		55.6		55.4		55.9
8″		133.1		132.7		132.4
9″	7.53 (d, 7.6)	124.9	7.49 (d, 7.6)	125.0	7.45 (d, 7.6)	124.9
10″	7.08 (ddd, 7.6, 7.6, 1.0)	123.6	7.06 (ddd, 7.6, 7.6, 0.9)	123.5	7.00 (ddd, 7.6, 7.6, 0.9)	123.4
11″	7.27 (ddd, 7.6, 7.6, 1.0)	128.2	7.24 (ddd, 7.6, 7.6, 0.9)	128.3	7.19 (ddd, 7.6, 7.6, 0.9)	128.1
12″	6.90 (d, 7.6)	106.8	6.87 (d, 7.6)	106.9	6.81 (d, 7.6)	106.7
13″		138.2		138.2		138.2
14″	2.54	38.0	2.65 (d, 10.5)	40.3	2.22 (m)	27.1
					2.14 (m)	
15″	3.20 (d, 8.9)	46.0	2.41 (m)	47.6	3.25 (t, 9.2)	41.6
16″	2.54	39.1	2.62 (td, 8.4, 3.4)	38.7	2.29 (m)	39.0
17″	4.34 (dd, 11.0. 3.6)	62.4	4.43 (dd, 11.3, 3.7)	62.2	4.24 (dd, 11.1, 3.2)	62.3
	4.27 (d, 11.0)		4.27 (d, 11.3)		4.13 (d, 11.1)	
18″	1.20 (t, 7.3)	10.2	1.01 (t, 7.3)	9.7	1.43 (d, 6.8)	10.6
19″	2.65 (m)	25.7	2.52 (m)	25.2	2.74 (qd, 6.8, 3.1)	41.3
	2.19 (m)		2.05 (m)			
20″		184.3		183.5		185.7
N-OMe″	3.90 (s)	63.4	3.92 (s)	63.6	3.85 (s)	63.4

[a] Overlapped signals were reported without designating multiplicity

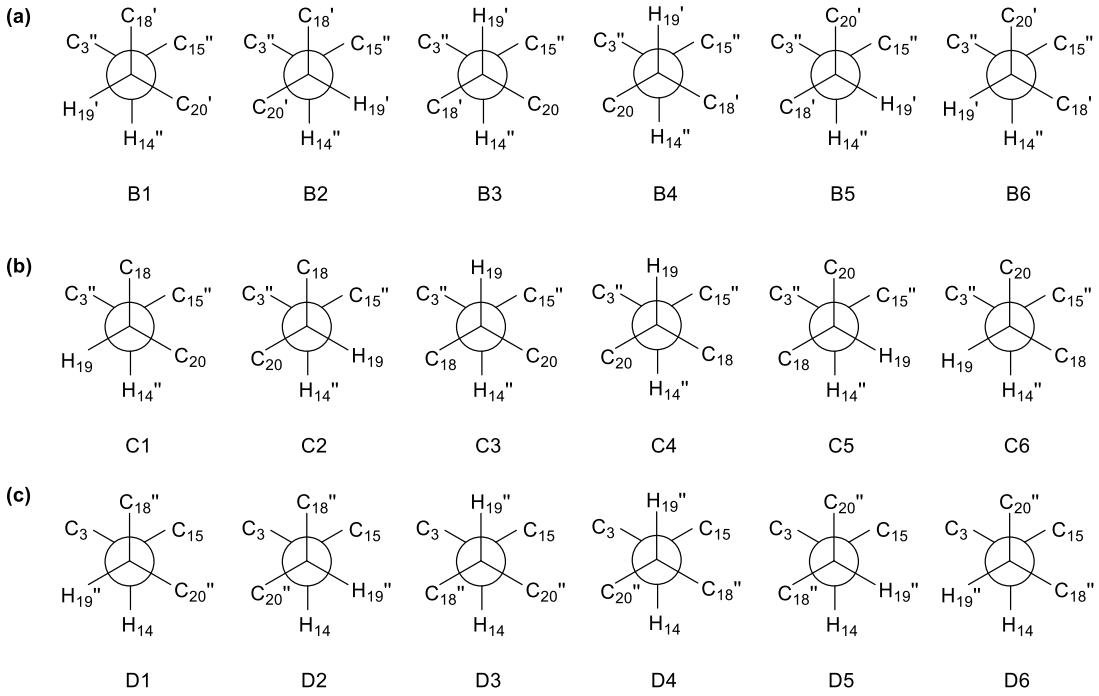

Fig. S1. All possible rotamers between C-19′ and C-14″ in **1** and **4** (a), between C-19 and C-14″ in **5** (b), and between C-19″ and C-14″ in **6** (c).

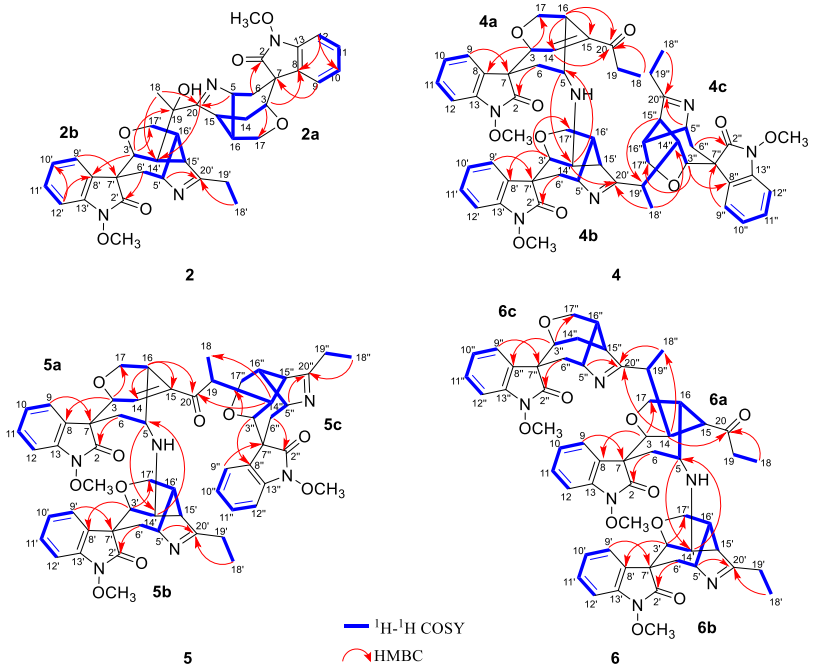

Fig. S2. Key ^{1}H-^{1}H COSY and HMBC correlations of **2** and **4**–**6**.

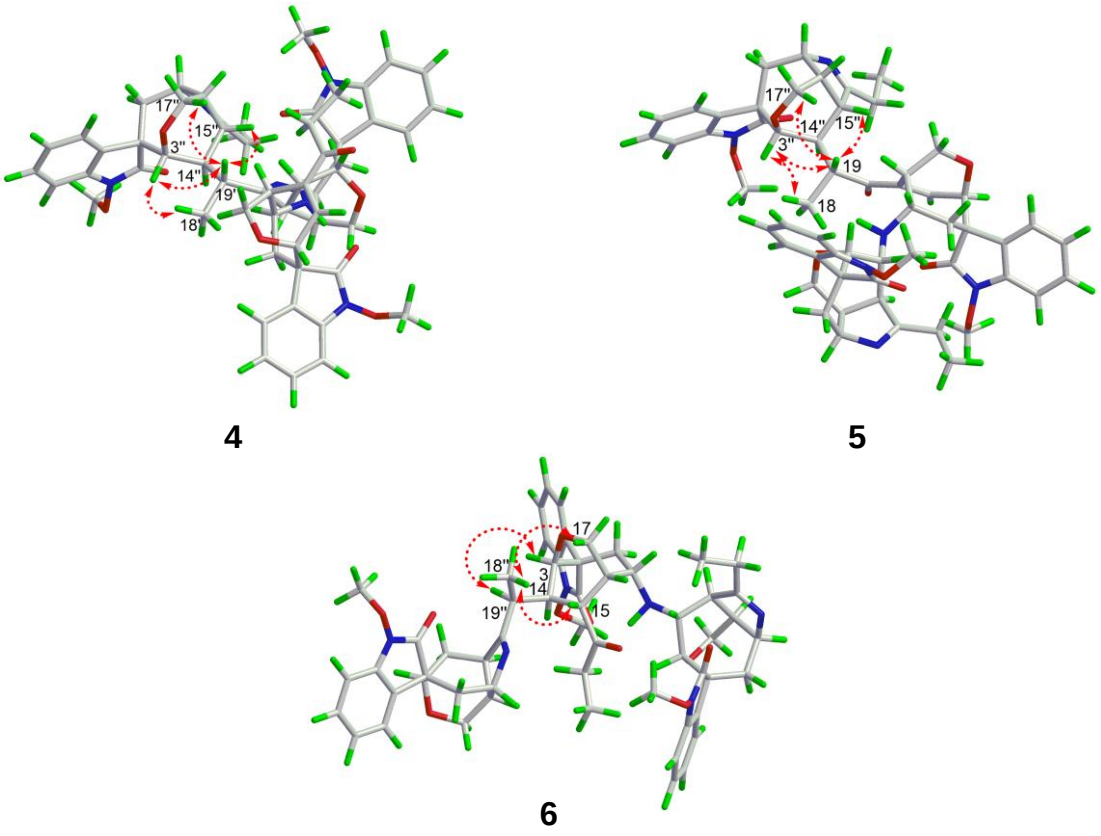

Fig. S3. Key NOESY correlations of **4**−**6**.

2. General experimental procedures

Melting points were recorded on an X-5 micro-melting point apparatus (Fukai Instrument, Beijing, China) without correction. Optical rotations were measured on a Jasco P-1020 polarimeter (Jasco, Tokyo, Japan) at room temperature. UV spectra were obtained on a Jasco V-550 UV/Vis spectrometer (Jasco, Tokyo, Japan). IR spectra (KBr disks, in cm^{-1}) were carried out using a Jasco FT/IR-480 Plus Fourier Transform spectrometer (Jasco, Tokyo, Japan). CD spectra were obtained on a Jasco J-810 spectropolarimeter (Jasco, Tokyo, Japan) at room temperature. X-ray crystallographic analysis was carried out on an Agilent Gemini S Ultra CCD diffractometer with Cu Kα radiation (λ = 1.54178 Å). HR-ESI-MS spectra were acquired from Agilent 6210 LC/MSD TOF-MS spectrometer (Agilent Technologies, CA, USA). NMR spectra were obtained on a Bruker AV-500 or AV-600 spectrometer (Bruker, Fällanden, Switzerland). Column chromatographies (CC) were performed on silica gel (200–300 mesh, Qingdao Marine Chemical Plant, China), ODS (Merck, Darmstadt, Germany) and Sephadex LH-20 (Pharmacia Uppsala, Sweden). Preparative HPLC was carried out on an Agilent 1260 systerm (G1310B Iso pump and G1365D MWDVL detector) with a Waters Xbridge ^{TM} C_{18} OBD reversed-phase column (19 × 250 mm, 5 μm, USA). All solvents used in CC and HPLC were of analytical grade (Shanghai Chemical Plant, Shanghai, China) and chromatographic grade (Fisher Scientific, New Jersey, USA), respectively.

3. Plant material

The flowers of *Gelsemium elegans* were corrected from Fujian Province of P. R. China in 2014, and authenticated by Prof. Guang-Xiong Zhou (Jinan University, Guangzhou, China). A voucher specimen (No. 20140901) is deposited in the Center for Bioactive Natural Molecules and Innovative Drugs, Jinan University, Guangzhou, China.

4. Extraction and isolation

The air-dried powder of the flowers (11.5 kg) of *Gelsemium elegans* were percolated with 95% (*v/v*) EtOH at room temperature. The combined crude extract (2 kg) was suspended in H_2O and acidified with 10% HCl to pH 3. The acidic suspension was partitioned with $CHCl_3$ to remove the neutral components. The aqueous layers was

basified with NH_4OH to pH 9 and extracted with $CHCl_3$ to obtain a total alkaloid fraction (200 g). The alkaloid fraction was subjected to silica gel column eluting with a gradient mixture of $CHCl_3/CH_3OH$ (100:0 → 0:100) to afford eleven fractions (Fr. 1–11). Fr. 4 (10.1 g) was then subjected to ODS column using CH_3OH/H_2O (20:80 → 100:0) as eluent to afford ten subfractions (Fr. 4a-Fr. 4j). Fr. 4i (1.2g) was chromatographed on Sephadex LH-20 ($CHCl_3/CH_3OH$, 1:1) and purified by reversed-phase preparative HPLC ($CH_3CN/H_2O/Et_2NH$, 40:60:0.01) to give compound **2** (7.5 mg) and **3** (13.4 mg). Fr. 4j (0.6 g) was purified by reversed-phase preparative HPLC ($CH_3OH/H_2O/Et_2NH$, 65:35:0.01) to yield compounds **1** (2.3 mg), **4** (4.0 mg), **5** (3.2 mg) and **6** (6.8 mg).

Gelsepolycine A (**1**): colorless crystals (CH_3OH); mp 290–291 ℃; $[\alpha]_D^{25}$ = –139.0° (*c* = 0.1, CH_3OH); UV (CH_3OH) λ_{max} (log ε) 211 (4.64), 258 (4.06) nm; IR (KBr) ν_{max} 3436, 2929, 1717, 1621, 1467, 1383, 1122, 1043, 752 cm^{-1}; HR-ESI-MS *m/z* 991.4607 $[M+H]^+$ (calcd for $C_{57}H_{63}N_6O_{10}$: 991.4600); ^1H and ^{13}C NMR see Table S1.

Gelsepolycine B (**2**): colorless crystals (CH_3OH); mp 222–223 ℃; $[\alpha]_D^{25}$ = –49.8 (*c* = 0.5, CH_3CN); UV (CH_3OH) λ_{max} (log ε) 210 (4.66), 258 (4.09) nm; IR (KBr) ν_{max} 3429, 2928, 1715, 1619, 1467, 1313, 1224, 1122, 1038, 965, 876, 753 cm^{-1}; HR-ESI-MS *m/z* 667.3128 $[M+H]^+$ (calcd for $C_{38}H_{43}N_4O_7$: 667.3126); ^1H and ^{13}C NMR see Table S1.

Gelsepolycine C (**3**): yellow amorphous powder; $[\alpha]_D^{25}$ = –144.2 (*c* = 0.5, CH_3OH); UV (CH_3OH) λ_{max} (log ε) 209 (4.59), 252 (4.18) nm; IR (KBr) ν_{max} 3432, 2928, 1721, 1672, 1624, 1467, 1322, 1235, 1114, 960, 749 cm^{-1}; HR-ESI-MS *m/z* 667.3132 $[M+H]^+$ (calcd for $C_{38}H_{43}N_4O_7$: 667.3126) ; ^1H and ^{13}C NMR see Table S1.

Gelsepolycine D (**4**): white amorphous powder; $[\alpha]_D^{25}$ = –136.0 (*c* = 0.25, CH_3OH); UV (CH_3OH) λ_{max} (log ε) 210 (4.61), 254 (4.16) nm; IR (KBr) ν_{max} 3431, 2927, 1720, 1626, 1468, 1325, 1240, 1116, 1043, 748 cm^{-1}; HR-ESI-MS *m/z* 991.4605 $[M+H]^+$ (calcd for $C_{57}H_{63}N_6O_{10}$: 991.4600); ^1H and ^{13}C NMR see Table S2.

Gelsepolycine E (**5**): white amorphous powder; $[\alpha]_D^{25}$ = –150.5 (*c* = 0.1, CH_3OH); UV (CH_3OH) λ_{max} (log ε) 210 (4.65), 254 (4.17) nm; IR (KBr) ν_{max} 3433, 2927, 1716, 1627, 1470, 1321, 1233, 1115, 1044, 751 cm^{-1}; HR-ESI-MS *m/z* 991.4601 $[M+H]^+$ (calcd for $C_{57}H_{63}N_6O_{10}$: 991.4600); ^1H and ^{13}C NMR see Table S2.

Gelsepolycine F (**6**): white amorphous powder; $[\alpha]_D^{25}$ = –98.0 (*c* = 0.1, CH_3OH); UV (CH_3OH) λ_{max} (log ε) 210 (4.60), 256 (4.02) nm; IR (KBr) ν_{max} 3435, 2927, 1720, 1626,

1467, 1317, 1234, 1117, 1039, 751 cm^{-1}; HR-ESI-MS *m/z* 993.4759 $[M+H]^+$ (calcd for $C_{57}H_{65}N_6O_{10}$: 993.4757); ^1H and ^{13}C NMR see Table S2.

5. X-ray crystal structures of 1 and 2

Single crystals of **1** and **2** were both obtained from CH_3OH solution by slow evaporation at room temperature. X-ray diffraction data were collected using an Agilent Gemini S Ultra CCD diffractometer using Cu Kα radiation (λ = 1.54178 Å). The structures were solved by direct methods and refined by full-matrix least squares on F2 using the SHELXL-97 program. The crystallographic data have been deposited with the Cambridge Crystallographic Data Centre (CCDC 2418509 for **1** and 2418511 for **2**).

Table S3 Crystal data and structure refinement for 1.

Empirical formula	$C_{57}H_{62}N_6O_{10}$
Formula weight	991.13
Temperature/K	150.00(10)
Crystal system	orthorhombic
Space group	$P2_12_12_1$
a/Å	13.79290(10)
b/Å	15.78840(10)
c/Å	22.5410(2)
α/°	90.00
β/°	90.00
γ/°	90.00
Volume/$Å^3$	4908.70(6)
Z	4
$\rho_{calc}g/cm^3$	1.341
μ/mm^{-1}	0.753
F(000)	2104.0
Crystal size/mm^3	0.26 × 0.21 × 0.03
Radiation	CuKα (λ = 1.54178)
2Θ range for data collection/°	6.84 to 148.12
Index ranges	$-11 \le h \le 16$, $-15 \le k \le 19$, $-26 \le l \le 27$
Reflections collected	36830
Independent reflections	9740 [R_{int} = 0.0286, R_{sigma} = 0.0241]
Data/restraints/parameters	9740/0/666
Goodness-of-fit on F^2	1.034
Final R indexes [I>=2σ (I)]	R_1 = 0.0300, wR_2 = 0.0734
Final R indexes [all data]	R_1 = 0.0331, wR_2 = 0.0754
Largest diff. peak/hole / e $Å^{-3}$	0.19/-0.14
Flack parameter	-0.10(10)

Table S4 Crystal data and structure refinement for 2.

Empirical formula	$C_{39}H_{46}N_4O_8$
Formula weight	698.80
Temperature/K	173(2)
Crystal system	monoclinic
Space group	$P2_1$
a/Å	9.4760(3)
b/Å	8.8438(3)
c/Å	20.4665(8)
α/°	90
β/°	93.324(3)
γ/°	90
Volume/Å^3	1712.29(10)
Z	2
ρ_{calc}g/cm^3	1.355
μ/mm^{-1}	0.778
F(000)	744.0
Crystal size/mm^3	0.31 × 0.18 × 0.15
Radiation	CuKα (λ = 1.54178)
2Θ range for data collection/°	12.378 to 122.294
Index ranges	$-7 \le h \le 10$, $-10 \le k \le 10$, $-22 \le l \le 23$
Reflections collected	6989
Independent reflections	4393 [R_{int} = 0.0365, R_{sigma} = 0.0456]
Data/restraints/parameters	4393/1/468
Goodness-of-fit on F^2	1.038
Final R indexes [I>=2σ (I)]	R_1 = 0.1151, wR_2 = 0.3241
Final R indexes [all data]	R_1 = 0.1160, wR_2 = 0.3267
Largest diff. peak/hole / e Å^{-3}	0.92/-0.52
Flack parameter	-0.02(19)

6. ECD spectra calculation details

The conformational analysis of **3**−**6** was performed using the SYBYL-X 2.1.1 program with the MMFF94s molecular force field. All conformers of **3**−**6** were fully optimized in the gas phase using DFT at the B3LYP/6-31+G(d) level with Gaussian09 software[1]. The optimized stable conformers of **3** were used for TDDFT computation of the excited stats at the same level, with the consideration of the first 50 excitations, and those of **4**−**6** were calculated at CAM-B3LYP/6-31+G(d) level in acetonitrile. The overall ECD curves of **3**−**6** were generated by weighting the contributions of each conformer according to their Boltzmann distribution. The calculated ECD spectra of

3–**6** were then compared with the experimental one. All ECD spectra were produced using SpecDis 1.71 software[2].

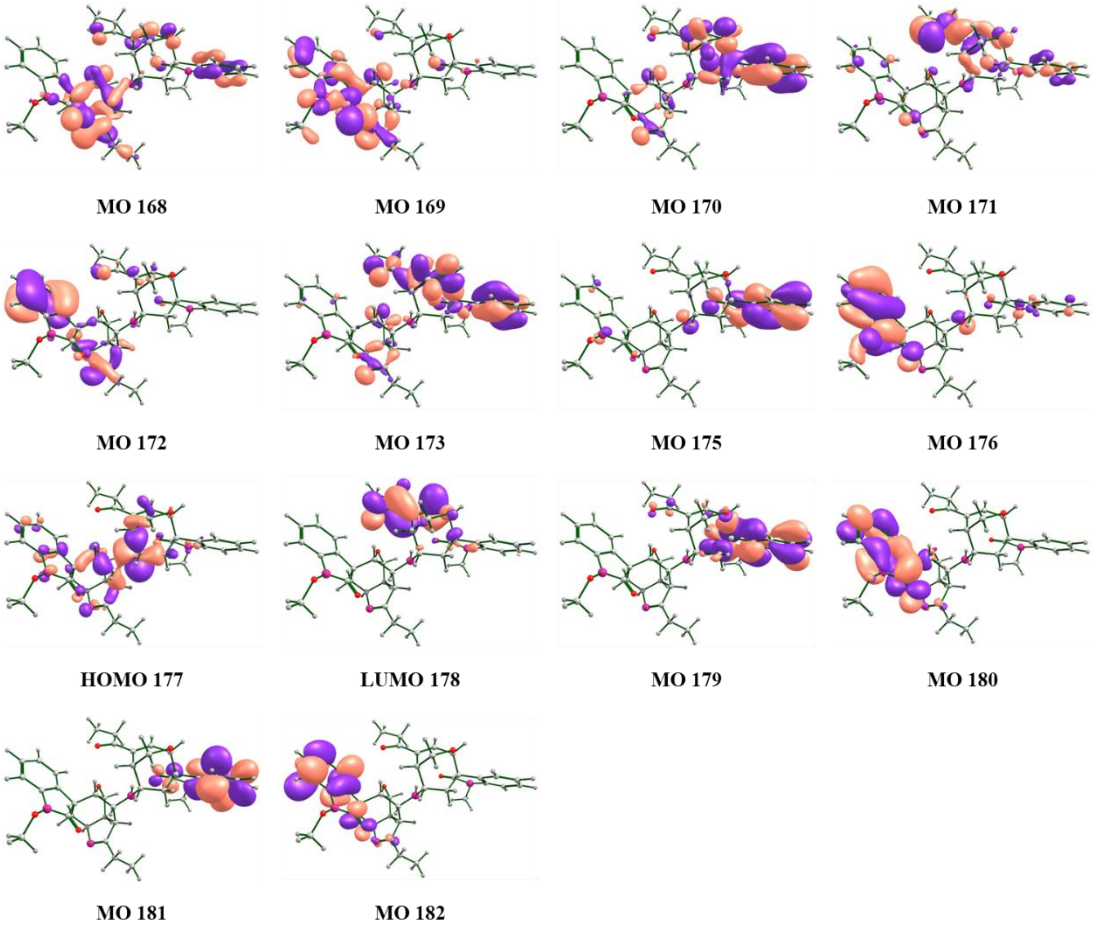

Fig. S4. Key molecular orbitals involved in important transitions regarding the ECD spectra of dominant conformer for **3** at the B3LYP/6-31+G(d) level in acetonitrile.

Table S5. Key transitions and their related rotatory and oscillator strengths of dominant conformer for **3** at the B3LYP/6-31+G(d) level in acetonitrile.

HOMO is 177					
No.	**Energy (cm^{-1})**	**Wavelength (nm)**	**Osc. Strength**	**R (length)**	**Major contribs**
1	25993.01	384.7188	0.0001	0.3556	HOMO->LUMO (98%)
2	30449.25	328.4153	0.0018	-14.6051	H-6->LUMO (36%), H-4->LUMO (14%), H-2->LUMO (39%)
3	30760.59	325.0913	0.0006	-7.2063	H-1->LUMO (85%)
4	31126.76	321.2669	0.0007	12.7479	H-6->LUMO (21%), H-2->LUMO (52%), H-1->LUMO (13%)
5	34451.4	290.2639	0.0017	4.8389	HOMO->L+1 (95%)
6	35291.84	283.3516	0.032	-49.1953	HOMO->L+2 (97%)

7	36195.99	276.2737	0.0828	21.5687	H-10->LUMO (16%), H-7->LUMO (12%), H-4->LUMO (50%)
8	36592.82	273.2776	0.0303	-6.8939	H-3->LUMO (83%)
9	37044.49	269.9456	0.0101	17.7573	H-1->L+2 (65%), HOMO->L+4 (18%)
10	37389.7	267.4533	0.0127	17.9112	H-2->L+1 (51%), HOMO->L+3 (26%)
11	37994.62	263.1951	0.0046	-12.3347	H-5->LUMO (89%)
12	38165.61	262.016	0.0289	-85.6773	H-2->L+1 (25%), HOMO->L+3 (61%)
13	38414.84	260.3161	0.0941	42.0379	H-1->L+2 (18%), HOMO->L+4 (65%)
14	38710.85	258.3255	0.0014	-6.7068	H-7->LUMO (55%), H-2->L+3 (12%)
15	39113.32	255.6674	0.0494	49.0479	H-1->L+4 (18%), HOMO->L+5 (56%)
16	39289.15	254.5232	0.0955	-11.9992	H-12->LUMO (10%), H-10->LUMO (24%), H-9->LUMO (33%), H-6->LUMO (12%)
17	39723.08	251.7428	0.0334	-35.5264	H-1->L+4 (48%), HOMO->L+4 (11%), HOMO->L+5 (19%)
18	39850.52	250.9378	0.1173	-46.3906	H-7->LUMO (14%), H-2->L+3 (40%), H-1->L+1 (13%)
19	39947.3	250.3298	0.0263	-8.9173	H-8->LUMO (79%)
20	39963.43	250.2287	0.0193	-11.0191	H-2->L+1 (11%), H-1->L+1 (77%)
21	40511.09	246.846	0.0434	7.7884	H-10->LUMO (29%), H-9->LUMO (56%)
22	40979.7	244.0233	0.009	0.6896	H-2->L+2 (13%), HOMO->L+5 (11%), HOMO->L+6 (67%)
23	41016.8	243.8025	0.0004	1.1433	H-2->L+2 (80%), HOMO->L+6 (11%)
24	41488.64	241.0298	0.0181	65.9445	H-9->L+2 (12%), H-8->L+2 (46%)
25	41737.87	239.5906	0.0072	46.4057	H-7->L+1 (29%), H-4->L+1 (13%)
26	42416.18	235.7591	0.0135	15.1054	HOMO->L+7 (74%)
27	42546.04	235.0395	0.0003	1.2219	H-1->L+3 (74%)
28	42770.26	233.8073	0.1024	26.9729	H-12->LUMO (14%), H-11->LUMO (64%), H-10->LUMO (10%)
29	42847.69	233.3848	0.0039	1.5205	H-1->L+3 (15%), H-1->L+5 (49%), HOMO->L+8 (11%)
30	43309.05	230.8986	0.0001	1.7561	HOMO->L+9 (40%), HOMO->L+10 (11%)
31	43371.15	230.568	0.0085	5.7553	H-2->L+4 (11%), HOMO->L+8 (34%)
32	43478.42	229.9991	0.005	-13.9392	H-3->L+2 (19%), H-2->L+4 (22%), HOMO->L+8 (18%)
33	43556.66	229.586	0.0518	41.6839	H-12->LUMO (23%), H-11->LUMO (10%), H-3->L+2 (10%), H-2->L+4 (32%)

34	43561.5	229.5605	0.0704	-25.6417	H-12->LUMO (37%), H-11->LUMO (16%), H-2->L+4 (20%)
35	43965.59	227.4506	0.0061	-7.293	H-2->L+6 (15%), HOMO->L+10 (51%)
36	43986.56	227.3422	0.0094	-10.9042	H-2->L+6 (28%), HOMO->L+9 (18%), HOMO->L+10 (18%)
37	44336.6	225.5473	0.0422	-9.8361	H-1->L+6 (28%), H-1->L+7 (45%)
38	44636.64	224.0312	0.012	-37.9868	H-9->L+2 (10%), H-3->L+2 (25%), H-3->L+5 (13%)
39	44899.58	222.7192	0.0825	-19.9737	H-6->L+1 (14%), H-4->L+1 (44%)
40	45374.65	220.3874	0.0195	18.9233	H-2->L+5 (68%), H-2->L+6 (10%)
41	45408.52	220.223	0.0266	-28.9773	H-3->L+1 (17%), H-1->L+6 (10%), HOMO->L+11 (31%)
42	45426.27	220.137	0.0045	1.4248	H-3->L+1 (59%)
43	45596.45	219.3153	0.1064	22.637	H-5->L+2 (26%), HOMO->L+11 (28%)
44	45723.89	218.7041	0.1446	-9.7539	H-5->L+2 (27%), H-1->L+6 (22%), HOMO->L+11 (11%)
45	45920.69	217.7668	0.0245	15.3898	H-6->L+2 (22%), H-4->L+2 (48%)
46	46311.06	215.9311	0.0588	-17.1658	H-6->L+1 (28%), H-5->L+1 (14%), H-4->L+3 (12%)
47	46381.23	215.6044	0.0301	14.8282	H-1->L+10 (10%), HOMO->L+12 (17%)
48	46465.12	215.2152	0.0242	-13.9093	H-9->L+2 (15%), HOMO->L+13 (11%)
49	46494.96	215.0771	0.0099	2.9916	H-9->L+2 (19%)
50	46618.36	214.5078	0.0038	4.1047	H-13->LUMO (92%)

Table S6. Cartesian coordinates of dominant conformer for **3**.

Center Number	**Atomic Number**	**Coordinates(Angstroms)**		
		X	**Y**	**Z**
1	6	0.842979	-1.56508	-1.47312
2	6	1.125213	-0.04251	-1.19569
3	6	5.091329	-0.13239	-1.04332
4	6	5.808599	0.4096	0.032
5	7	4.96977	0.407068	1.159191
6	6	3.756032	-0.21473	0.940008
7	6	3.69585	-0.53343	-0.58042
8	6	5.70602	-0.23233	-2.28539
9	6	7.031971	0.210588	-2.42773
10	6	7.725157	0.744732	-1.33761
11	6	7.119166	0.85409	-0.07705
12	8	2.920518	-0.43351	1.804478
13	6	3.433154	-2.06541	-0.83285
14	8	3.11631	-2.26194	-2.21906

15	6	2.629942	0.326265	-1.3228
16	6	1.734099	-2.11068	-2.60409
17	6	1.084312	-2.45	-0.26884
18	1	-0.20016	-1.67099	-1.78685
19	7	0.556489	0.518582	0.023145
20	1	4.376045	-2.59946	-0.68668
21	1	0.647355	0.49936	-2.02303
22	6	2.368979	-2.66015	0.05496
23	6	-0.05926	-3.13725	0.402116
24	8	-1.16804	-3.12324	-0.12083
25	6	0.183462	-3.85997	1.722078
26	6	-1.08609	-4.45692	2.329269
27	6	-1.51839	2.161516	2.252951
28	6	-2.96697	2.617264	1.918403
29	6	-4.27964	-0.75231	0.420018
30	6	-5.08228	-0.82371	-0.72538
31	7	-4.77718	0.278345	-1.54128
32	6	-3.68747	1.00208	-1.08746
33	6	-3.38564	0.48968	0.355283
34	6	-4.4192	-1.72732	1.399944
35	6	-5.34853	-2.76249	1.208554
36	6	-6.13003	-2.81383	0.050939
37	6	-6.00988	-1.83338	-0.9441
38	8	-3.12006	1.86064	-1.74284
39	6	-1.8699	0.094675	0.509943
40	8	-1.61494	-0.29854	1.864772
41	6	-3.89423	1.479143	1.460891
42	6	-1.34267	0.753114	2.808812
43	6	-0.78499	1.100888	0.024871
44	6	-0.80398	2.395098	0.906743
45	1	-1.11378	2.858419	2.999289
46	6	-1.66946	3.511734	0.325765
47	7	-2.81879	3.645108	0.876246
48	1	-1.73593	-0.82827	-0.05718
49	1	-3.45103	3.073814	2.791681
50	1	0.236229	2.710769	1.027921
51	6	-1.21388	4.389491	-0.80617
52	6	-0.12293	5.393606	-0.38721
53	1	-1.01651	1.374642	-1.00651
54	8	5.460251	0.661085	2.424173
55	6	4.935667	1.900022	2.944591
56	8	-5.16219	0.302711	-2.87002
57	6	-6.03883	1.416373	-3.12955
58	1	5.173929	-0.66359	-3.12838
59	1	7.52334	0.131219	-3.39344
60	1	8.751738	1.078898	-1.4627
61	1	7.650364	1.255357	0.779822
62	1	2.740251	1.372241	-1.01829
63	1	2.902663	0.277558	-2.3817

64	1	1.367226	-3.09538	-2.91816
65	1	1.718986	-1.4458	-3.47726
66	1	0.792475	-0.00651	0.86069
67	1	2.68026	-3.27621	0.89239
68	1	0.65125	-3.14854	2.416164
69	1	0.931627	-4.64775	1.553479
70	1	-0.85192	-4.95908	3.274975
71	1	-1.54484	-5.18574	1.653704
72	1	-1.82807	-3.67687	2.523819
73	1	-3.798	-1.70129	2.289693
74	1	-5.45129	-3.53688	1.963781
75	1	-6.83992	-3.62545	-0.08598
76	1	-6.60231	-1.86401	-1.85268
77	1	-4.84922	1.910707	1.138205
78	1	-4.1171	0.868845	2.343153
79	1	-0.30902	0.622689	3.159797
80	1	-2.00381	0.590174	3.671631
81	1	-0.83532	3.755245	-1.61871
82	1	-2.0881	4.922329	-1.19311
83	1	0.176226	6.010771	-1.24241
84	1	-0.4887	6.062635	0.400445
85	1	0.775537	4.888074	-0.01298
86	1	3.850902	1.832704	3.063382
87	1	5.416401	2.012654	3.918723
88	1	5.205183	2.736051	2.289647
89	1	-6.30241	1.317112	-4.18501
90	1	-6.93783	1.350717	-2.50635
91	1	-5.51576	2.361124	-2.95777

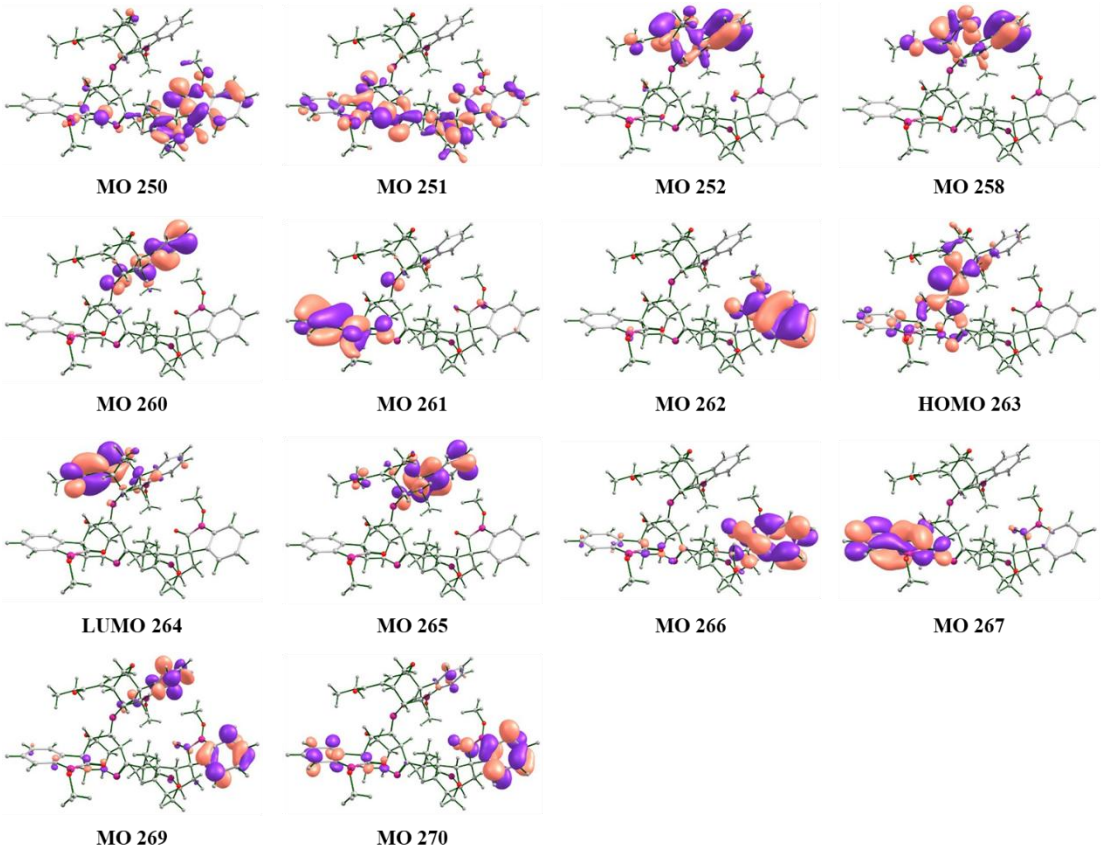

Fig. S5. Key molecular orbitals involved in important transitions regarding the ECD spectra of dominant conformer for **4** at the CAM-B3LYP/6-31+G(d) level in acetonitrile.

Table S7. Key transitions and their related rotatory and oscillator strengths of dominant conformer for **4** at the CAM-B3LYP/6-31+G(d) level in acetonitrile.

HOMO is 263					
No.	**Energy (cm^{-1})**	**Wavelength (nm)**	**Osc. Strength**	**R (length)**	**Major contribs**
1	33141.55	301.736	0.0005	-9.1195	H-14->LUMO (11%), H-9->LUMO (56%)
2	34141.68	292.8971	0.012	26.6004	HOMO->LUMO (82%)
3	39840.84	250.9987	0.0245	-23.3486	H-3->LUMO (20%), H-3->L+1 (42%)
4	40127.97	249.2027	0.0201	13.3243	H-2->L+3 (56%)
5	40261.86	248.374	0.0247	-10.674	H-1->L+2 (56%), H-1->L+5 (10%)
6	41621.72	240.2592	0.0925	-18.6665	H-3->L+4 (21%), H-3->L+5 (14%), HOMO->L+1 (18%)
7	41960.48	238.3195	0.179	-31.4038	H-2->L+6 (10%), H-2->L+7 (28%)
8	42015.32	238.0084	0.1716	-81.8662	H-1->L+2 (25%), H-1->L+5 (10%), H-1->L+6 (31%)

9	43342.92	230.7182	0.2894	31.744	H-11->LUMO (14%), H-5->LUMO (18%), HOMO->L+1 (11%)
10	43439.71	230.2041	0.0815	76.9897	
11	43681.68	228.9289	0.0881	-25.7638	H-5->LUMO (27%), H-3->LUMO (10%), HOMO->L+1 (19%)
12	43907.51	227.7515	0.0153	80.1241	H-12->L+3 (12%)
13	43964.78	227.4548	0.0113	51.7477	H-13->L+2 (31%)
14	45290.76	220.7956	0.0186	-11.8761	H-14->LUMO (13%), H-3->LUMO (39%), H-3->L+1 (17%)
15	45529.51	219.6378	0.0047	17.1314	H-8->L+17 (11%)
16	45919.88	217.7706	0.0352	-75.056	HOMO->L+1 (27%)
17	46358.65	215.7095	0.034	-20.025	H-14->LUMO (30%), H-3->LUMO (15%), H-2->LUMO (13%)
18	46669.17	214.2742	0.0288	-26.883	H-14->LUMO (11%), H-2->LUMO (15%), HOMO->L+3 (23%)
19	46788.55	213.7275	0.0872	-24.3013	H-2->LUMO (38%), HOMO->L+3 (31%)
20	47322.49	211.316	0.0224	35.2992	HOMO->L+4 (28%), HOMO->L+6 (10%), HOMO->L+8 (12%)
21	47646.73	209.878	0.0151	3.1896	H-2->LUMO (12%), H-2->L+10 (15%)
22	47921.76	208.6735	0.0019	-8.6628	H-1->L+4 (14%), H-1->L+9 (24%), H-1->L+11 (10%)
23	48726.71	205.2263	0.0213	6.6146	HOMO->L+10 (10%)
24	49190.48	203.2914	0.035	-33.6997	HOMO->L+12 (11%)
25	49735.72	201.0628	0.2334	116.3593	H-5->L+1 (10%), HOMO->L+5 (23%), HOMO->L+6 (10%)
26	50016.4	199.9344	0.023	-52.7433	HOMO->L+4 (14%), HOMO->L+7 (10%)
27	50329.34	198.6912	0.0006	-0.7348	H-1->LUMO (82%)
28	50476.14	198.1134	0.1639	7.9132	HOMO->L+9 (18%)
29	50611.64	197.583	0.0115	28.8256	H-7->LUMO (29%), H-6->LUMO (17%)
30	50652.77	197.4226	0.3178	110.3971	H-4->L+2 (13%)
31	51047.99	195.8941	0.1527	217.3059	H-5->L+1 (25%)
32	51192.36	195.3416	0.8375	-290.427	H-4->L+2 (16%)
33	51235.92	195.1756	0.0727	-115.317	H-4->L+2 (10%), HOMO->L+7 (13%)
34	51408.52	194.5203	0.0743	-41.2241	HOMO->L+4 (16%), HOMO->L+5 (10%)
35	51725.5	193.3282	0.3906	-1.4767	H-6->L+3 (33%), H-2->L+7 (11%), HOMO->L+7 (11%)
36	52174.75	191.6636	0.0004	10.7269	HOMO->L+2 (28%), HOMO->L+9 (17%)
37	52511.9	190.433	0.0623	-50.2868	
38	52544.16	190.3161	0.0291	9.618	H-24->LUMO (10%), H-17->LUMO (10%)

39	52565.13	190.2402	0.0301	19.527	H-1->L+10 (10%), H-1->L+20 (11%)
40	52855.49	189.1951	0.0569	-194.463	HOMO->L+2 (13%)
41	52911.95	188.9932	0.0073	57.1574	HOMO->L+8 (12%), HOMO->L+10 (12%), HOMO->L+13 (10%)
42	52980.51	188.7487	0.07	106.1546	
43	53141.82	188.1757	0.0384	14.9558	H-1->L+8 (10%)
44	53403.14	187.2549	0.0077	-68.8554	
45	53636.24	186.4411	0.0285	-37.3771	H-10->L+2 (13%), H-8->L+2 (28%), H-7->L+2 (11%)
46	53666.08	186.3374	0.02	25.8092	H-11->LUMO (18%), H-5->L+1 (12%)
47	53699.15	186.2227	0.0425	-35.6012	H-7->L+3 (22%)
48	53808.04	185.8458	0.0007	2.3733	H-1->L+1 (61%)
49	54002.42	185.1769	0.0731	90.1144	H-1->L+1 (12%), H-1->L+18 (11%)
50	54116.95	184.785	0.1249	69.0867	H-3->L+11 (13%)

Table S8. Cartesian coordinates of dominant conformer for **4**.

Center Number	**Atomic Number**	**Coordinates(Angstroms)**		
		X	**Y**	**Z**
1	6	2.941156	-4.41293	-1.33076
2	6	4.275095	-3.84219	-1.86585
3	6	5.43176	-2.09431	1.405281
4	6	6.000423	-0.82434	1.466717
5	7	5.467729	-0.06401	0.42113
6	6	4.525104	-0.72679	-0.32465
7	6	4.501133	-2.18889	0.198373
8	6	5.789432	-3.03543	2.354813
9	6	6.710456	-2.6832	3.348083
10	6	7.271967	-1.40974	3.376992
11	6	6.923506	-0.44875	2.424608
12	8	3.845129	-0.20133	-1.18698
13	6	3.068812	-2.60339	0.668441
14	8	3.106404	-3.95776	1.097233
15	6	5.154935	-3.19724	-0.79466
16	6	2.939921	-4.95608	0.087205
17	6	1.874186	-2.34603	-0.27285
18	6	1.986497	-3.2286	-1.54509
19	1	2.639288	-5.23419	-1.9916
20	6	2.683198	-2.5248	-2.70032
21	7	3.895081	-2.86718	-2.89016
22	1	2.897359	-2.03793	1.584985
23	1	4.881998	-4.62511	-2.33493
24	1	0.988455	-3.56409	-1.83531
25	6	1.995215	-1.51635	-3.56847
26	6	1.071561	-2.17848	-4.59841
27	1	1.911287	-1.29105	-0.55985

28	6	-1.76038	-1.02844	-2.10577
29	6	-2.24945	-2.48804	-1.94927
30	6	-5.61505	-1.79445	-0.10913
31	6	-6.06818	-2.53932	0.977951
32	7	-4.94972	-3.05659	1.646035
33	6	-3.76172	-2.56059	1.160872
34	6	-4.09055	-1.82282	-0.15846
35	6	-6.54032	-1.19027	-0.94205
36	6	-7.90325	-1.33636	-0.66192
37	6	-8.32713	-2.08044	0.435567
38	6	-7.40614	-2.70234	1.281992
39	8	-2.68836	-2.71205	1.711178
40	6	-3.52375	-0.3704	-0.16291
41	8	-3.79521	0.206533	-1.43646
42	6	-3.67692	-2.6382	-1.41772
43	6	-2.81268	0.00975	-2.45363
44	6	-2.04844	-0.12435	0.248441
45	6	-1.05683	-0.79253	-0.75748
46	1	-1.01498	-1.01261	-2.90882
47	6	-0.62648	-2.2202	-0.43041
48	7	-1.2633	-3.12137	-1.07131
49	1	-4.12334	0.216483	0.53595
50	1	-2.23043	-3.01064	-2.91325
51	1	-0.1881	-0.13355	-0.84934
52	6	-2.20574	3.029018	2.04461
53	6	-1.23067	1.970318	1.446226
54	6	1.665373	4.478692	0.424037
55	6	2.262673	4.532956	-0.83499
56	7	1.383903	3.94893	-1.75609
57	6	0.197135	3.553498	-1.20676
58	6	0.281695	3.858834	0.305203
59	6	2.329967	5.025848	1.507768
60	6	3.5825	5.618261	1.305685
61	6	4.152474	5.660934	0.035884
62	6	3.495626	5.110929	-1.06814
63	8	-0.71236	3.020096	-1.82267
64	6	-0.78366	4.917447	0.755815
65	8	-0.73348	5.011594	2.175478
66	6	0.172511	2.555426	1.144086
67	6	-1.5298	4.080418	2.920459
68	6	-2.90377	3.736839	0.913424
69	1	-2.95269	2.502322	2.64438
70	7	-1.88265	1.31365	0.329002
71	1	-0.45214	5.895289	0.398245
72	1	-1.061	1.211861	2.220031
73	6	-2.17956	4.644667	0.260827
74	6	-4.3114	3.368449	0.580606
75	8	-4.97203	2.724911	1.377519
76	6	-4.87784	3.793626	-0.75807

77	6	-6.30455	3.313065	-0.98314
78	1	-1.9094	-0.53819	1.24647
79	6	0.523976	-2.58813	0.479371
80	1	0.419917	-3.66186	0.662608
81	6	0.44415	-1.86381	1.828607
82	8	5.781109	1.25271	0.238896
83	6	4.837385	2.099073	0.911101
84	8	1.678366	3.850135	-3.08527
85	6	2.099497	2.514449	-3.41942
86	8	-5.0564	-3.5597	2.917109
87	6	-4.68788	-4.94292	2.949411
88	1	5.346627	-4.02552	2.336403
89	1	6.989763	-3.41259	4.101927
90	1	7.991929	-1.15546	4.149076
91	1	7.35677	0.545456	2.427428
92	1	6.007252	-2.71277	-1.28321
93	1	5.569286	-4.00577	-0.18511
94	1	1.991982	-5.47387	0.280291
95	1	3.746913	-5.68735	0.223086
96	1	1.419646	-0.83145	-2.93388
97	1	2.763569	-0.92507	-4.07374
98	1	0.556741	-1.4234	-5.20175
99	1	1.64745	-2.81611	-5.27617
100	1	0.308592	-2.80144	-4.11907
101	1	-6.20814	-0.59381	-1.78514
102	1	-8.63618	-0.85564	-1.30235
103	1	-9.38858	-2.17764	0.642925
104	1	-7.71854	-3.27569	2.147657
105	1	-3.87422	-3.70084	-1.23893
106	1	-4.35412	-2.33115	-2.22027
107	1	-3.35066	-0.2847	-3.36368
108	1	-2.32729	0.973254	-2.65621
109	1	1.871783	5.020101	2.491171
110	1	4.108057	6.058806	2.147238
111	1	5.120838	6.132064	-0.10429
112	1	3.920615	5.143419	-2.06507
113	1	0.654622	2.772969	2.101858
114	1	0.780237	1.776949	0.668568
115	1	-0.86991	3.613964	3.662238
116	1	-2.29122	4.653954	3.459752
117	1	-1.71022	1.77215	-0.5586
118	1	-2.54195	5.19883	-0.59863
119	1	-4.20795	3.405915	-1.5352
120	1	-4.82132	4.887903	-0.82832
121	1	-6.66476	3.640697	-1.96349
122	1	-6.98042	3.703594	-0.21746
123	1	-6.35544	2.222226	-0.94121
124	1	-0.55771	-1.9662	2.247343
125	1	1.140521	-2.30045	2.54823

126	1	0.679579	-0.79599	1.733262
127	1	3.843924	1.98008	0.473247
128	1	4.818937	1.873742	1.982305
129	1	5.1944	3.114504	0.746754
130	1	2.93766	2.201335	-2.79018
131	1	1.260683	1.822696	-3.3144
132	1	2.409315	2.574315	-4.46318
133	1	-4.84173	-5.24894	3.985173
134	1	-3.6374	-5.06181	2.673554
135	1	-5.33206	-5.52541	2.283049

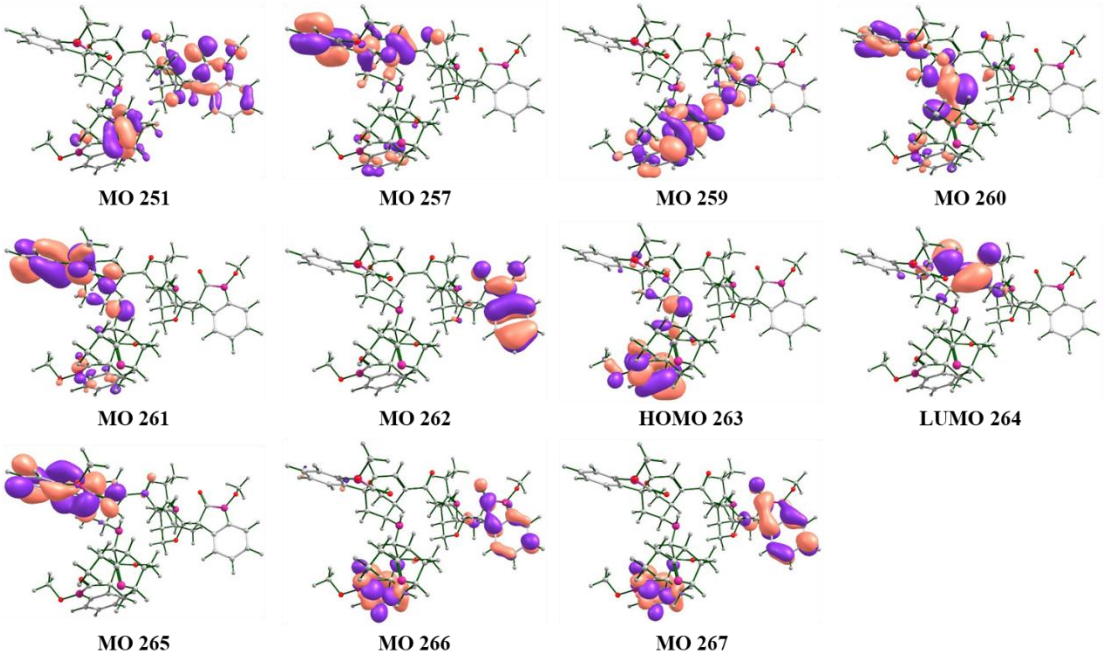

Fig. S6. Key molecular orbitals involved in important transitions regarding the ECD spectra of dominant conformer for **5** at the CAM-B3LYP/6-31+G(d) level in acetonitrile.

Table S9. Key transitions and their related rotatory and oscillator strengths of dominant conformer for **5** at the CAM-B3LYP/6-31+G(d) level in acetonitrile.

HOMO is 263					
No.	**Energy (cm^{-1})**	**Wavelength (nm)**	**Osc. Strength**	**R (length)**	**Major contribs**
1	31601.83	316.4374	0.0026	-5.356	H-15->LUMO (11%), H-9->LUMO (54%)
2	38826.19	257.5581	0.0125	-2.5382	H-3->LUMO (47%), H-2->LUMO (22%), HOMO->LUMO (19%)
3	39865.84	250.8413	0.0182	-24.4766	H-3->LUMO (13%), H-2->L+1 (45%)

4	39948.11	250.3247	0.0245	-11.0737	H-1->L+2 (27%), H-1->L+3 (46%)
5	40055.38	249.6543	0.02	-11.4149	HOMO->L+2 (32%), HOMO->L+3 (22%)
6	41937.09	238.4524	0.1598	-167.299	H-1->L+7 (45%)
7	41998.39	238.1044	0.1802	129.6885	HOMO->L+2 (10%), HOMO->L+6 (40%)
8	42190.35	237.021	0.049	-43.9925	H-2->L+1 (12%), H-2->L+5 (36%)
9	42450.87	235.5665	0.4972	97.9432	H-15->LUMO (12%), H-14->LUMO (14%), H-6->LUMO (36%)
10	43429.22	230.2597	0.0054	-3.241	H-13->L+2 (11%)
11	43638.93	229.1532	0.0017	-20.2182	H-18->L+1 (19%)
12	43738.94	228.6292	0.0231	83.4721	H-12->L+3 (16%)
13	44088.99	226.814	0.0107	-8.2735	H-3->LUMO (18%), H-2->LUMO (41%)
14	45292.38	220.7877	0.0011	2.4821	
15	45585.96	219.3658	0.023	16.9974	H-15->LUMO (43%), H-14->LUMO (24%), H-9->LUMO (10%)
16	45740.02	218.6269	0.0025	12.9913	
17	46265.09	216.1457	0.0031	-6.0158	H-1->LUMO (87%)
18	47114.4	212.2494	0.0072	-10.4491	HOMO->L+4 (25%), HOMO->L+10 (26%), HOMO->L+12 (10%)
19	47149.88	212.0896	0.0198	1.2891	H-1->L+8 (19%), H-1->L+11 (26%)
20	47906.44	208.7402	0.0109	-2.2066	H-2->L+9 (12%), HOMO->LUMO (32%)
21	47947.57	208.5611	0.0095	4.2375	H-2->L+9 (10%), HOMO->LUMO (46%)
22	48568.62	205.8942	0.0064	-12.5418	H-3->L+1 (48%), HOMO->L+1 (10%)
23	49621.18	201.5268	0.0045	22.8517	H-8->LUMO (10%), H-7->LUMO (17%), H-5->LUMO (13%), H-4->LUMO (38%)
24	50035.76	199.8571	0.2032	73.6379	H-3->L+2 (23%)
25	50235.78	199.0613	0.0988	-42.3219	
26	50343.86	198.6339	0.1606	-74.2573	H-3->L+4 (22%)
27	50512.43	197.9711	0.5402	134.6369	H-6->L+1 (21%)
28	50754.4	197.0272	0.0975	-298.739	
29	50996.37	196.0924	0.4165	356.4056	H-5->L+3 (14%)
30	51154.45	195.4864	0.1043	-210.052	
31	51177.04	195.4001	0.2174	83.5566	H-11->LUMO (10%), H-10->LUMO (13%)
32	51735.18	193.2921	0.2605	-128.696	
33	51803.74	193.0363	0.0475	-46.4513	H-18->LUMO (20%), H-8->LUMO (11%), H-4->LUMO (18%)
34	52111.04	191.8979	0.0564	-20.0447	H-18->LUMO (15%), H-11->LUMO (20%), H-7->LUMO (10%)
35	52148.94	191.7584	0.193	-40.3787	

36	52432.85	190.7201	0.0028	7.72	H-12->LUMO (14%), H-5->LUMO (27%)
37	52494.96	190.4945	0.021	2.8465	HOMO->L+8 (10%), HOMO->L+14 (11%)
38	52516.73	190.4155	0.1648	-7.5545	H-5->L+7 (16%), H-1->L+12 (11%)
39	52769.19	189.5045	0.0241	-46.0702	
40	53102.3	188.3158	0.1649	94.7804	H-2->L+13 (10%)
41	53253.93	187.7796	0.0239	15.9444	H-1->L+13 (19%), H-1->L+16 (15%)
42	53348.3	187.4474	0.0175	-1.9919	H-18->LUMO (16%), H-14->LUMO (21%), H-6->LUMO (23%)
43	53430.57	187.1588	0.0387	-5.4683	H-7->L+2 (10%), H-7->L+3 (13%)
44	53573.33	186.66	0.0104	18.9795	H-4->L+2 (12%), H-4->L+3 (12%)
45	53754	186.0327	0.0183	-12.0833	H-2->L+14 (12%)
46	53851.59	185.6955	0.0073	-17.5409	HOMO->L+15 (10%), HOMO->L+18 (17%)
47	53937.89	185.3984	0.0307	-1.9298	H-1->L+11 (14%), H-1->L+16 (13%), H-1->L+20 (10%)
48	54141.95	184.6997	0.0145	39.368	H-3->L+6 (16%)
49	54329.88	184.0608	0.0562	4.7836	H-3->L+5 (17%)
50	54488.77	183.524	0.1072	4.328	HOMO->L+1 (29%)

Table S10. Cartesian coordinates of dominant conformer for **5**

Center Number	**Atomic Number**	**Coordinates(Angstroms)**		
		X	**Y**	**Z**
1	6	0.774767	-1.67949	-1.6687
2	6	1.893602	-0.81579	-1.0362
3	6	4.698529	-3.58771	-0.62364
4	6	5.242683	-4.00766	0.589552
5	7	4.311042	-3.73366	1.604729
6	6	3.23193	-3.01504	1.154402
7	6	3.327365	-2.98099	-0.38497
8	6	5.413432	-3.78937	-1.79081
9	6	6.674677	-4.39047	-1.71619
10	6	7.203008	-4.78153	-0.48877
11	6	6.486962	-4.59785	0.696969
12	8	2.38545	-2.51396	1.873787
13	6	2.225773	-3.87391	-1.05628
14	8	2.184374	-3.55967	-2.44735
15	6	3.263964	-1.53477	-0.92979
16	6	1.308326	-2.50297	-2.84851
17	6	0.13366	-2.67605	-0.725
18	1	0.021031	-0.98715	-2.05676
19	7	1.402593	-0.20176	0.194277
20	1	2.55899	-4.91317	-1.01123
21	1	2.066692	-0.00527	-1.753
22	6	0.867298	-3.74815	-0.43123

23	6	-1.2659	-2.58446	-0.19501
24	8	-1.91205	-3.60619	-0.03645
25	6	0.832899	2.386678	2.336501
26	6	1.807991	3.5705	2.541887
27	6	2.415087	4.410615	-1.22295
28	6	3.646337	4.63006	-1.83867
29	7	4.609913	3.888635	-1.1493
30	6	4.117423	3.223887	-0.0504
31	6	2.592802	3.508581	-0.00507
32	6	1.28597	5.01272	-1.75005
33	6	1.413992	5.830382	-2.8786
34	6	2.659555	6.044472	-3.46228
35	6	3.808913	5.440727	-2.94643
36	8	4.796623	2.531996	0.682292
37	6	1.751488	2.203545	-0.19691
38	8	0.379109	2.532492	-0.0896
39	6	2.1762	4.322286	1.257433
40	6	-0.18916	2.518824	1.223502
41	6	2.139614	0.979752	0.662999
42	6	1.811704	1.219404	2.155569
43	1	0.278992	2.245479	3.272131
44	6	3.006626	1.735083	2.947262
45	7	2.991719	2.987298	3.176381
46	1	1.875975	1.919573	-1.24577
47	1	1.38181	4.319356	3.219335
48	1	1.437694	0.285651	2.587914
49	6	4.102636	0.819552	3.396142
50	6	5.261852	1.521499	4.091558
51	1	3.222406	0.843342	0.559843
52	6	-1.83809	-1.23801	0.23346
53	1	-1.19112	-0.43992	-0.13948
54	6	-1.75208	-1.23195	1.770445
55	1	-3.8363	-1.96728	-0.01697
56	6	-5.84099	-3.62256	-3.28246
57	6	-4.52308	-3.12225	-2.70608
58	1	-2.31968	-1.42466	-2.24254
59	1	-5.18723	1.208568	-3.40812
60	1	-3.87418	0.068986	1.382537
61	7	-5.33877	-0.82603	-2.94743
62	6	-4.44238	-1.63662	-2.54457
63	1	-2.9224	0.606373	-3.29979
64	6	-3.24797	-0.97985	-1.86584
65	6	-3.27523	-1.08036	-0.31803
66	6	-2.84066	1.509034	-1.3813
67	6	-5.75204	1.034623	-1.37327
68	8	-3.25068	1.346806	-0.01901
69	6	-3.95904	0.152385	0.297677
70	8	-6.15821	-2.01437	-0.1847
71	6	-7.91719	1.324066	2.667999

72	6	-7.51526	2.59905	3.073271
73	6	-6.41631	3.223824	2.489926
74	6	-5.68452	2.584994	1.482651
75	6	-5.47809	0.388158	0.017717
76	6	-6.31978	-0.89375	0.249167
77	7	-7.36349	-0.53556	1.080137
78	6	-7.17429	0.719397	1.671322
79	6	-6.06516	1.3181	1.075504
80	6	-4.94864	0.535533	-2.57635
81	6	-3.42077	0.474167	-2.33181
82	8	4.682611	-3.73695	2.923867
83	6	3.966824	-4.73966	3.656449
84	8	-8.14745	-1.4823	1.690875
85	6	-9.21548	-1.89063	0.829213
86	8	5.948322	4.039302	-1.38957
87	6	6.495868	2.873242	-2.01696
88	1	4.999005	-3.49171	-2.74891
89	1	7.247175	-4.55053	-2.62432
90	1	8.187102	-5.2384	-0.44804
91	1	6.887467	-4.89346	1.660186
92	1	3.696001	-1.57759	-1.93357
93	1	3.946076	-0.91049	-0.3429
94	1	0.469314	-2.94514	-3.39758
95	1	1.875256	-1.8701	-3.54124
96	1	1.428827	-0.90781	0.927288
97	1	0.492795	-4.53434	0.216607
98	1	0.314862	4.84395	-1.29697
99	1	0.53309	6.30587	-3.29852
100	1	2.74369	6.690746	-4.33086
101	1	4.787858	5.602406	-3.3839
102	1	2.967846	5.041851	1.492116
103	1	1.301789	4.912342	0.967056
104	1	-0.75759	3.451186	1.331774
105	1	-0.90634	1.694043	1.267173
106	1	3.660383	0.051474	4.04632
107	1	4.466068	0.275617	2.514699
108	1	6.020974	0.793276	4.395438
109	1	5.722626	2.250714	3.420826
110	1	4.920448	2.059165	4.980585
111	1	-1.95076	-0.23662	2.174706
112	1	-2.46888	-1.94032	2.198145
113	1	-0.75162	-1.52495	2.104318
114	1	-5.82136	-4.71219	-3.38776
115	1	-6.6695	-3.35117	-2.62366
116	1	-6.03805	-3.18097	-4.26344
117	1	-3.68	-3.43674	-3.33933
118	1	-4.33455	-3.57748	-1.72634
119	1	-1.74457	1.480492	-1.40482
120	1	-3.14369	2.51875	-1.68679

121	1	-6.81943	0.944992	-1.60232
122	1	-5.54956	2.10441	-1.26349
123	1	-8.76429	0.819227	3.118721
124	1	-8.06978	3.106044	3.857323
125	1	-6.11928	4.213475	2.822929
126	1	-4.81698	3.062138	1.039041
127	1	4.368094	-4.68375	4.669045
128	1	4.153094	-5.73005	3.229539
129	1	2.897932	-4.51397	3.662444
130	1	-8.81641	-2.37171	-0.06666
131	1	-9.84037	-1.03228	0.562692
132	1	-9.78957	-2.60815	1.417185
133	1	7.542658	3.119744	-2.19946
134	1	6.422889	2.014273	-1.34625
135	1	5.984838	2.67423	-2.9647

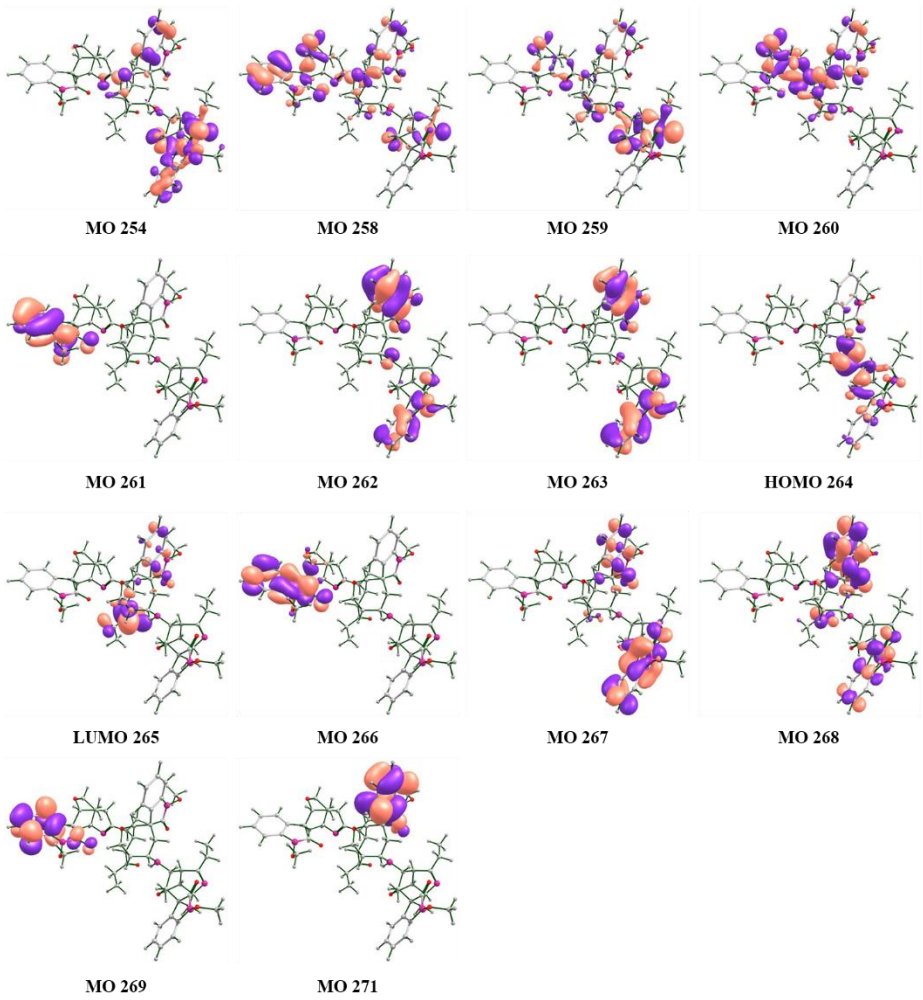

Fig. S7. Key molecular orbitals involved in important transitions regarding the ECD spectra of dominant conformer for **6** at the CAM-B3LYP/6-31+G(d) level in acetonitrile.

Table S11. Key transitions and their related rotatory and oscillator strengths of dominant conformer for 6 at the CAM-B3LYP/6-31+G(d) level in acetonitrile.

HOMO is 264					
No.	**Energy (cm^{-1})**	**Wavelength (nm)**	**Osc. Strength**	**R (length)**	**Major contribs**
1	32897.97	303.9701	0.0012	3.2281	HOMO->LUMO (94%)
2	34868.4	286.7927	0.0049	1.7658	H-7->LUMO (11%), HOMO->L+2 (19%), HOMO->L+3 (42%)
3	34946.63	286.1506	0.0044	5.0343	H-9->LUMO (12%), H-7->LUMO (22%), HOMO->L+3 (23%)
4	35383.79	282.6153	0.0286	-41.7342	HOMO->L+2 (69%), HOMO->L+3 (29%)
5	37468.74	266.8891	0.0003	-1.6125	HOMO->L+1 (98%)
6	37523.59	266.499	0.0167	-13.8051	H-2->LUMO (17%), H-2->L+2 (11%), H-2->L+3 (22%), H-1->LUMO (11%), H-1->L+3 (14%)
7	37573.6	266.1443	0.0118	10.7797	H-2->L+2 (16%), H-1->L+2 (38%), H-1->L+3 (11%), HOMO->L+5 (15%)
8	38084.15	262.5764	0.0339	5.0846	H-3->L+1 (81%)
9	39016.53	256.3016	0.0042	-11.4388	H-1->LUMO (53%), HOMO->L+6 (24%)
10	39063.31	255.9947	0.0716	21.8436	HOMO->L+5 (67%)
11	39203.66	255.0783	0.0059	-8.1603	H-2->LUMO (35%), H-1->LUMO (32%), HOMO->L+6 (26%)
12	39281.89	254.5702	0.0187	-0.6854	H-2->LUMO (35%), H-2->L+3 (14%), HOMO->L+6 (32%)
13	39454.5	253.4565	0.0001	-0.1908	H-3->LUMO (96%)
14	40132.01	249.1777	0.0247	18.4905	H-2->L+5 (11%), H-1->L+5 (22%), HOMO->L+8 (45%)
15	40354.62	247.8031	0.0034	-5.9449	HOMO->L+7 (95%)
16	40476.41	247.0575	0.0414	6.7452	H-1->L+5 (18%), HOMO->L+8 (40%)
17	40495.76	246.9394	0.0556	138.1159	H-3->L+4 (23%), H-2->L+6 (21%), H-1->L+6 (13%)
18	40519.96	246.7919	0.1429	-181.304	H-3->L+4 (30%), H-2->L+6 (18%), H-1->L+6 (11%)
19	40677.24	245.8377	0.0114	12.0718	H-2->L+3 (20%), H-1->L+2 (12%), H-1->L+3 (38%)
20	40696.6	245.7208	0.0031	-1.39	H-2->L+1 (39%), H-1->L+1 (52%)
21	40808.71	245.0457	0.0015	-0.0764	HOMO->L+4 (97%)
22	40861.14	244.7313	0.0016	-1.6225	H-2->L+2 (47%), H-2->L+3 (17%), H-1->L+2 (22%)
23	41116.01	243.2143	0.0123	-20.1686	H-4->L+3 (12%)
24	41274.9	242.278	0.0004	-0.3362	H-3->L+2 (31%), H-3->L+3 (65%)

25	41328.13	241.9659	0.0007	1.0497	H-2->L+1 (54%), H-1->L+1 (43%)
26	41465.25	241.1658	0.0385	88.7769	H-14->L+1 (23%), H-6->L+1 (14%), H-4->L+1 (17%)
27	41670.92	239.9755	0.0409	98.4146	H-10->L+2 (19%)
28	41827.4	239.0778	0.0063	-39.7117	H-7->L+7 (11%), H-4->L+7 (42%)
29	41930.63	238.4891	0.0001	0.0262	H-3->L+2 (67%), H-3->L+3 (32%)
30	42761.39	233.8558	0.0003	-3.4392	H-4->LUMO (74%)
31	43342.11	230.7225	0.0098	4.2177	H-3->L+7 (93%)
32	43566.34	229.535	0.0024	-8.588	H-5->L+2 (32%), H-5->L+8 (15%)
33	43617.96	229.2634	0.001	3.3146	H-2->L+7 (47%), H-1->L+7 (38%)
34	43630.86	229.1956	0.002	8.8188	H-4->L+1 (59%)
35	43841.38	228.095	0.0003	-0.205	H-2->L+6 (35%), H-1->L+6 (62%)
36	43922.84	227.672	0	0.017	H-2->L+4 (36%), H-1->L+4 (61%)
37	43992.2	227.313	0.0032	2.0134	H-5->LUMO (47%), H-2->L+5 (19%)
38	44003.49	227.2547	0.001	-0.9479	H-5->LUMO (19%), H-2->L+5 (47%), H-1->L+5 (22%)
39	44229.33	226.0943	0	0.0063	H-3->L+6 (98%)
40	44430.16	225.0723	0.0038	-1.2839	H-6->LUMO (15%), H-2->L+4 (30%), H-1->L+4 (18%)
41	44430.16	225.0723	0.0034	-1.7424	H-6->LUMO (15%), H-2->L+4 (31%), H-1->L+4 (19%)
42	44482.59	224.8071	0.0022	0.0086	HOMO->L+9 (83%)
43	44559.21	224.4205	0.0076	1.7262	HOMO->L+10 (89%)
44	44751.98	223.4538	0	0.0079	H-3->L+5 (98%)
45	44842.32	223.0036	0.0928	-36.8079	H-4->L+2 (14%), H-4->L+3 (32%)
46	44925.39	222.5913	0.0082	-6.1972	H-2->L+8 (26%), H-1->L+8 (60%)
47	45020.57	222.1207	0.0003	-1.1432	H-2->L+7 (40%), H-1->L+7 (55%)
48	45108.48	221.6878	0.0072	-0.293	H-5->L+2 (13%), H-5->L+8 (23%)
49	45423.85	220.1487	0.0045	-2.2311	H-7->LUMO (26%), H-6->LUMO (41%)
50	45763.41	218.5152	0.0522	-23.3768	H-6->L+1 (31%), H-5->L+1 (32%), H-4->L+1 (13%)

Table S12. Cartesian coordinates of dominant conformer for **6**

Center Number	**Atomic Number**	**Coordinates(Angstroms)**		
		X	**Y**	**Z**
1	6	0.065179	-0.75675	0.336163
2	6	1.392336	0.045499	0.556363
3	6	-0.32274	3.201369	2.206056
4	6	-0.17935	4.56952	1.937427
5	7	0.266183	4.713685	0.613976

6	6	0.608834	3.4995	0.02688
7	6	0.095229	2.381717	0.985384
8	6	-0.79577	2.810905	3.453805
9	6	-1.10031	3.790963	4.412513
10	6	-0.93079	5.147819	4.12145
11	6	-0.46479	5.562417	2.866143
12	8	1.185538	3.399889	-1.0402
13	6	-1.16856	1.662294	0.383293
14	8	-1.66021	0.697627	1.324604
15	6	1.226565	1.371942	1.357761
16	6	-0.90738	-0.51738	1.496529
17	6	-0.79519	-0.45235	-0.93139
18	1	0.328533	-1.8225	0.335881
19	7	2.161658	0.259968	-0.66103
20	1	-1.96818	2.40858	0.36179
21	1	1.966964	-0.59241	1.254794
22	6	-0.97294	1.069529	-1.0462
23	6	-0.30587	-1.14584	-2.20818
24	8	0.459589	-0.61749	-3.00329
25	6	-0.86128	-2.53912	-2.44358
26	6	-0.1843	-3.30857	-3.5762
27	6	4.835835	0.010223	-2.81106
28	6	6.308169	-0.15697	-2.33864
29	6	5.748056	-3.09154	0.201412
30	6	6.383271	-3.16124	1.448714
31	7	6.655438	-1.85161	1.874841
32	6	6.062451	-0.89025	1.066354
33	6	5.589964	-1.6292	-0.22302
34	6	5.392498	-4.27279	-0.43985
35	6	5.668373	-5.50087	0.184611
36	6	6.297552	-5.54046	1.432413
37	6	6.67033	-4.35936	2.09011
38	8	5.965925	0.285337	1.370771
39	6	4.086803	-1.3107	-0.5543
40	8	3.726831	-1.96423	-1.77387
41	6	6.552295	-1.38148	-1.43792
42	6	4.020911	-1.26292	-3.00066
43	6	3.616463	0.175245	-0.56278
44	6	4.273972	0.963166	-1.73612
45	1	4.851255	0.532077	-3.77703
46	6	5.550948	1.690423	-1.31814
47	7	6.639808	1.099749	-1.64908
48	1	3.490381	-1.82693	0.206212
49	1	6.986962	-0.27323	-3.19397
50	1	3.518189	1.65203	-2.12316
51	6	5.540038	2.991758	-0.56713
52	6	4.9925	4.168512	-1.3976
53	1	-1.76938	-0.90633	-0.72481
54	6	-5.81233	1.493017	-1.89568

55	6	-5.47868	0.098423	-2.50251
56	6	-7.20197	-1.98621	0.341517
57	6	-6.73453	-3.05571	1.115952
58	7	-5.33116	-2.98749	1.15145
59	6	-4.81733	-2.02147	0.301723
60	6	-6.02005	-1.17728	-0.1974
61	6	-8.57351	-1.82003	0.188311
62	6	-9.44824	-2.73373	0.798457
63	6	-8.95152	-3.80123	1.552143
64	6	-7.57202	-3.97995	1.726417
65	8	-3.63312	-1.89523	0.039853
66	6	-6.01705	0.237714	0.499603
67	8	-7.18568	0.958225	0.110411
68	6	-6.07355	-1.11337	-1.75803
69	6	-7.1307	1.643434	-1.14926
70	6	-4.75683	1.115083	0.377437
71	6	-4.559	1.744709	-1.03412
72	1	-5.82823	2.214535	-2.72392
73	6	-3.5121	1.026656	-1.89478
74	7	-4.00836	0.100561	-2.63417
75	1	-6.17201	0.046703	1.567136
76	1	-5.87633	0.021364	-3.52327
77	1	-4.34062	2.811853	-0.92787
78	6	-2.06216	1.457756	-2.09233
79	1	-1.76341	0.934432	-3.00705
80	6	-2.00989	2.966348	-2.42139
81	1	-0.04325	1.47563	-1.45489
82	1	3.912605	0.62928	0.385209
83	8	0.848736	5.90222	0.203235
84	6	0.120364	6.485344	-0.89297
85	8	6.95207	-1.59483	3.202923
86	6	8.244817	-0.97064	3.327241
87	8	-4.57652	-4.07031	1.563601
88	6	-3.93114	-3.79937	2.822237
89	1	-0.93071	1.759711	3.68801
90	1	-1.46546	3.489633	5.390529
91	1	-1.16015	5.895129	4.876631
92	1	-0.31847	6.610887	2.628071
93	1	2.18957	1.892578	1.324199
94	1	1.076015	1.109428	2.409914
95	1	-1.6491	-1.32084	1.527823
96	1	-0.3887	-0.48565	2.464908
97	1	1.806805	-0.2304	-1.47252
98	1	-0.82013	-3.09553	-1.49601
99	1	-1.93645	-2.40366	-2.63844
100	1	0.880371	-3.46212	-3.3687
101	1	-0.65459	-4.2902	-3.70396
102	1	-0.26133	-2.76373	-4.52231
103	1	4.887904	-4.2418	-1.40045

104	1	5.383853	-6.42759	-0.30639
105	1	6.501512	-6.49815	1.904431
106	1	7.150995	-4.37324	3.062841
107	1	7.584818	-1.3466	-1.07034
108	1	6.482015	-2.27093	-2.07383
109	1	4.553014	-1.97144	-3.65088
110	1	3.062978	-1.02628	-3.48086
111	1	4.929126	2.872457	0.337867
112	1	6.564399	3.197555	-0.23993
113	1	5.040523	5.095402	-0.81411
114	1	5.584769	4.313535	-2.30927
115	1	3.946396	4.0135	-1.68281
116	1	-8.96704	-0.9905	-0.39032
117	1	-10.5211	-2.60953	0.680078
118	1	-9.6406	-4.50564	2.01053
119	1	-7.17128	-4.80906	2.300419
120	1	-5.62358	-2.02339	-2.17199
121	1	-7.13332	-1.15083	-2.03342
122	1	-7.96399	1.275412	-1.76647
123	1	-7.32177	2.706423	-0.94706
124	1	-4.89609	1.923178	1.105947
125	1	-3.87315	0.55975	0.697655
126	1	-1.00734	3.231904	-2.77089
127	1	-2.72574	3.219195	-3.2128
128	1	-2.23729	3.598218	-1.55427
129	1	0.63933	7.424604	-1.09732
130	1	0.162283	5.833521	-1.7697
131	1	-0.91836	6.682285	-0.60372
132	1	9.025183	-1.61915	2.913323
133	1	8.246619	0.003843	2.831456
134	1	8.386703	-0.84712	4.40331
135	1	-3.22515	-2.97006	2.720538
136	1	-4.67317	-3.57927	3.597845
137	1	-3.39639	-4.72114	3.061826

7. Biological assay

7.1 Materials

7.1.1 Culture of cells

The murine macrophage cell line RAW 264.7 was sourced from the American Type Culture Collection (ATCC, Manassas, VA), while the Human hepatic stellate cell line LX-2 was purchased from Fuheng Biology (Fuheng, Hunan, China). The cells were grown in Dulbecco′s Modified Eagle Medium (DMEM, Gibco, Cat#11965092, USA) supplemented with 10% (*v/v*) fetal bovine serum (Invitrogen) and 1% (*v/v*) penicillin/streptomycin (Gibco), and maintained at 37 °C in a humidified incubator with an atmosphere of 5% CO_2.

For in vitro experiments, compounds were dissolved in DMSO and further diluted to the required concentration. LX-2 were trypsinized and seeded at 2.5×10^5 cells/well into 6-well plates. At the same time, we treated LX-2 cells with 10 ng/mL TGF-β1 and different concentrations of compounds for 48 h. After that, samples were collected from each group for subsequent experiments.

7.1.2 Culture of zebrafish embryos

Wild-type and transgenic line Tg (*corolla*: GFP; *Lyz*: DsRed) zebrafish were provided by professor Wenqing Zhang (South China University of Technology). Zebrafish cultured in an experimental culture system (Shanghai Haisheng) were placed in the oviposition tank with a female-to-male ratio of 1:2 or 1:1 in the evening with the separator placed. The separator was removed on the next morning, and embryos were collected after nearly 30 min of chase between the female and male fish. Then the embryos were washed and placed in Petri dishes and incubated in an incubator (Shanghai Zhicheng) at 28 ^oC.

7.1.3 Reagents

Copper (II) sulfate pentahydrate was purchased from Guangzhou Chemical Reagent Factory (Guangzhou, China). LPS, Tricaine and Thioacetamide (TAA) were purchased from Sigma Aldrich (St. Louis, USA). Dexamethasone Sodium Phosphate Injection (DEX) was purchased from Guangzhou Baiyunshan Tianxin Pharmaceutical (Guangzhou, China). Silymarin was purchased from MedChemExpress (USA). TRIzolTM reagent was purchased from Invitrogen (Leicestershire, United Kingdom). ReverTra Ace® qPCR RT Kit was purchased from TOYOBO (Osaka, Japan).

7.2 Methods

7.2.1 *In vitro* anti-inflammatory assay

5×10^4 cells/well RAW 264.7 macrophage cells were cultured in a 96-well plate for 24 h and then treated with different compounds in the presence or absence of LPS (1 μg/mL) for another 24 h. The secretion of IL-6 and TNF-α were quantified with ELISA kits according to the manufacturers′ protocol[3].

Table S13 The anti-inflammatory effects of **2**–**6** on LPS-induced RAW264.7 cells.

No.	Concertration	TNF-α (%)	IL-6 (%)
LPS	100 ng/mL	100	100
2	10 μM	73.49 ± 0.01***	73.49 ± 0.01***
	5 μM	–	83.57 ± 0.02***
3	5 μM	56.13 ± 0.03***	21.72 ± 0.04***
	2.5 μM	73.84 ± 0.04***	66.21 ± 0.03***
4	5 μM	53.78 ± 0.02***	59.37 ± 0.01***
	2.5 μM	73.54 ± 0.02***	73.75 ± 0.01***
5	10 μM	66.96 ± 0.05***	57.34 ± 0.02***
	5 μM	88.93 ± 0.02***	69.96 ± 0.01***
6	10 μM	77.01 ± 0.00***	51.50 ± 0.01***
	5 μM	91.99 ± 0.02***	64.20 ± 0.01***

Note: The generation of TNF-α and IL-6 was considered as 100%. ***$P < 0.001$, v.s. LPS.

7.2.2 *In vivo* anti-inflammatory assay

(1) Determination of embryo survival

Zebrafish at 72 hours post fertilization (hpf) were randomly placed in 12-well plates with 20 fish/well and 2 mL of egg water, then different concentrations of compound **3** (300, 200 and 100 μM) was added to the wells, and 2 mL of egg water was added to the control group. The embryo survival was recorded every 24 h and the dead embryos were discarded in time. This process lasted for 72 h.

(2) $CuSO_4$ inflammation model

Zebrafish at 72 hpf were randomly placed in 12-well plates with 20 fish in each well. Zebrafish in drug groups were treated with compound **3** at different concentrations (300, 200 and 100 μM) in the presence of 20 μM $CuSO_4$ [4]. Zebrafish in the positive group were treated with 2 ml of egg water containing 4 μg/mL DEX and 20 μM $CuSO_4$. Zebrafish in the model group were treated with 2 ml of egg water containing 20 μM $CuSO_4$ and zebrafish in the control group were treated with the same volume of egg

water. After 2 h, the migration of neutrophils in zebrafish was observed under a fluorescence microscope (Olympus, Japan) and photographed for statistical analysis.

(3) Tail transection inflammation model

Zebrafish at 72 hpf were anesthetized with 1% Tricaine and placed on a slide, then the tail fins were cut off quickly at the same position in all groups except the control group[5]. Zebrafish in drug groups were added with 2 ml of egg water containing compound **3** at the dosages of 100, 200 and 300 μM, respectively. Zebrafish in the positive drug group were added with 2 ml of egg water containing 4 μg/mL DEX. Zebrafish in the model group and the control group were added with 2 ml of egg water. After 4 h treatment, the migration of neutrophils in zebrafish was observed under a fluorescence microscope (Olympus, Japan) and photographed for statistical analysis.

(4) LPS-Microinjection inflammation model

Zebrafish at 72 hpf were anesthetized with 1% Tricaine and placed on 1% agar plates. Zebrafish in the control group was microinjected with 2 nL of PBS and in the other groups were injected with 2 nL of LPS (5 mg/mL)[6]. Treatment was performed according to the same group assignment as described above, and photographs were taken 12 h later.

(5) H&E staining and Survival analysis

After LPS-microinjection and treated with compound **3** for 12 h, zebrafish were fixed with 4% paraformaldehyde at room temperature for 24 h and then wrapped in mirror paper for routine dehydration. Dehydrated zebrafish were embedded in paraffin at 65 ^{o}C, sectioned with a paraffin microtome, and finally stained with H&E dyes[6]. The stained slides were dropped and sealed with neutral gum. When the slides were dried, the infiltration of inflammatory cells in the yolk sac of the zebrafish was observed by a KF-PRO digital pathology slide scanner (Ningbo Jiangfeng). The survival of embryos was also observed for 96 h and recorded every 24 h after LPS-microinjection and treated with compound **3** for 12 h[6].

7.2.3 *In vitro* anti-fibrotic assay

(1) CCK-8 assay

LX-2 cells were seeded in 96-well plates. After attachment, LX-2 cells were treated with different concentrations of compounds for 24 h. Then, 10 μL of CCK-8 solution were added to each well and incubated at 37 ℃ with 5% CO_2 for 2 h. The absorbance was read at a wavelength of 450 nm using a microplate reader.

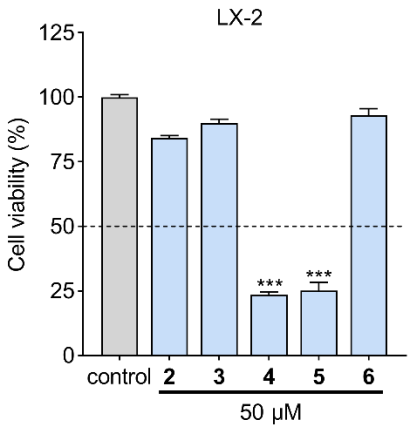

Fig. S8. The effects of **2**−**6** on the proliferation of LX-2 cells.

(2) Quantitative real-time PCR

LX-2 cells were treated with 10 ng/mL TGF-β1 and different concentrations of compounds for 48 h. After 48 h, samples were collected from each group for subsequent experiments.

(3) Western blot analysis

The cells were washed with cold PBS and subsequently lysed in RIPA buffer (Beyotime, China) with protease inhibitor (Roche, Swiss) for 30 min at 4 ℃, and then centrifuged (14000 rpm, 15 min, 4 ℃) to take the supernatant. The concentration of total protein was measured by a BCA kit (Beyotime, China). Then, the proteins were boiled for 10 min at 80 ℃ after addition of 5× loading buffer and subjected to 10% SDS-PAGE and electrophoretically transferred to PVDF membranes (Roche, Swiss). After incubation in 5% nonfat milk for 1 h at room temperature, the membranes were incubated overnight with the primary antibodie Fibronectin (abmart, China) at 1:1000 dilution at 4 ℃ and then incubated with horseradish peroxide (HRP)-conjugated secondary antibodies at 1:10000 dilution for 1 h at room temperature. The protein bands were detected by an enhanced chemiluminescence reagent (ECL) kit (Thermo Fisher Scientific, USA).

(4). Immunofluorescence assay

LX-2 cells were incubated with or without TGF-β1 (10 ng/mL), followed by the addition of Hydronidone (200 μM), 12.5 μM/25 μM/50 μM compound **3** or vehicle (DMSO) for 48 h. Then, cells were washed with PBS buffer and fixed with 4% paraformaldehyde (Biosharp, China) for 30 min at room temperature. Next, after washed with PBS for three times, the cells were permeabilization with 0.5% Triton X-100 (Beyotime, China) for 15 min and blocked with 5% BSA (Beyotime, China) for 1

h at room temperature, followed by incubation with the primary antibodies Fibronectin (abmart, 1:200, China) overnight at 4 ℃. The next day, Alexa 555 labeled anti-rabbit secondary antibody (red) (Proteintech, 1:1000, USA) was incubated at room temperature for 1 h. After three times PBS washing, the DAPI (Beyotime, China) was used for nuclear staining. The images were taken by laser scanning confocal microscope (Leica, Germany).

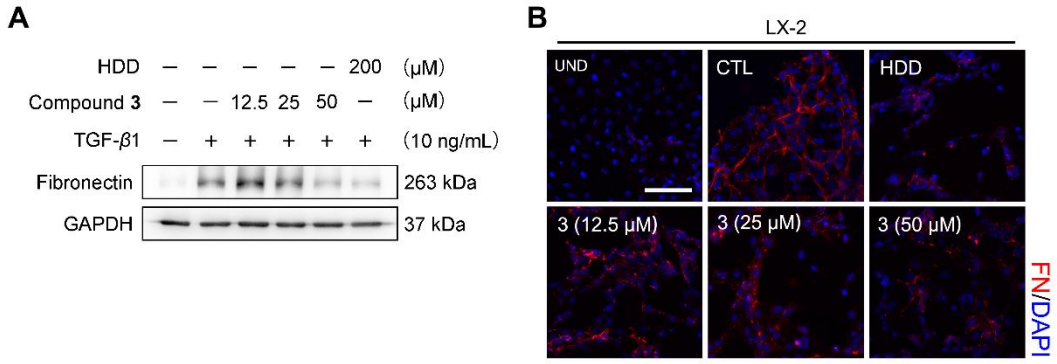

Fig. S9. Compound **3** reduced the protein expression of Fibronectin in the LX-2 cell. (A) Compound **3** suppressed the protein levels of Fibronectin in a dose-dependent manner in TGF-β1-stimulated LX-2 cells. (B) Immunostaining of Fibronectin (red) in LX-2 cells. TGF-β1-activated LX-2 cells were treated with vehicle, Hydronidone (HDD) or compound **3** for 48 h. Scale bar: 100 μm.

7.2.4 *In vivo* anti-fibrotic assay

Wild-type zebrafish at 2 dpf were randomly placed in 6-well plates with 30 fish in each well. Zebrafish in drug groups were treated with compound **3** at different concentrations (100, 200 and 300 μM) in the presence of 0.06% TAA until 9 dpf [7]. Zebrafish in the positive group were treated with 2 ml of egg water containing 20 μM Silymarin and 0.06% TAA. The treated zebrafish were collected and routinely dehydrated. After dehydration, zebrafish were embedded in paraffin and sectioned with a paraffin microtome. Paraffin sections stained with H&E dyes to observe the fibrosis of zebrafish liver.

7.2.5 Statistical analysis

The experimental data were analyzed by Graph Pad Prism 5.0. Kaplan-Meier method was used for survival analysis, and Log rank test was used for comparison between groups. One-way ANOVA and Turkey Post *hoc* test were used to analyze the means of

multiple samples. All experimental data are presented as SEM. When $P<0.05$ the difference was considered statistically significant.

8. Synthetic experimental procedures of compound 3 from 14-OH-gelsenicine (8).

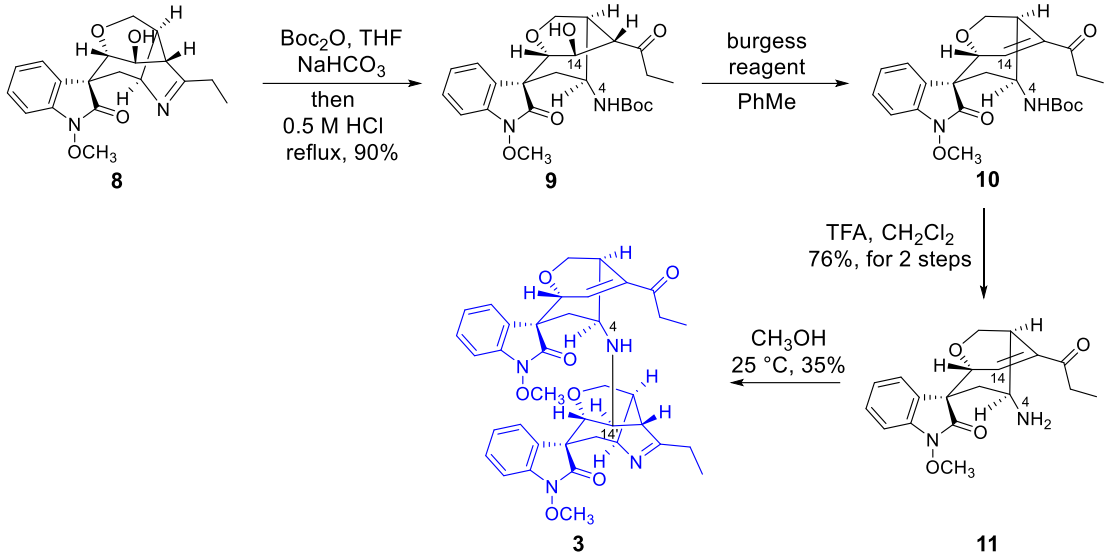

8.1 Synthesis of compound 9.

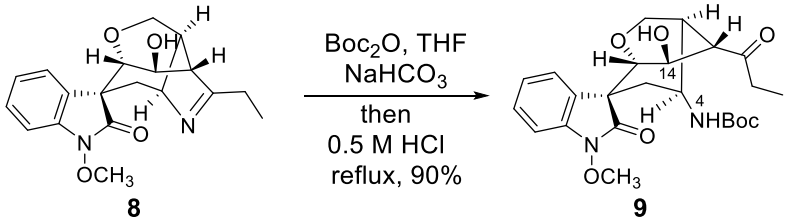

Boc_2O (2.18 g, 100 mmol, 100 equiv.) was added to a solution of 14-OH-gelsenicine (**8**) (342 mg, 1 mmol) and $NaHCO_3$ (840 mg, 10 mmol, 10 equiv.) in THF (10 mL). This solution was stirred for overight and HCl (25 mL, 0.5 M) was solwly added. The mixture was warmed up to reflux. Upon completion of the reaction, as determined by TLC, it was quenched with saturated aqueous sodium bicarbonate and extracted with dichloromethane. The combined organic layers were dried over Na_2SO_4, filtered and concentrated *in vacuo*. The crude residue was purified by silica gel column chromatography (1%-10% CH_2Cl_2-CH_3OH) to afford compound **9** (414 mg, 90%): yellow oil; $[\alpha]_D^{25}$ –140.5 (c = 1.0, CH_3CN); **IR** (KBr) ν_{max} 3403, 2980, 2939, 2881, 1709, 1620, 1503, 1462, 1393, 1367, 1317, 1242, 1201, 1173, 1132, 1078, 997, 957, 839, 750 cm^{-1}; **^{1}H NMR** (400 MHz, $CDCl_3$) δ 7.42 (d, J = 7.6 Hz, 1H), 7.28 (dd, J = 7.6, 7.6 Hz, 1H) , 7.07 (dd, J = 7.6, 7.6 Hz, 1H), 6.95 (d, J = 7.6 Hz, 1H), 5.77 (d, J = 8.1 Hz, 1H),

5.28 (d, *J* = 5.0 Hz, 1H), 4.20 (m, 1H), 4.17 (d, *J* =10.3 Hz, 1H), 4.09 (d, *J* = 10.3 Hz, 1H), 3.91 (s, 3H), 3.67 (br s, 1H), 3.64 (s, 1H), 2.86 (br s, 1H), 2.73~2.78 (overlapped, 3H), 1.80 (t, *J* = 13.3 Hz, 1H), 1.55 (d, *J* = 13.3 Hz, 1H), 1.38 (s, 9H), 1.12 (t, *J* = 7.4 Hz, 3H); **^{13}C NMR** (100 MHz, $CDCl_3$) δ 212.9, 172.2, 155.1, 138.6, 128.5, 127.0, 127.0, 123.6, 107.5, 79.6, 78.3, 69.9, 65.6, 63.5, 56.3, 52.2 (2C), 39.8, 34.4, 33.8, 28.5 (3C), 8.1; HR-ESI-MS *m/z* 461.2289 $[M+H]^+$ (calcd for $C_{24}H_{33}H_2O_7$: 461.2282).

8.2 Synthesis of compound 11.

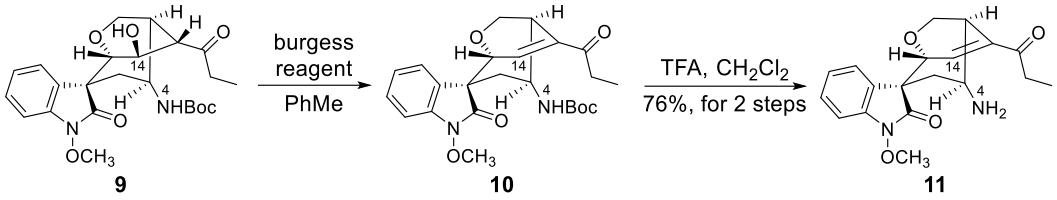

Burgess reagent (142.8 mg, 0.6 mmol, 1.2 equiv.) was added to a solution of **9** (230 mg, 0.5 mmol, 1.0 equiv.) in PhMe (5 mL). The solution was warmed up to reflux. Upon completion of the reaction, as determined by TLC, it was quenched with saturated aqueous sodium bicarbonate and extracted with dichloromethane. The combined organic layers were dried over Na_2SO_4, filtered and concentrated *in vacuo* to yield curde **10**. To a solution of curde **10** in CH_2Cl_2 (5 mL) was added trifluoroacetic acid (TFA; 1 mL, 5 equiv) was added. Upon completion of the reaction, as determined by TLC, it was quenched with saturated aqueous sodium bicarbonate and extracted with dichloromethane. Next, the combined organic layers were dried over Na_2SO_4, filtered and concentrated *in vacuo*. The crude residue was purified by silica gel column chromatography (2%-10% CH_2Cl_2-CH_3OH) to afford compound **11** (130 mg, 76%): yellow amorphous powder; $[\alpha]_D^{25}$ –153.0 (*c* = 1.43, CH_3OH); **IR** (KBr) ν_{max} 3428, 2935, 2873, 1722, 1674, 1615, 1460, 1383, 1321, 1234, 1190, 1112, 1069, 1042, 745 cm^{-1}; **^{1}H NMR** (500 MHz, CD_3OD) δ 7.51 (d, *J* = 7.7 Hz, 1H), 7.42 (overlapped, 1H), 7.38 (overlapped, 1H), 7.18 (ddd, *J* = 7.7, 7.7, 1.0 Hz, 1H), 7.12 (d, *J* = 7.7 Hz, 1H), 4.29 (d, *J* = 6.2 Hz, 1H), 4.24 (m, 1H), 4.02 (s, 3H), 3.59 (dd, *J* = 9.3, 2.9 Hz, 1H), 3.43 (overlapped, 1H), 3.41 (overlapped, 1H), 3.02 (m, 1H), 2.90 (m, 1H), 1.66 (m, 1H), 1.74 (m, 1H), 1.21 (t, *J* = 7.3 Hz, 1H); **^{13}C NMR** (125 MHz, CD_3OD) δ 201.6, 173.4, 140.7, 140.5, 138.3, 129.7, 128.4, 127.9, 124.3, 108.6, 72.8, 68.8, 64.1, 54.5, 50.7, 41.8, 39.1, 31.2, 8.7; HR-ESI-MS *m/z* 343.1652 $[M+H]^+$ (calcd for $C_{19}H_{23}N_2O_4$: 343.1652).

8.3 Synthesis of compound 3.

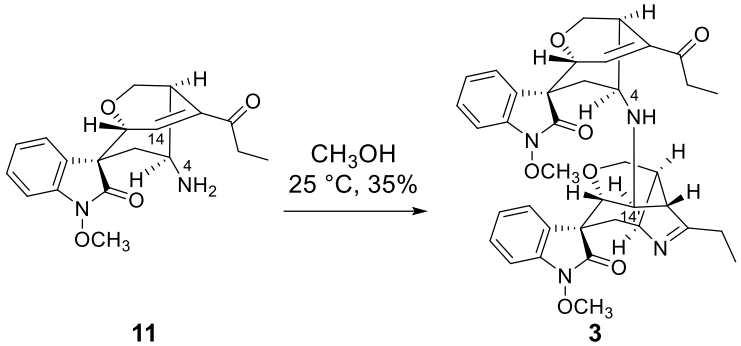

11 **3**

The solution of **11** (68.6 mg) in methanol (MeOH, 1 mL) was stirred at 25 ºC for 24 h. The mixture was directly concentrated *in vacuo* to yield curde **3**. The curde **3** was preparative HPLC ($CH_3CN/H_2O/Et_2NH$, 40:60:0.01) to afford compound **3** (23.3 mg, 35%): yellow amorphous powder; $[\alpha]_D^{25} = -133.4$ (*c* = 1.20, CH_3OH); **IR** (KBr) ν_{max} 3437, 2972, 2940, 2874, 1719, 1668, 1618, 1461, 1321, 1234, 1192, 1116, 1072, 1041, 748 cm^{-1}; **^{1}H NMR** (500 MHz, $CDCl_3$) δ 7.50 (d, *J* = 7.6 Hz, 1H), 7.33 (overlapped, 2H), 7.27 (overlapped, 2H), 7.07 (dd, *J* = 7.6, 7.6 Hz, 2H), 7.01 (d, *J* = 7.6 Hz, 1H), 6.89 (d, *J* = 7.6 Hz, 1H), 4.37 (m, 1H), 4.31 (dd, *J* = 10.9, 3.4 Hz, 1H), 4.21 (d, *J* = 6.1 Hz, 1H), 4.20 (d, *J* = 10.9 Hz,1H), 4.04 (d, *J* = 9.2 Hz, 1H), 3.99 (s, 3H), 3.89 (s, 3H), 3.62 (dd, *J* = 9.2, 3.1 Hz,, 1H), 3.61 (br s, 1H), 3.60 (br s, 1H), 3.44 (br s, 1H), 3.07 (dd, *J* = 11.3, 4.8 Hz, 1H), 2.85 (m, 1H), 2.71 (overlapped, 2H), 2.59 (d, *J* = 8.7 Hz, 1H), 2.48 (td, *J* = 8.7, 3.4 Hz, 1H), 2.43 (overlapped, 1H), 2.40 (dd, *J* = 15.5, 4.8 Hz, 1H), 2.26 (dd, *J* = 15.5, 1.9 Hz, 1H), 1.72 (dd, *J* = 13.8, 11.3 Hz, 1H), 1.57 (dd, *J* = 13.8, 4.8 Hz, 1H), 1.31 (t, *J* = 7.4 Hz, 1H), 1.07 (t, *J* = 7.3 Hz, 1H); **^{13}C NMR** (125 MHz, $CDCl_3$) δ 199.4, 182.1, 171.9, 171.3, 139.6, 139.5, 138.0, 136.6, 132.1, 128.7, 128.3, 127.0, 126.4, 124.8, 123.6, 123.3, 107.6, 106.9, 78.3, 72.0, 71.4, 68.1, 63.6, 63.4, 61.4, 54.7, 53.5, 53.3, 51.3, 49.5, 38.9, 37.4, 37.3, 36.9, 30.4, 25.9, 10.2, 8.5; HR-ESI-MS *m/z* 667.3126 $[M+H]^+$ (calcd for $C_{38}H_{43}N_4O_7$: 667.3126).

Table S14. NMR spectral data comparison of synthetic **3** and the natural product in $CDCl_3$ (δ in ppm, J in Hz)[a]

no.	^{1}H			^{13}C		
	natural **3**	synthetic **3**	error	natural **3**	synthetic **3**	error
2	-	-	-	171.9	171.9	0
3	4.21 (d, 6.1)	4.21 (d, 6.1)	0	71.4	71.4	0
5	3.07 (dd, 11.3, 4.8)	3.07 (dd, 11.3, 4.8)	0	53.5	53.5	0
6	1.72 (dd, 13.8, 11.3)	1.72 (dd, 13.8, 11.3)	0	37.3	37.3	0
	1.56 (dd, 13.8, 4.8)	1.57 (dd, 13.8, 4.8)	-0.01	-	-	-
7	-	-	-	53.3	53.3	0
8	-	-	-	127.0	127.0	0
9	7.33	7.33	0	126.4	126.4	0
10	7.07 (dd, 7.6, 7.6)	7.07 (dd, 7.6, 7.6)	0	123.3	123.3	0
11	7.33	7.33	0	128.7	128.7	0
12	7.01 (d, 7.6)	7.01 (d, 7.6)	0	107.6	107.6	0
13	-		-	139.6	139.6	0
14	7.27	7.27	0	136.6	136.6	0
	-	-	-	139.5	139.5	0
15	-	-	-	36.8	36.9	-0.1
16	3.45 (br s)	3.44 (br s)	0.01	68.1	68.1	0
17	3.62 (dd, 9.2, 3.1)	3.62 (dd, 9.2, 3.1)	0	-	-	-
	4.04 (d, 9.2)	4.04 (d, 9.2)	0	8.5	8.5	0
18	1.06 (t, 7.3)	1.06(t, 7.3)	0	30.4	30.4	0
19	2.85 (m)	2.85 (m)	0	-	-	-
	2.71	2.71	0	-	-	-
20	-	-	-	199.4	199.4	0
N-OMe	3.99 (s)	3.99 (s)	0	63.6	63.6	0
2′	-	-	-	171.3	171.3	0
3′	3.61 (br s)	3.61 (br s)	0	78.3	78.3	0
5′	4.36 (m)	4.37 (m)	-0.01	72.1	72.0	0.1
6′	2.39 (dd, 15.5, 4.8)	2.40 (dd, 15.5, 4.8)	-0.01	37.3	37.4	-0.1
	2.25 (dd, 15.5, 1.9)	2.26 (dd, 15.5, 1.9)	-0.01	-	-	-
7′	-	-	-	54.7	54.7	0
8′	-	-	-	132.2	132.1	0.1
9′	7.50 (d, 7.6)	7.50 (d, 7.6)	0	124.8	124.8	0
10′	7.07 (dd, 7.6, 7.6)	7.08 (dd, 7.6, 7.6)	-0.01	123.5	123.6	-0.1
11′	7.27	7.27	0	128.2	128.3	-0.1
12′	6.89 (d, 7.6)	6.89 (d, 7.6)	0	106.9	106.9	0
13′	-	-	-	138.0	138.0	0
14′	3.59 (br s)	3.60 (br s)	-0.01	51.3	51.3	0
15′	2.59 (d, 8.7)	2.59 (d, 8.7)	0	49.5	49.5	0
16′	2.47 (td, 8.7, 3.4)	2.48 (td, 8.7, 3.4)	-0.01	38.9	38.9	0
17′	4.31 (dd, 10.9, 3.4)	4.31 (dd, 10.9, 3.4)	0	61.4	61.4	0
	4.20 (d, 10.9)	4.20 (d, 10.9)	0	-	-	-
18′	1.31 (t, 7.4)	1.31 (t, 7.4)	0	10.2	10.2	0
19′	2.71	2.71	0	25.9	25.9	0
	2.42	2.43	-0.01	-	-	-
20′	-	-	-	181.8	182.1	-0.3
N-OMe′	3.88 (s)	3.89 (s)	-0.01	63.4	63.4	0

[a] Overlapped signals were reported without designating multiplicity.

9. UV, IR, HRESIMS, 1D, and 2D NMR spectra of 1–6.

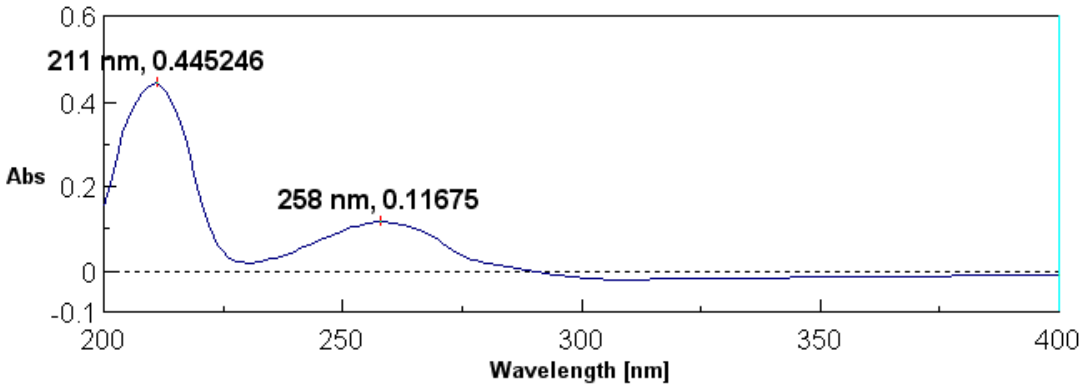

Fig. S9. UV spectrum of **1**

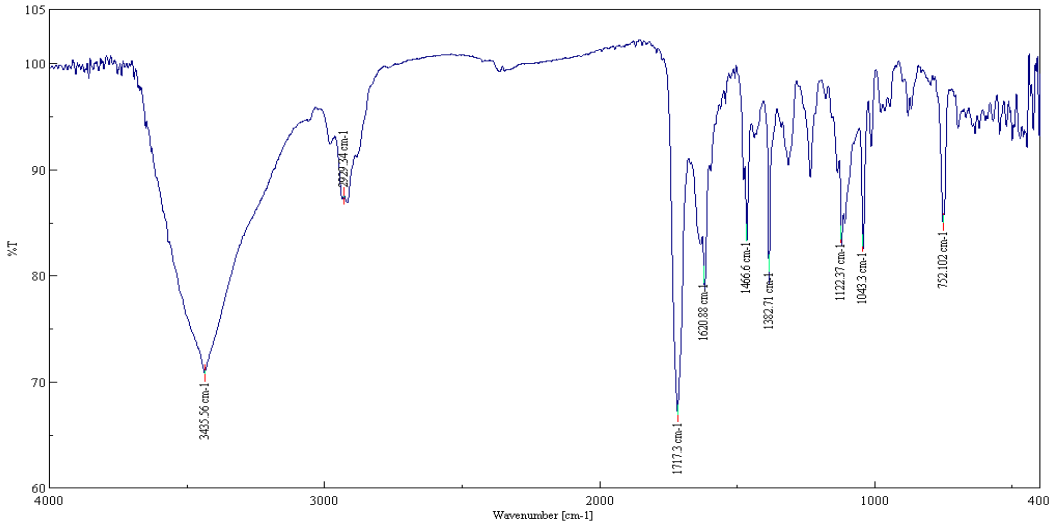

Fig. S10. IR (KBr disc) spectrum of **1**

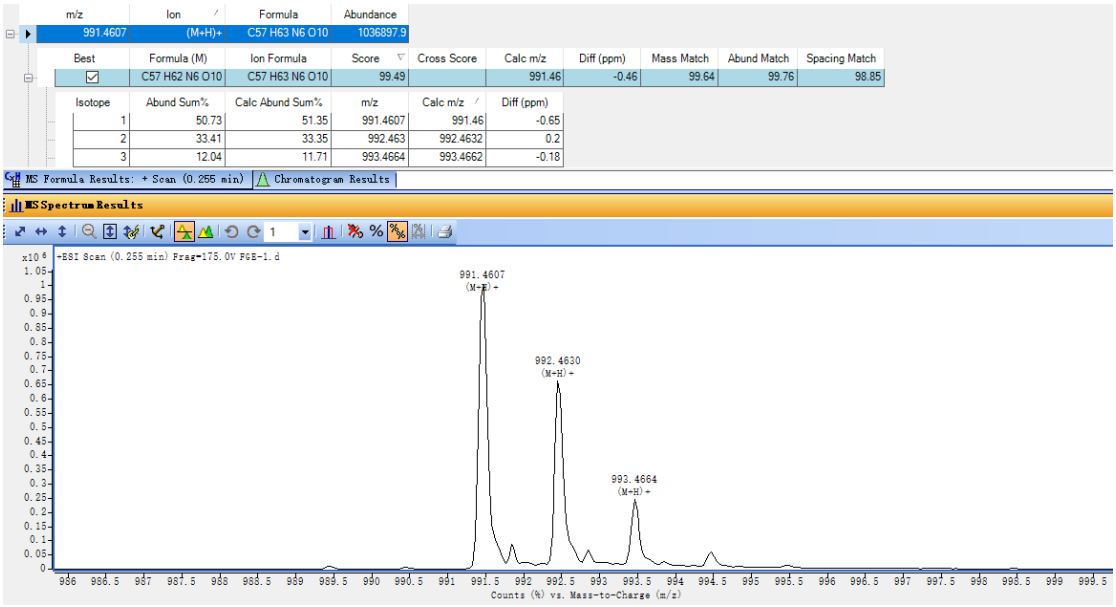

Fig. S11. HR-ESI-MS spectrum of **1**

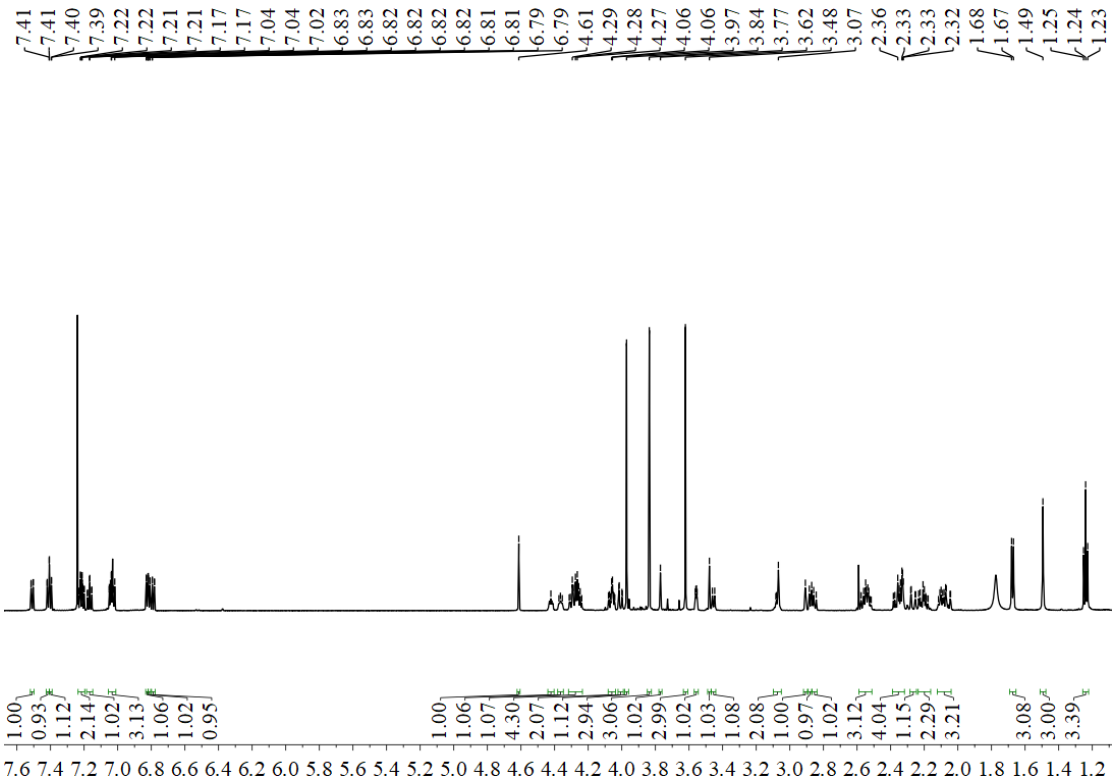

Fig. S12. ^{1}H NMR spectrum of **1** in $CDCl_3$ (500 MHz)

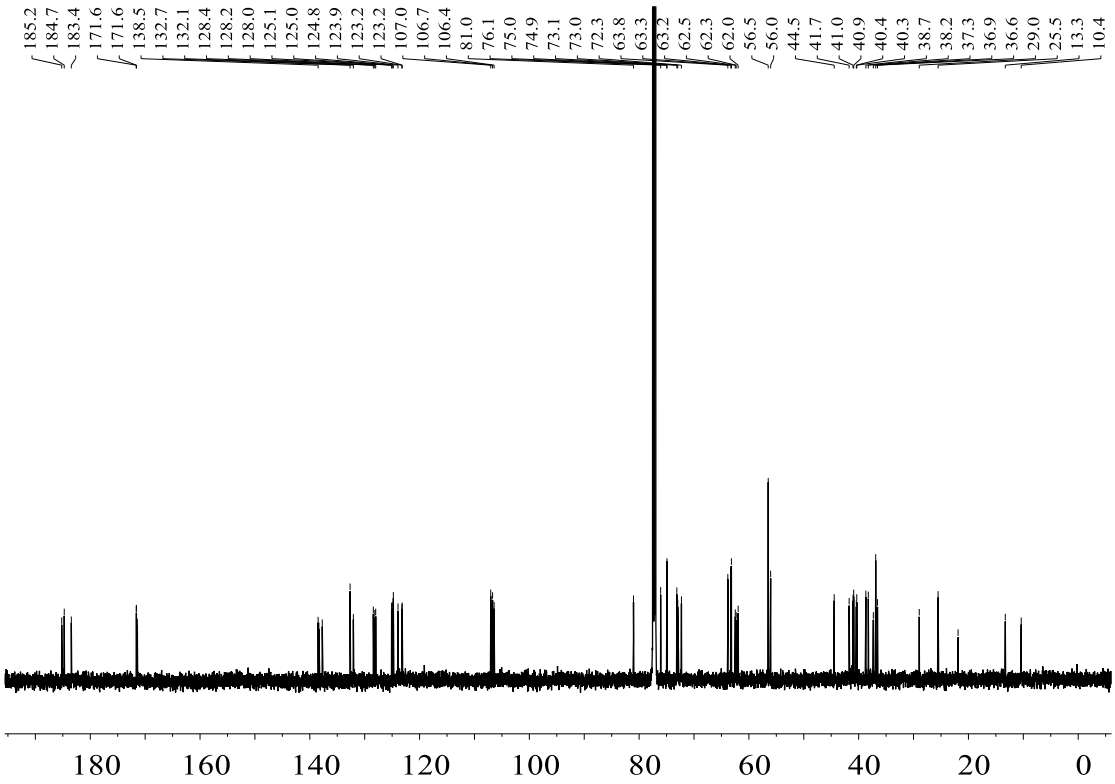

Fig. S13. ^{13}C NMR spectrum of **1** in $CDCl_3$ (125 MHz)

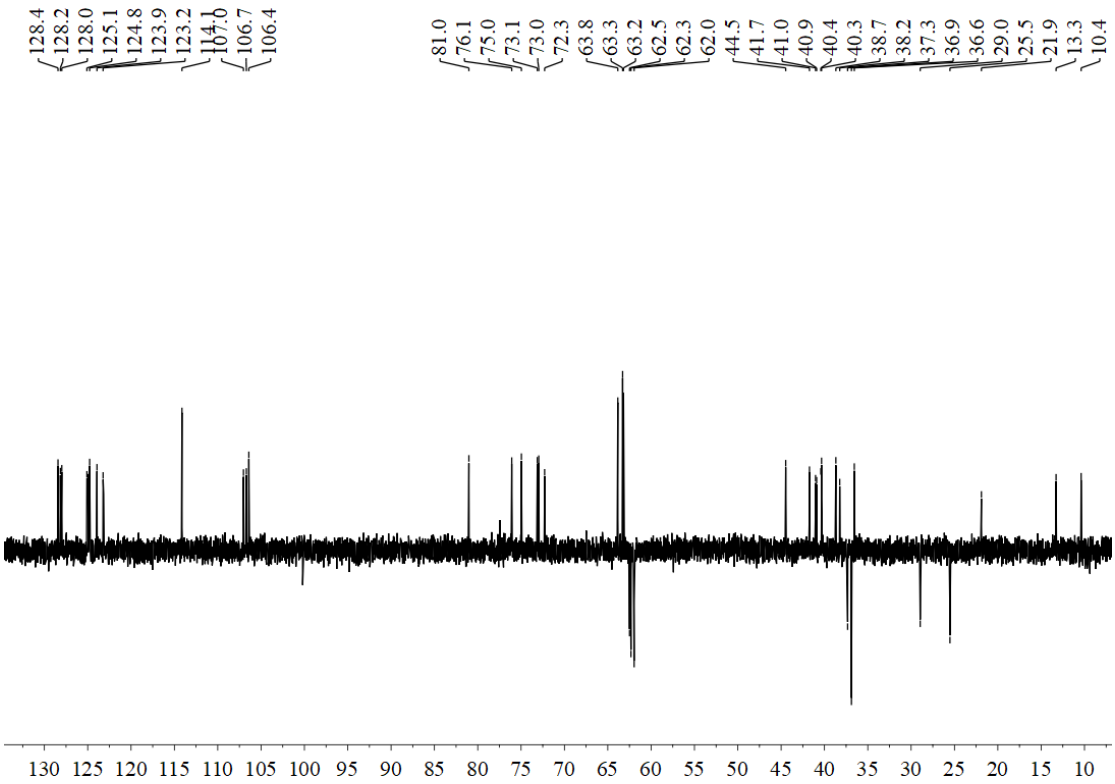

Fig. S14. DEPT-135 spectrum of **1** in $CDCl_3$

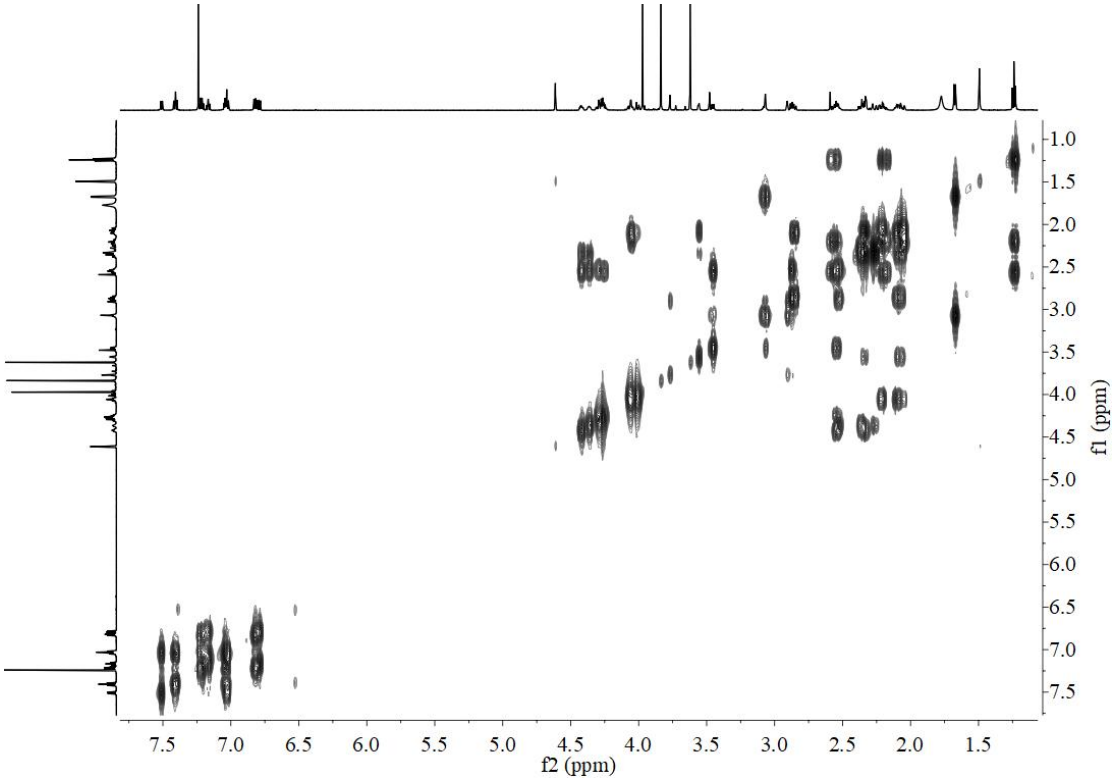

Fig. S15. ^{1}H-^{1}H COSY spectrum of **1** in $CDCl_3$

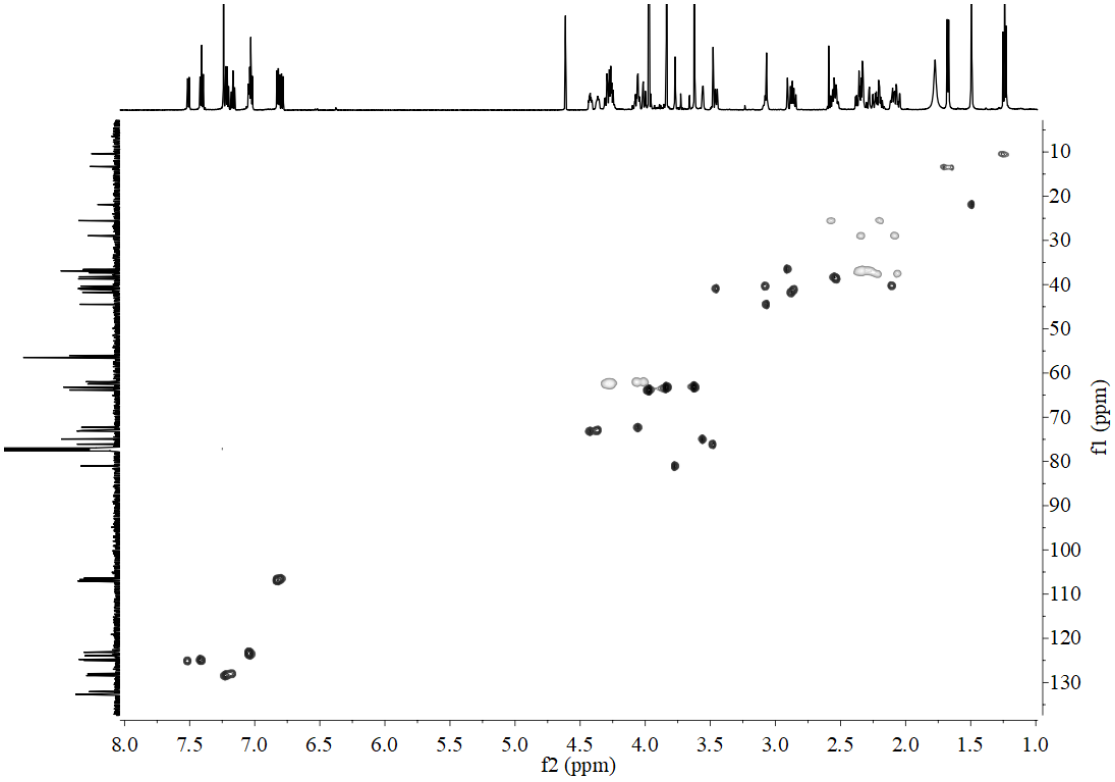

Fig. S16. HSQC spectrum of **1** in $CDCl_3$

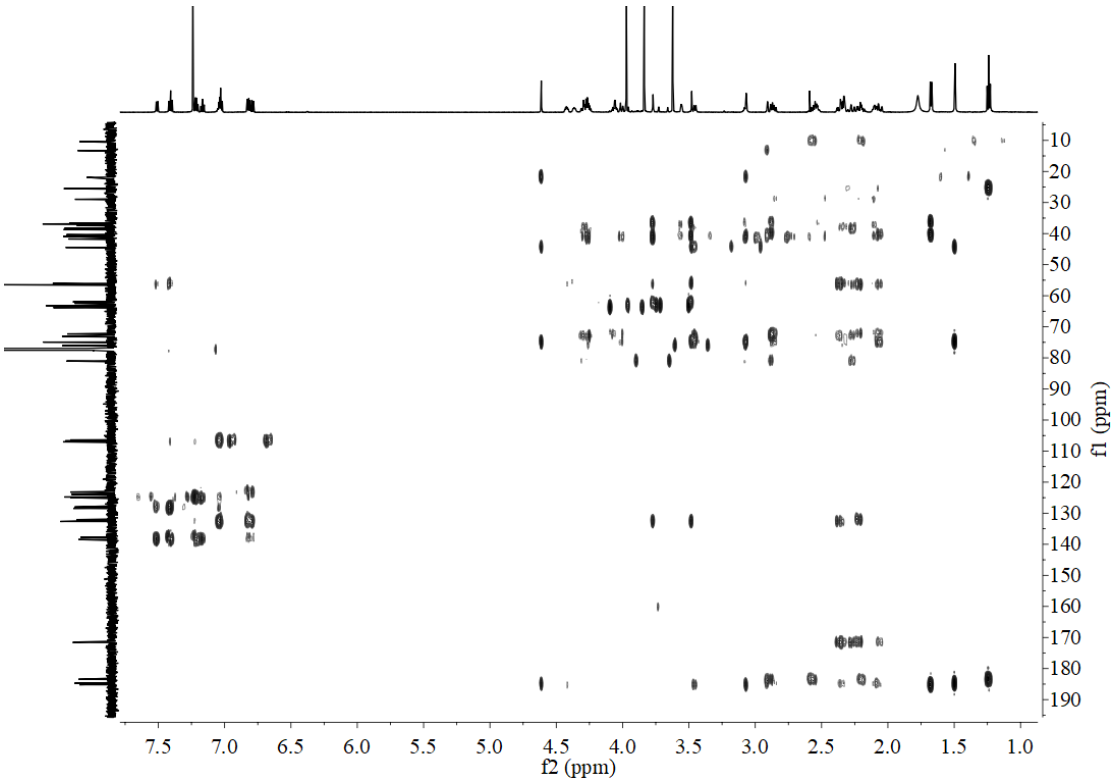

Fig. S17. HMBC spectrum of **1** in $CDCl_3$

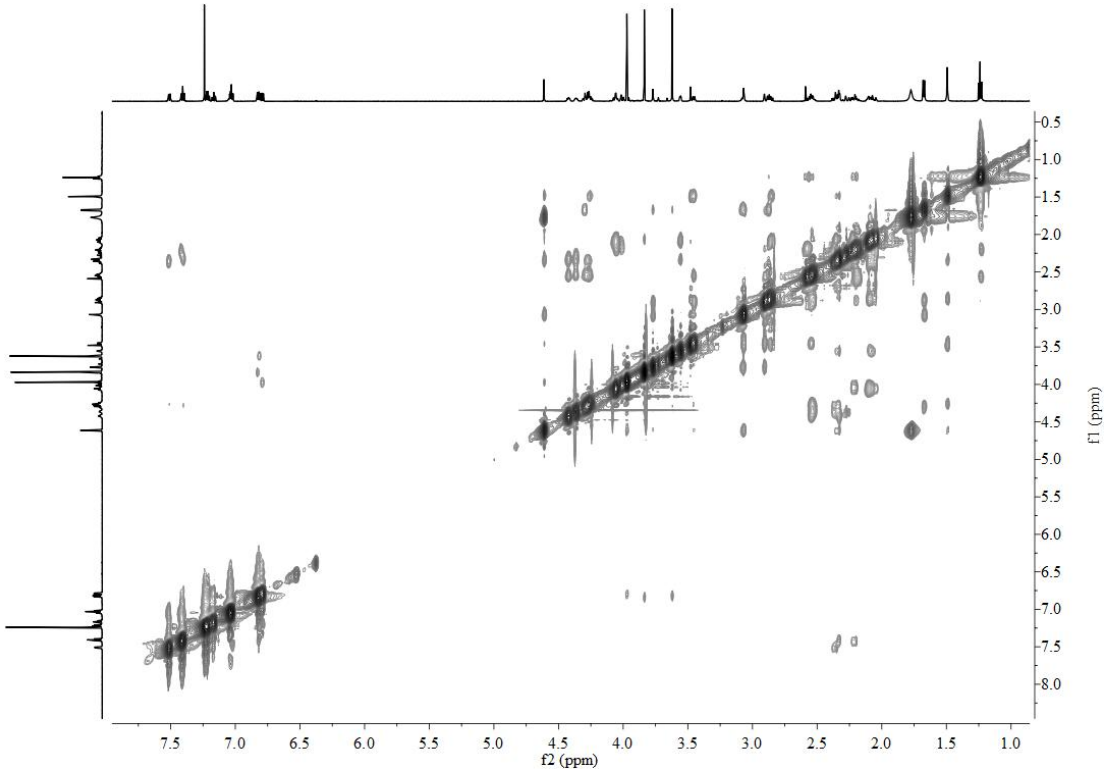

Fig. S18. NOESY spectrum of **1** in $CDCl_3$

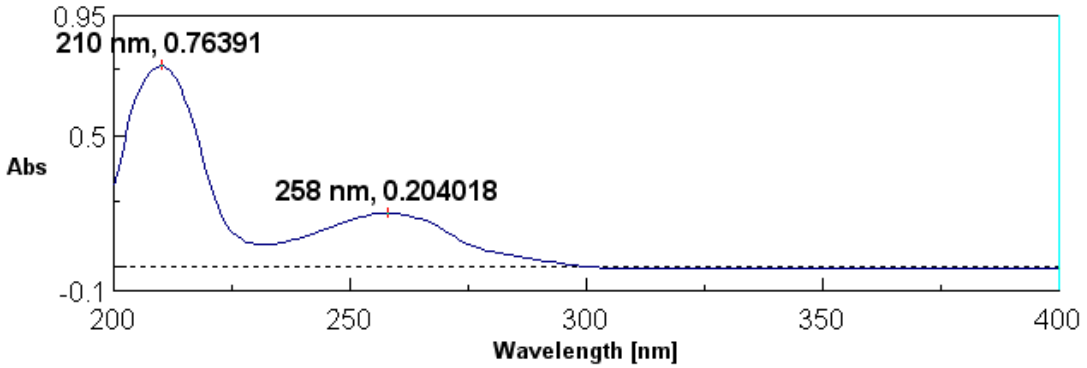

Fig. S19. UV spectrum of **2**

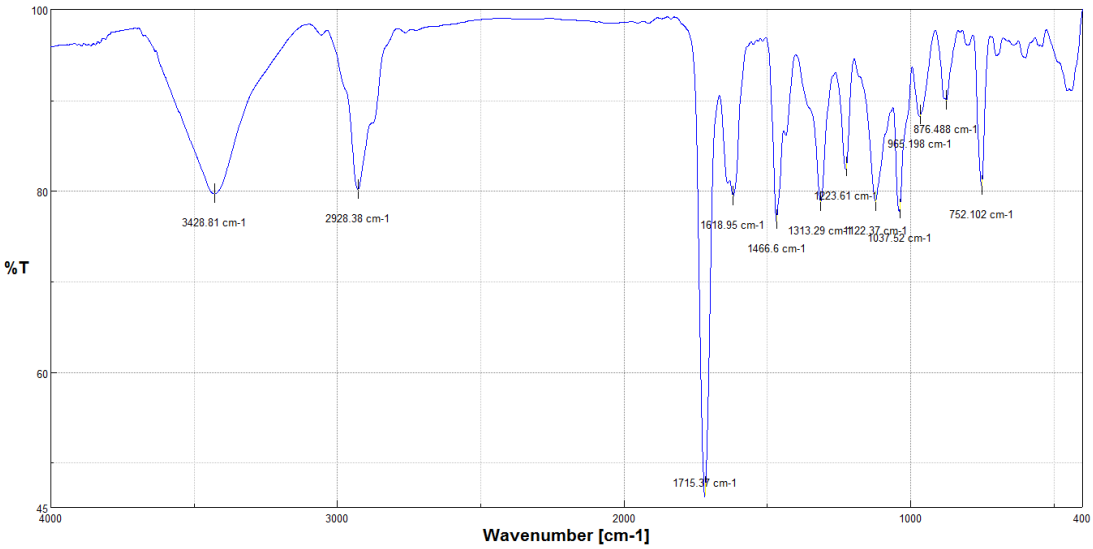

Fig. S20. IR (KBr disc) spectrum of **2**

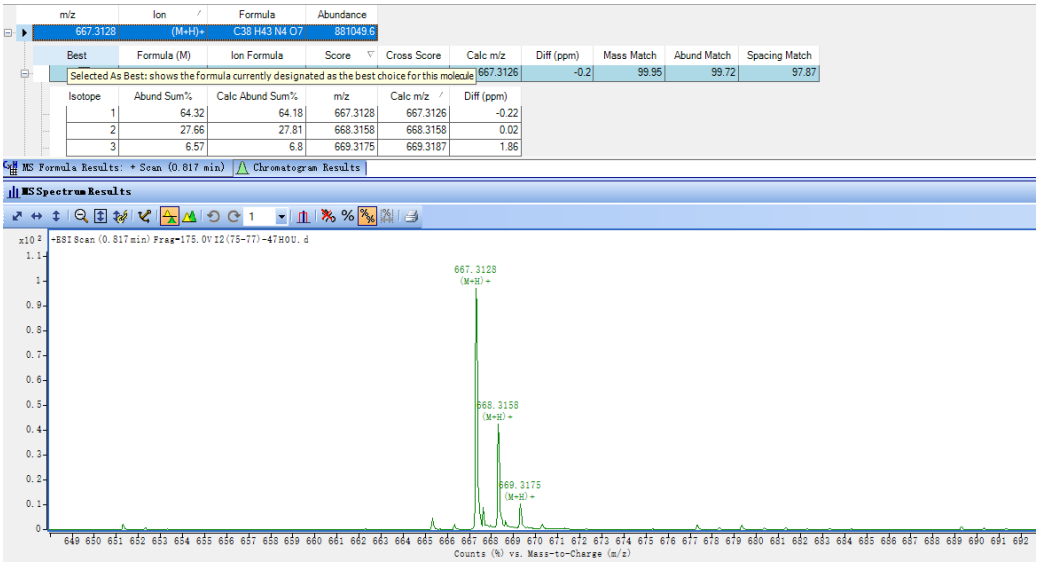

Fig. S21. HR-ESI-MS spectrum of **2**

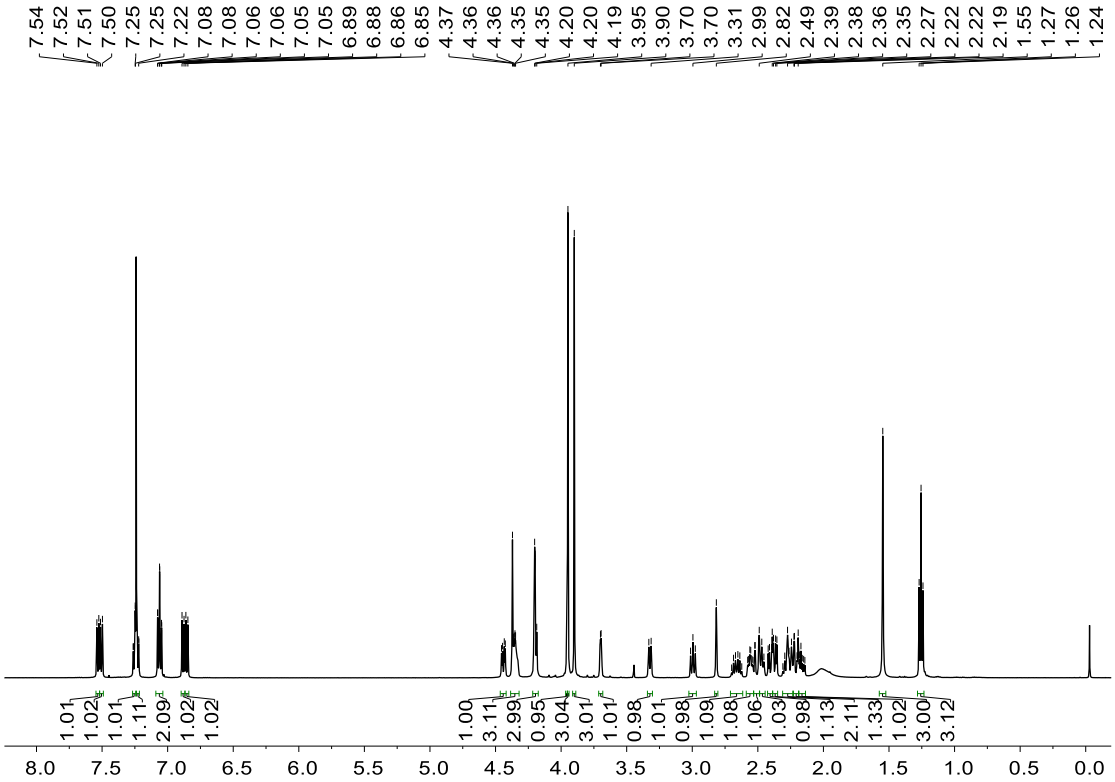

Fig. S22. ^{1}H NMR spectrum of **2** in $CDCl_3$

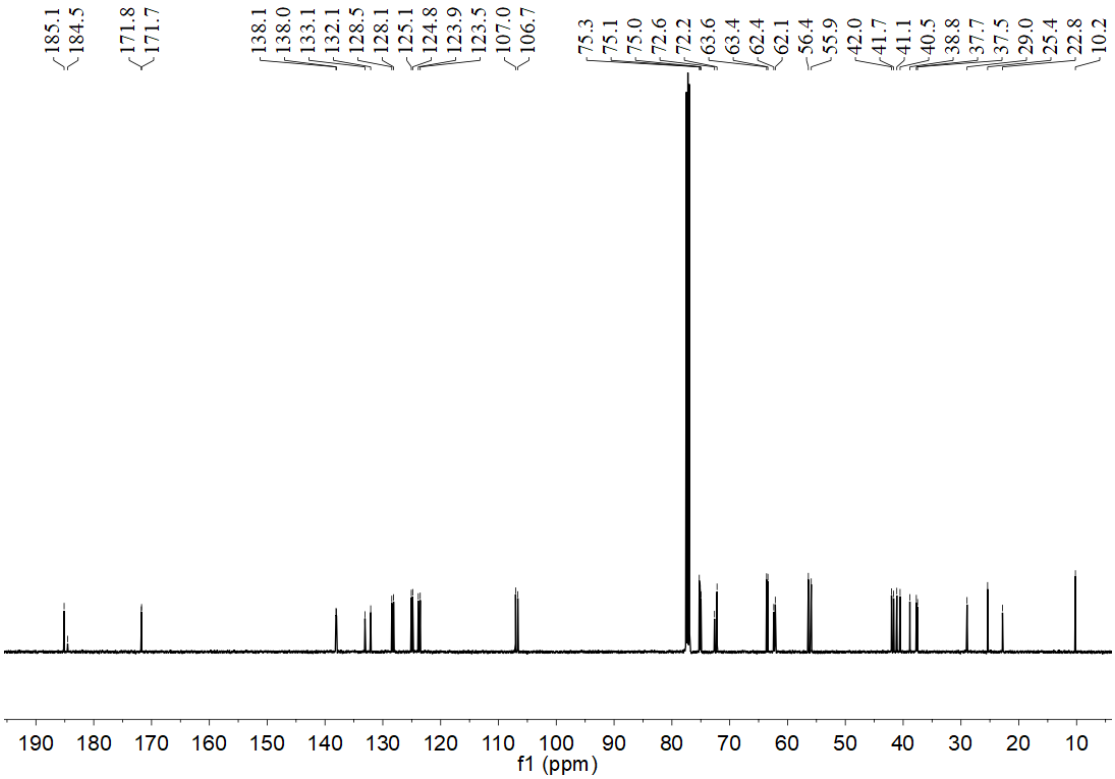

Fig. S23. ^{13}C NMR spectrum of **2** in $CDCl_3$

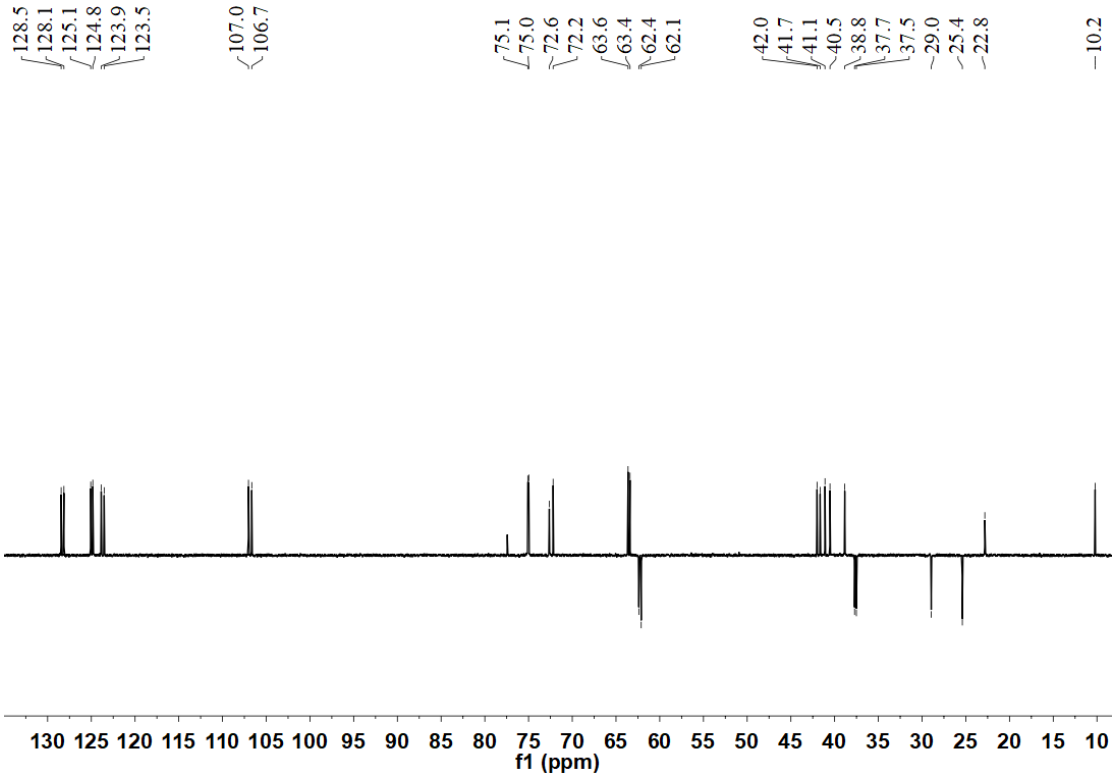

Fig. S24. DEPT-135 spectrum of **2** in $CDCl_3$

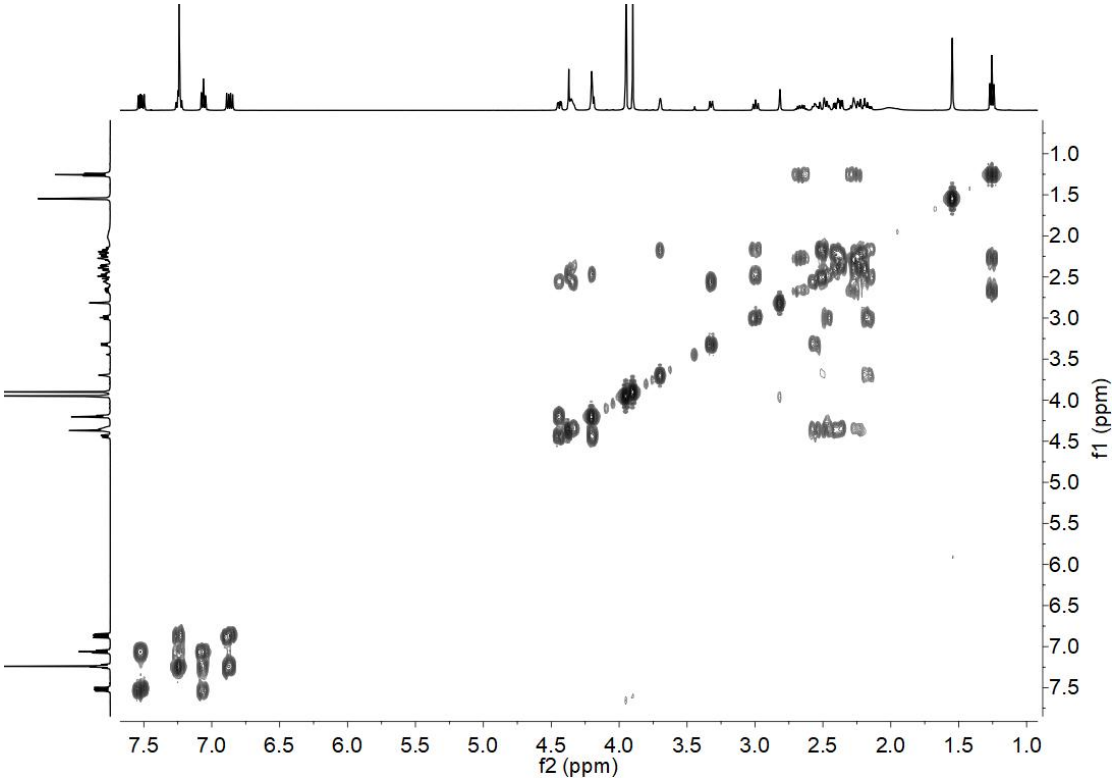

Fig. S25. ^{1}H-^{1}H COSY spectrum of **2** in $CDCl_3$

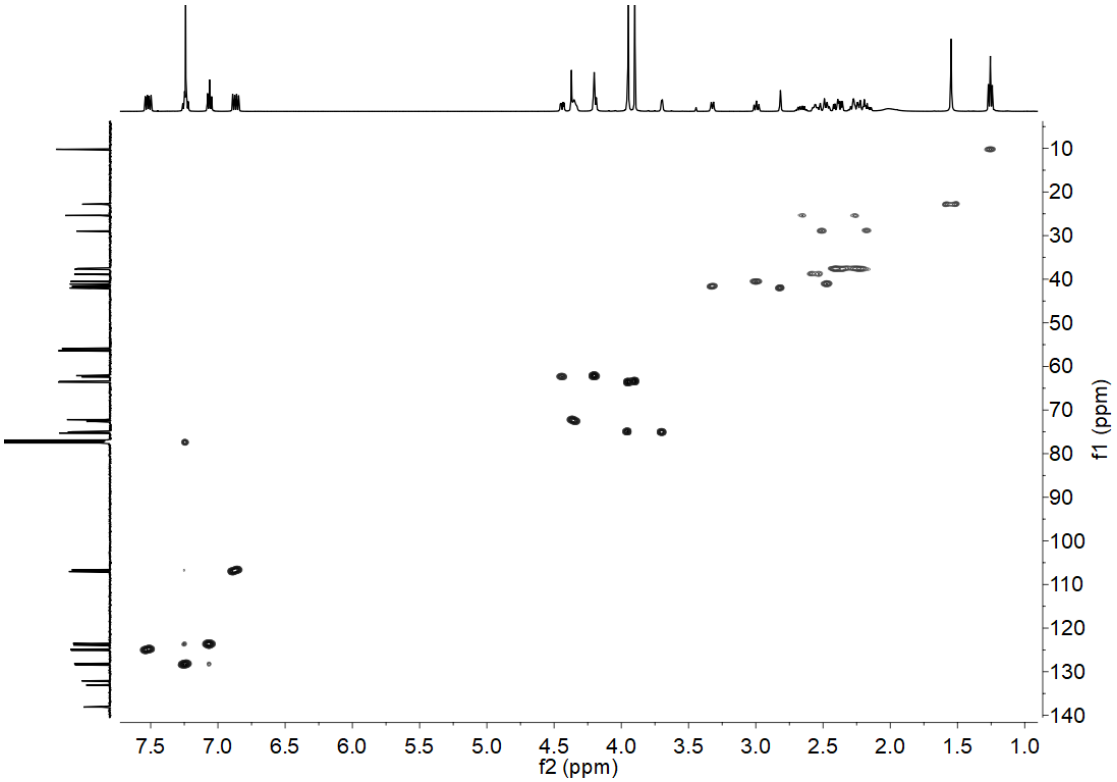

Fig. S26. HSQC spectrum of **2** in $CDCl_3$

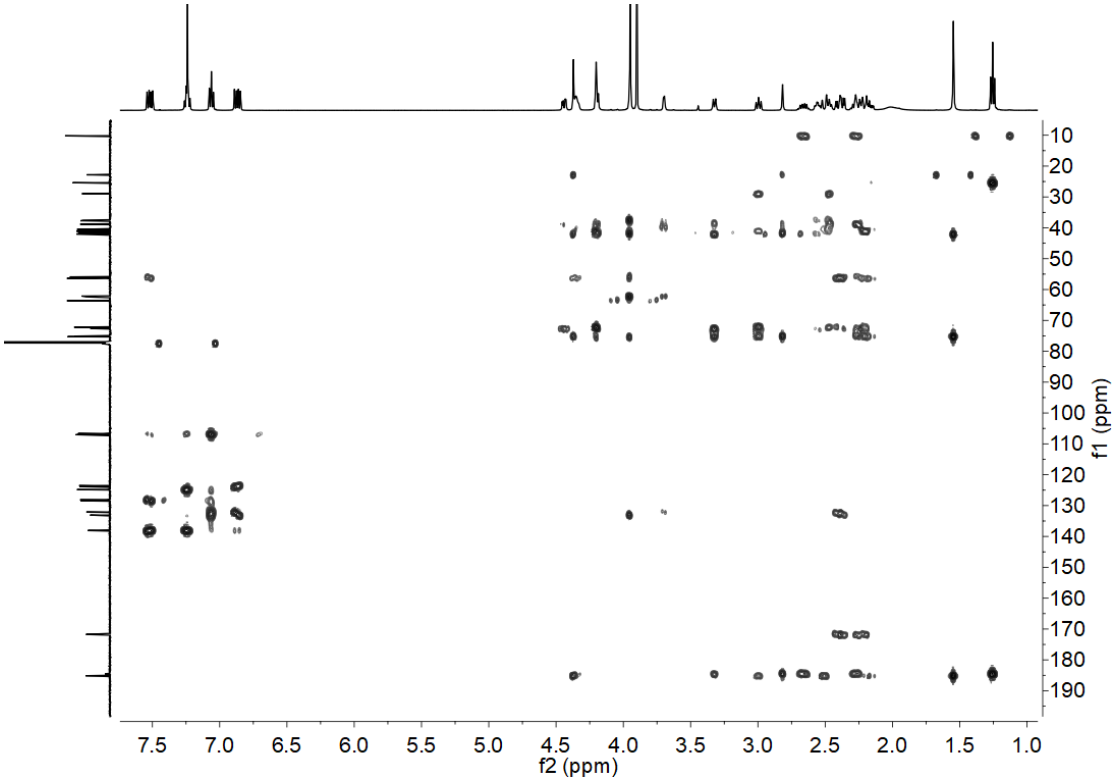

Fig. S27. HMBC spectrum of **2** in $CDCl_3$

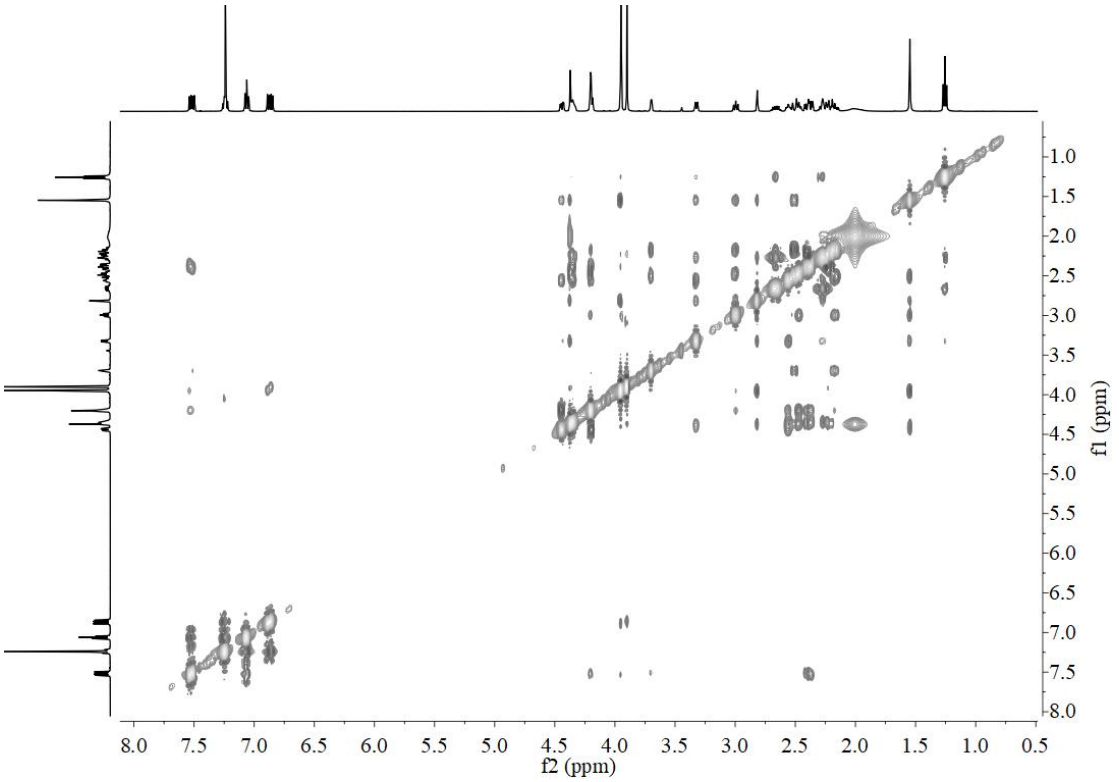

Fig. S28. NOESY spectrum of **2** in $CDCl_3$

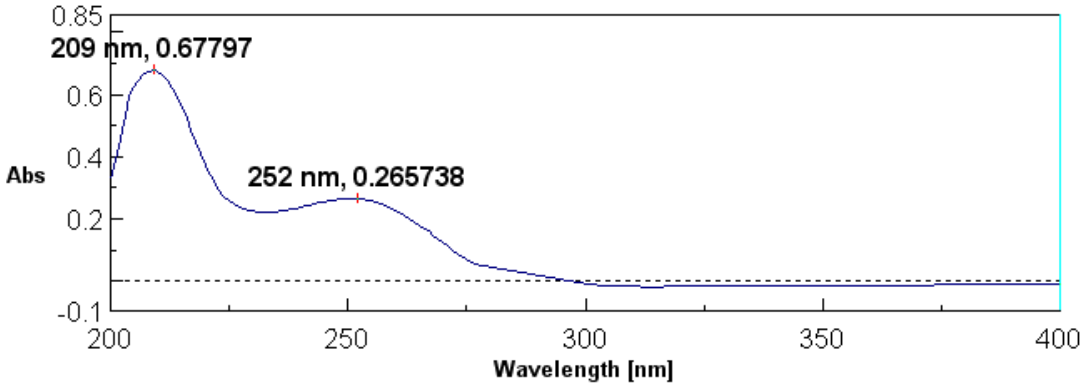

Fig. S29. UV spectrum of **3**

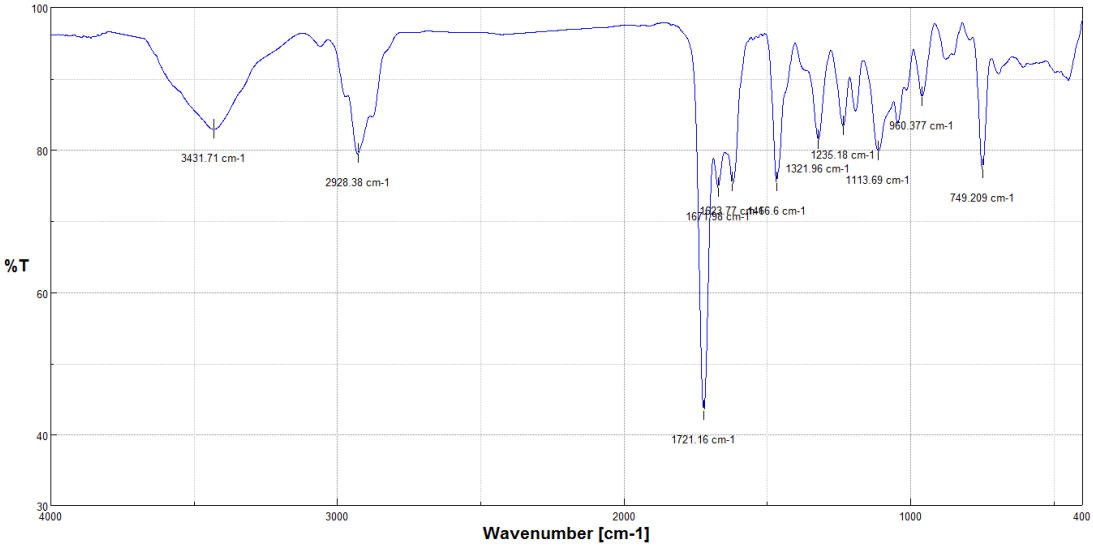

Fig. S30. IR (KBr disc) spectrum of **3**

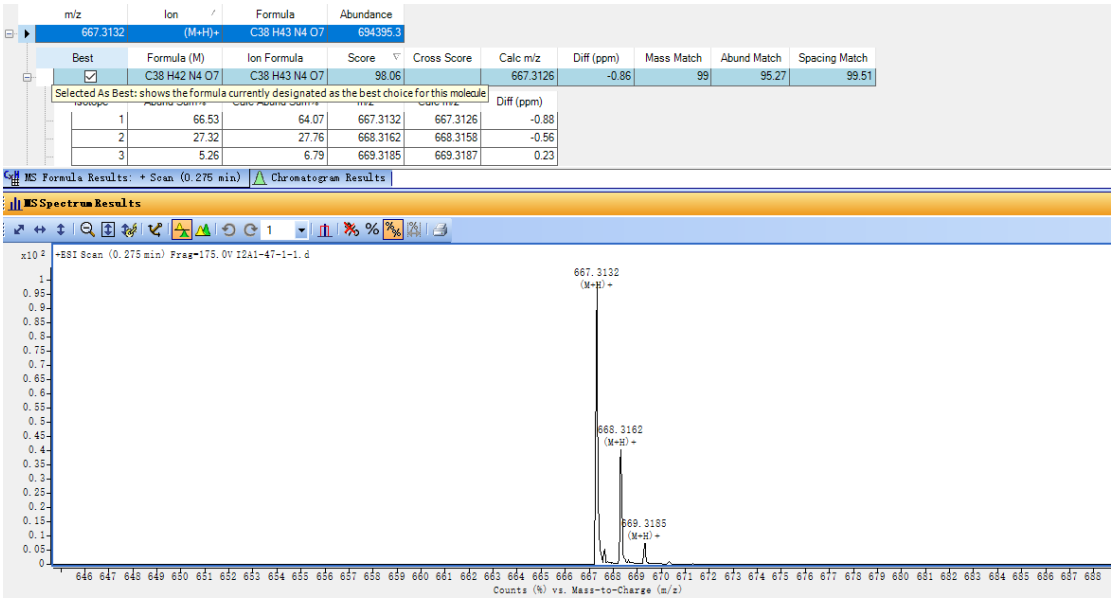

Fig. S31. HR-ESI-MS spectrum of **3**

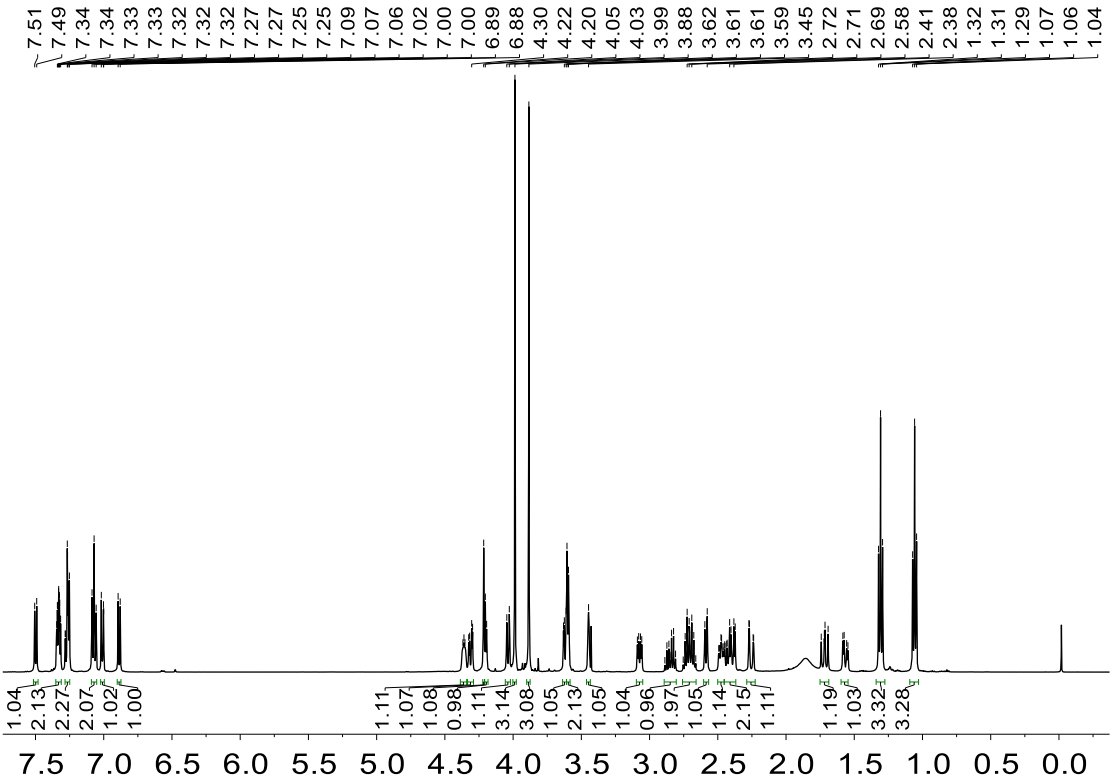

Fig. S32. ^{1}H NMR spectrum of **3** in $CDCl_3$

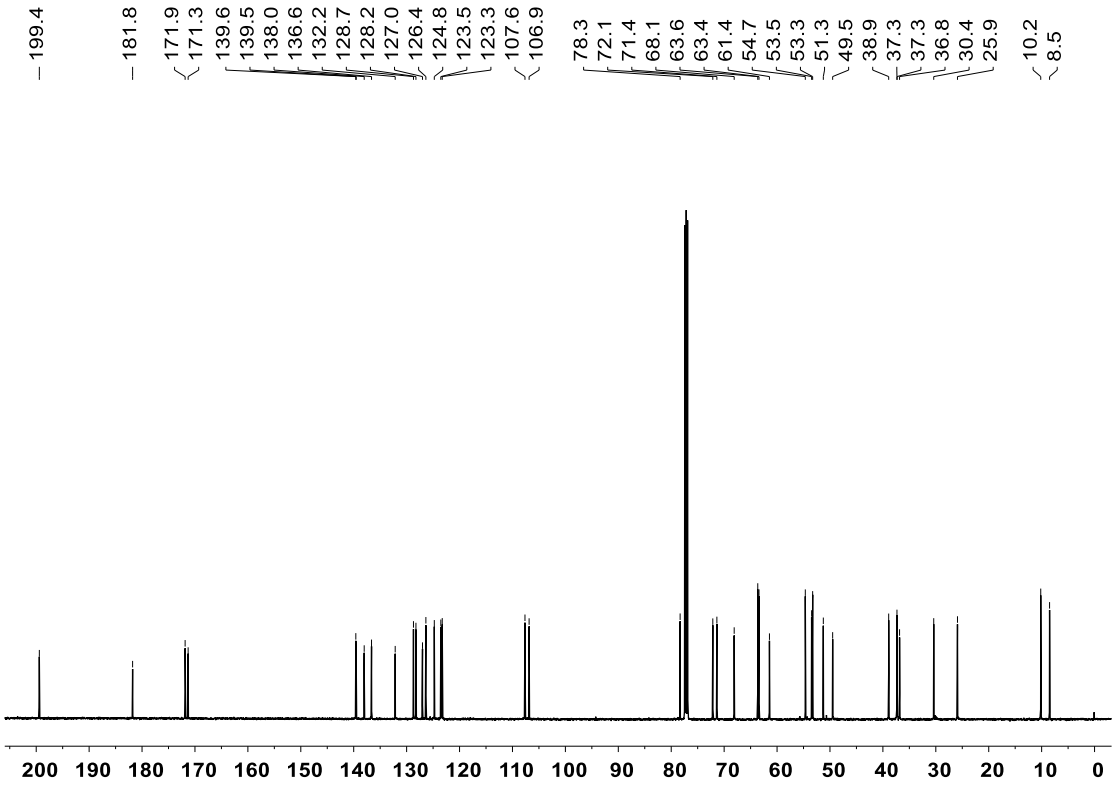

Fig. S33. ^{13}C NMR spectrum of **3** in $CDCl_3$

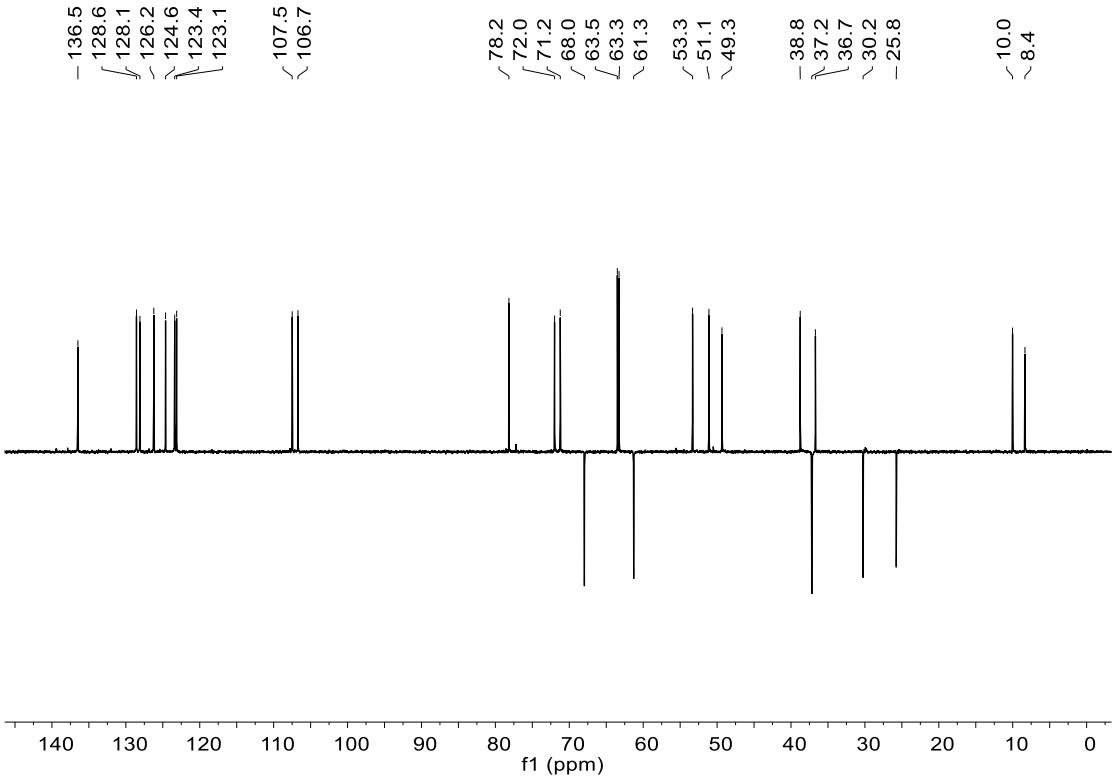

Fig. S34. DEPT-135 spectrum of **3** in $CDCl_3$

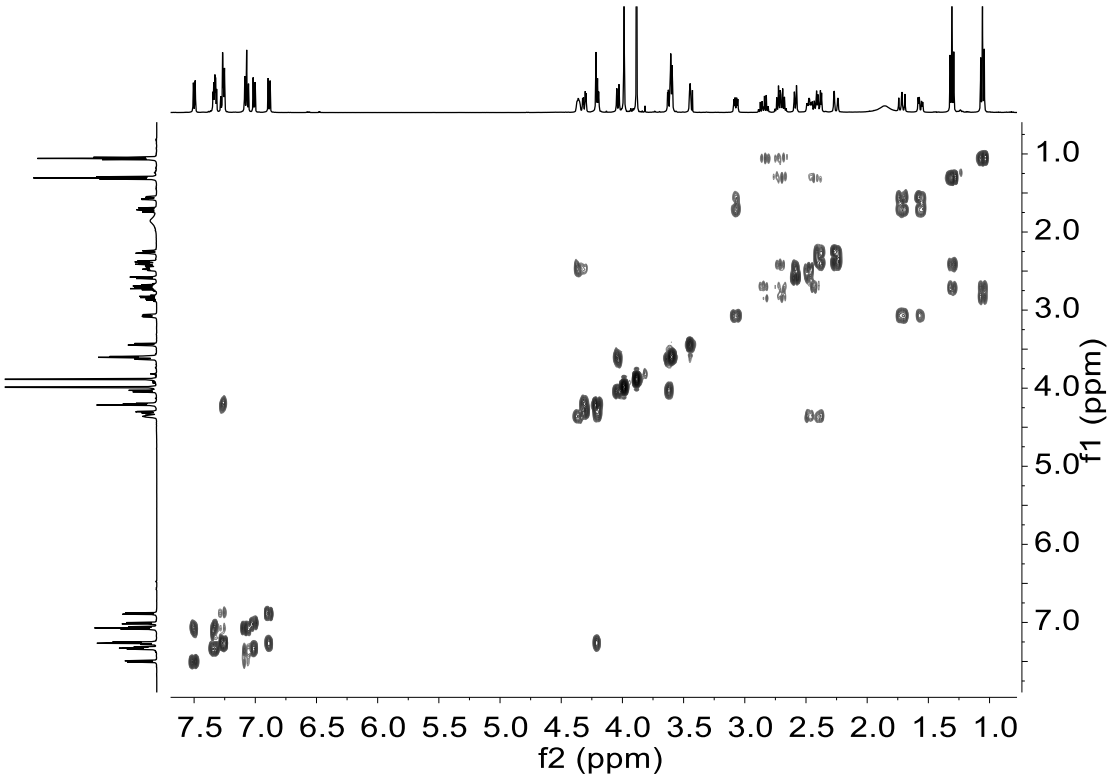

Fig. S35. ^{1}H-^{1}H COSY spectrum of **3** in $CDCl_3$

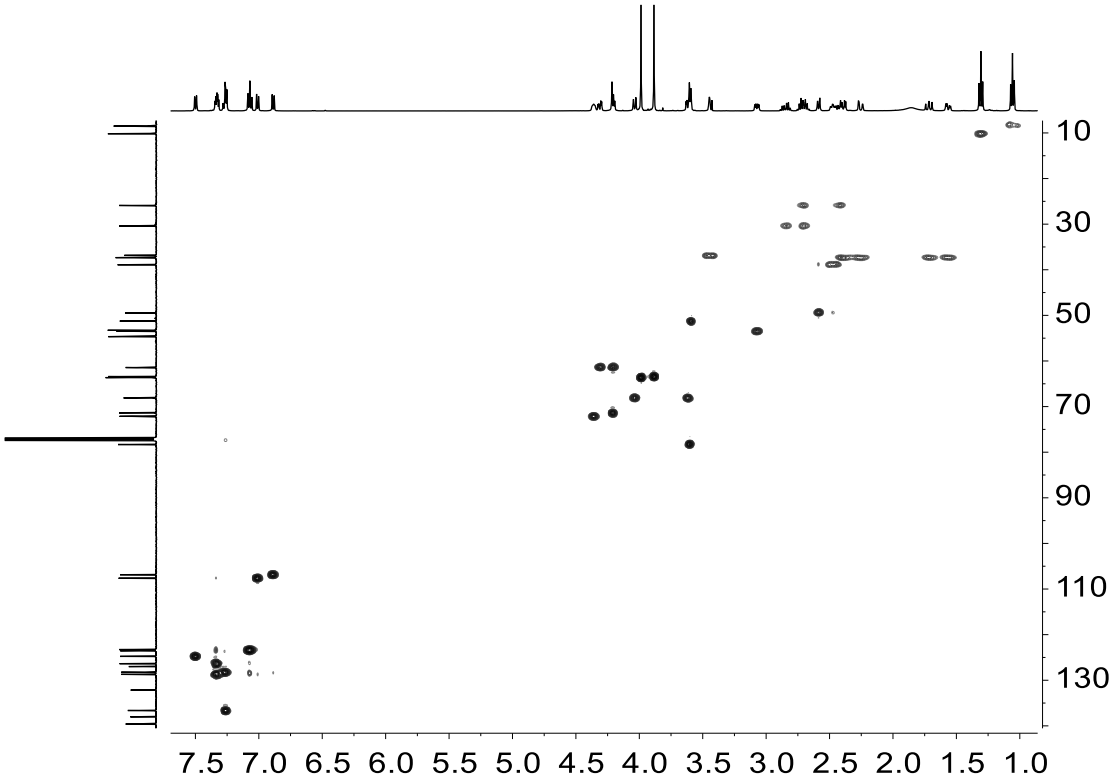

Fig. S36. HSQC spectrum of **3** in $CDCl_3$

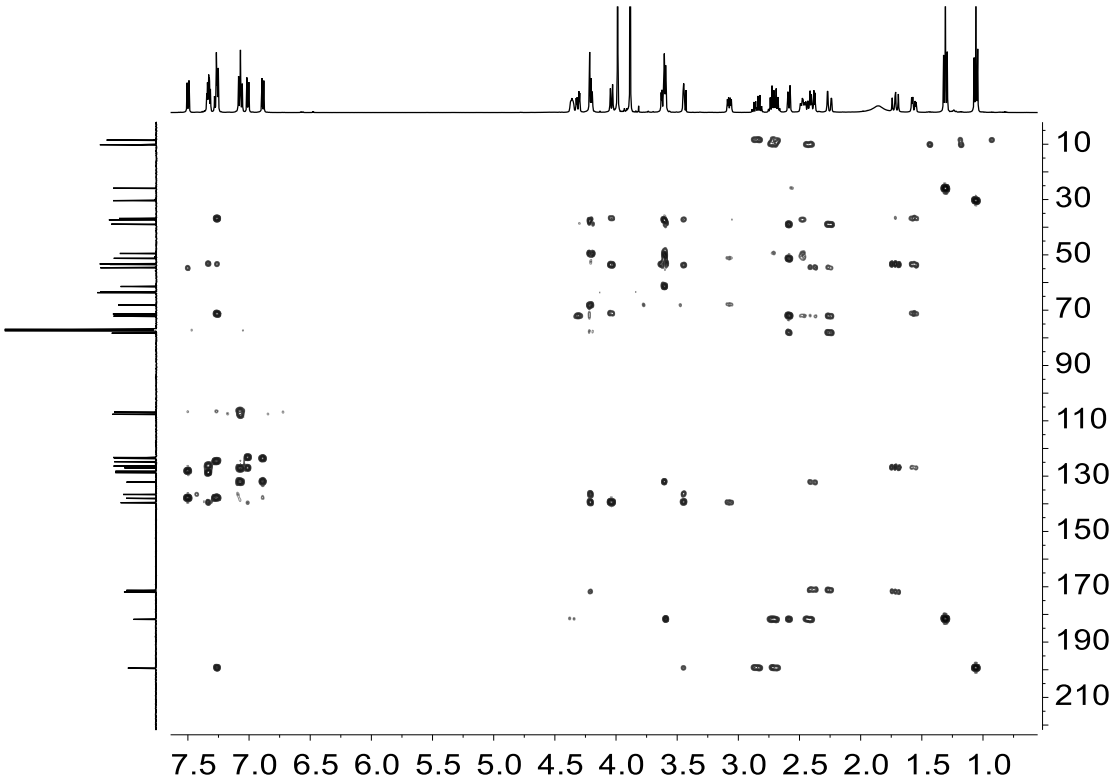

Fig. S37. HMBC spectrum of **3** in $CDCl_3$

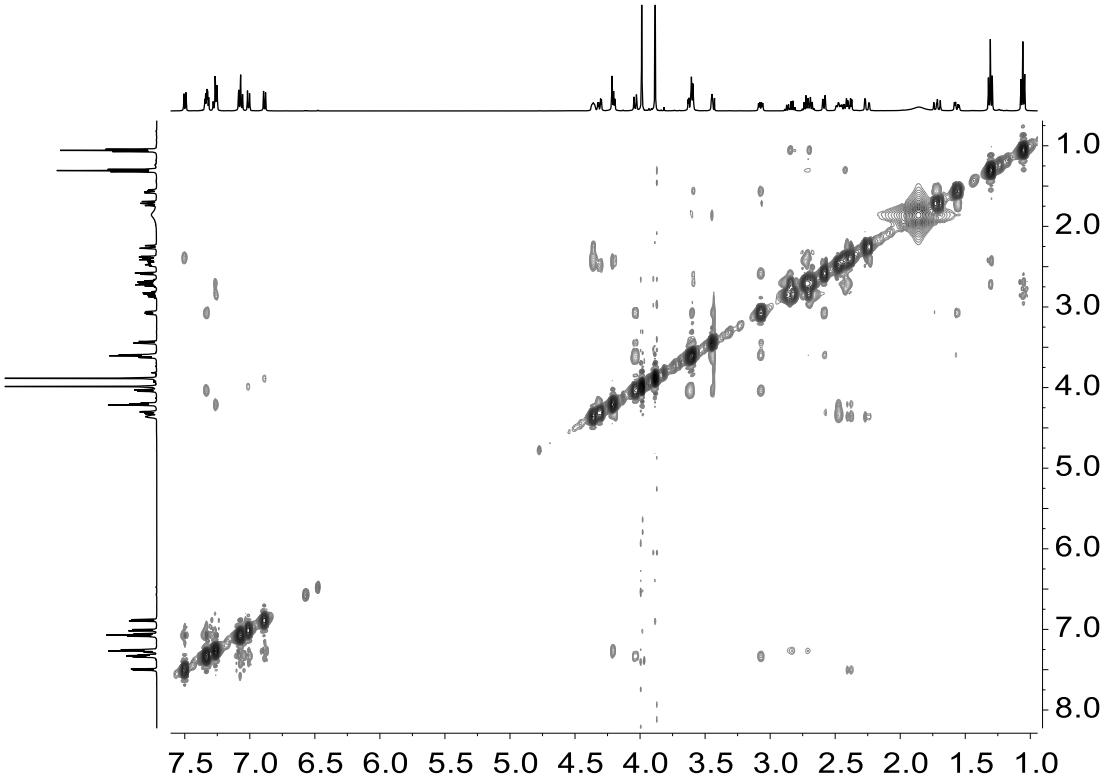

Fig. S38. NOESY spectrum of **3** in $CDCl_3$

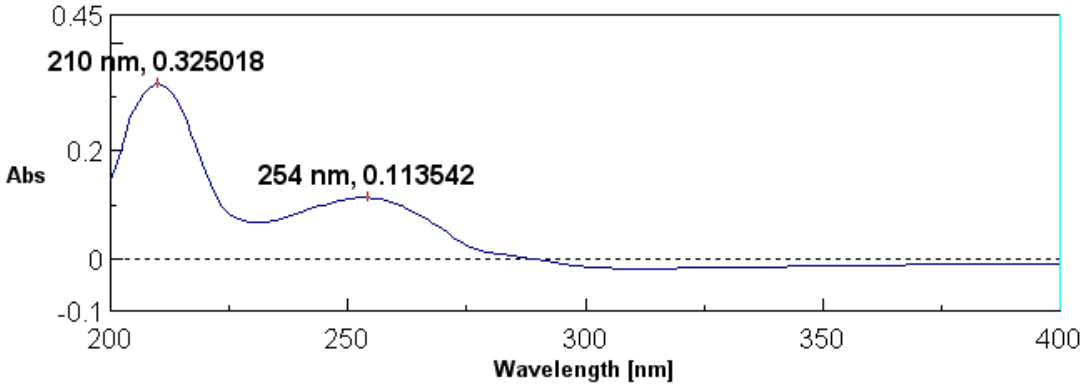

Fig. S39. UV spectrum of **4**

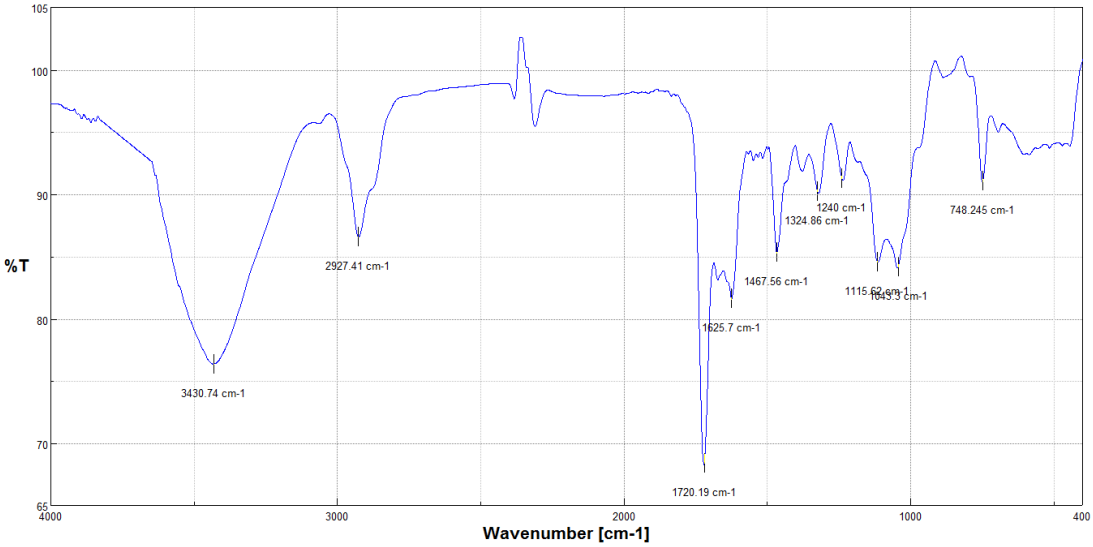

Fig. S40. IR (KBr disc) spectrum of **4**

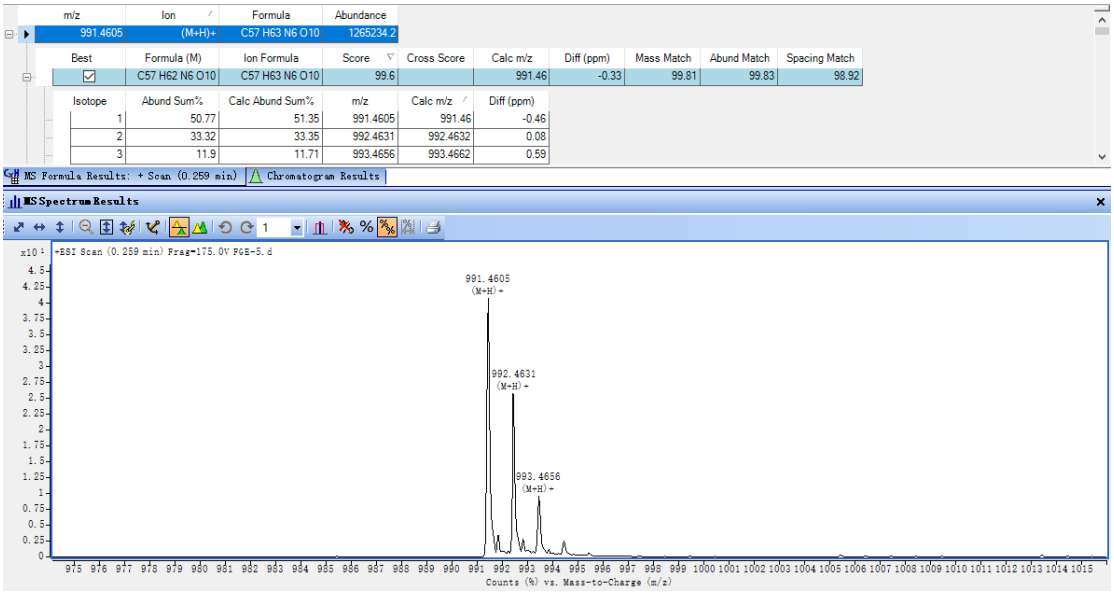

Fig. S41. HR-ESI-MS spectrum of **4**

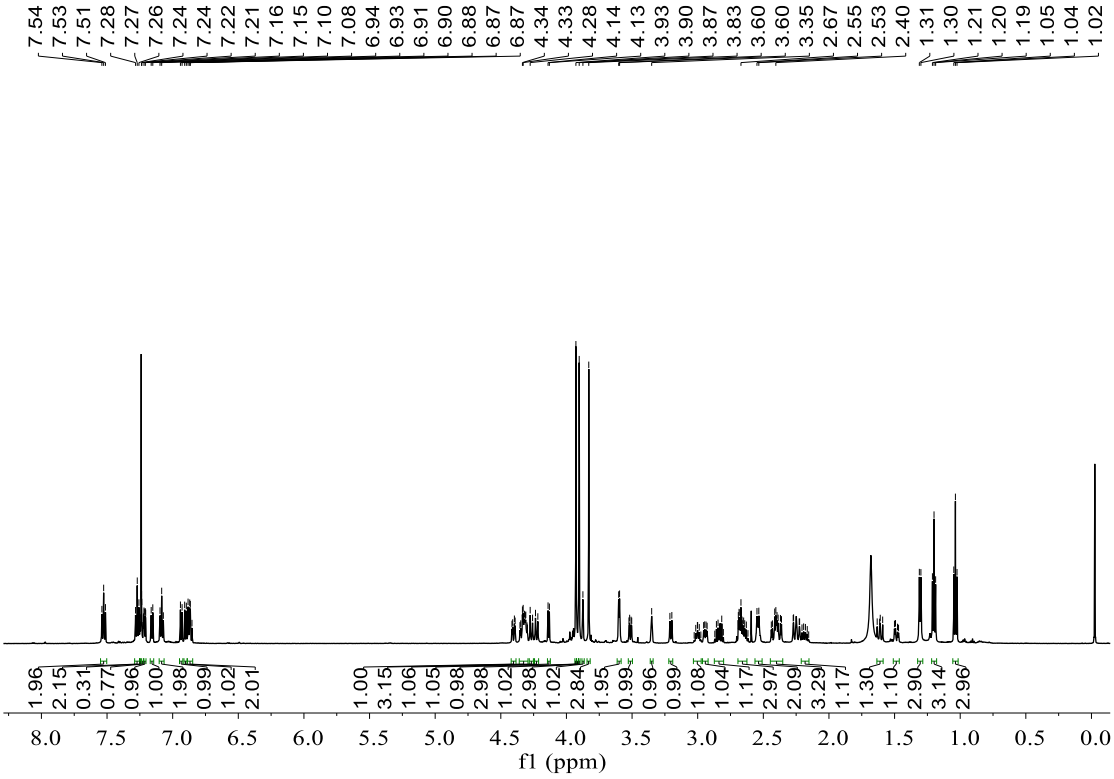

Fig. S42. ^{1}H NMR spectrum of **4** in $CDCl_3$

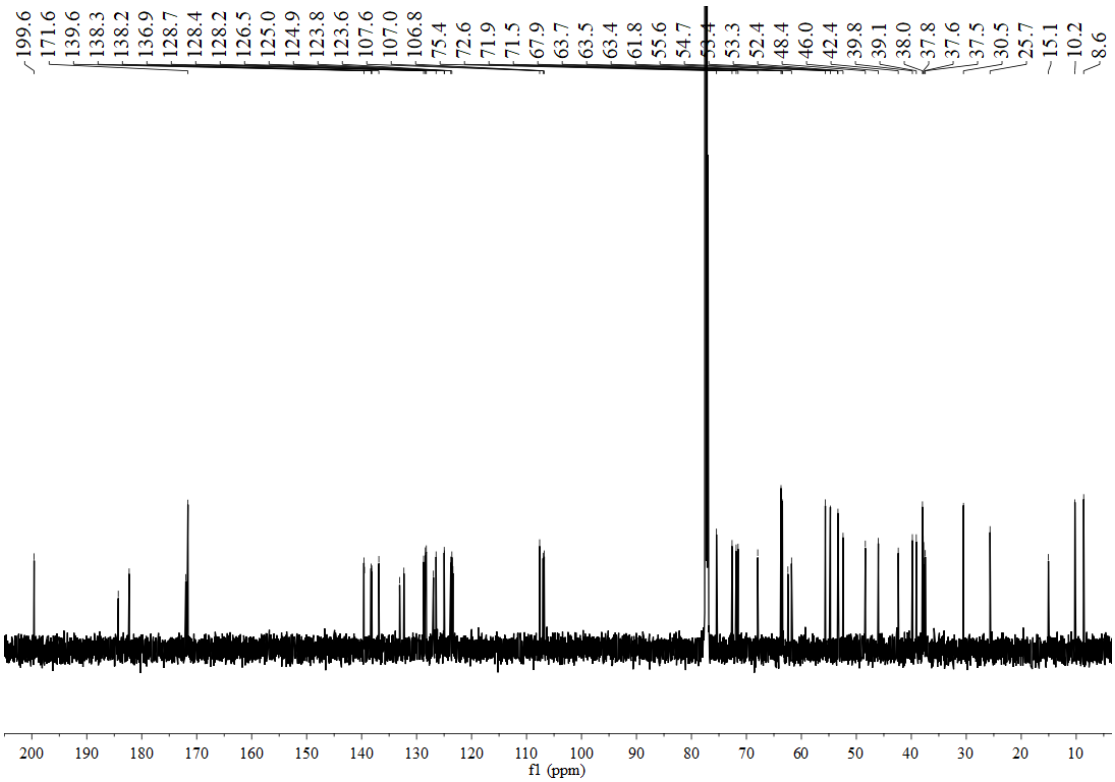

Fig. S43. ^{13}C NMR spectrum of **4** in $CDCl_3$

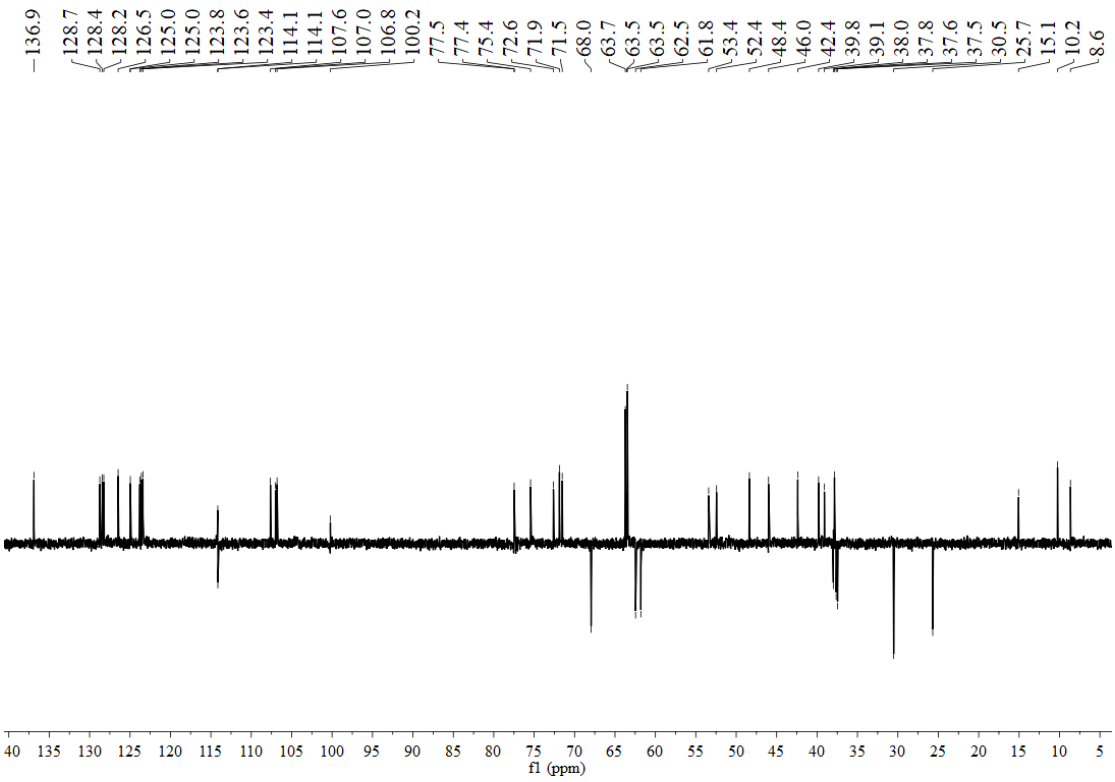

Fig. S44. DEPT-135 spectrum of **4** in $CDCl_3$

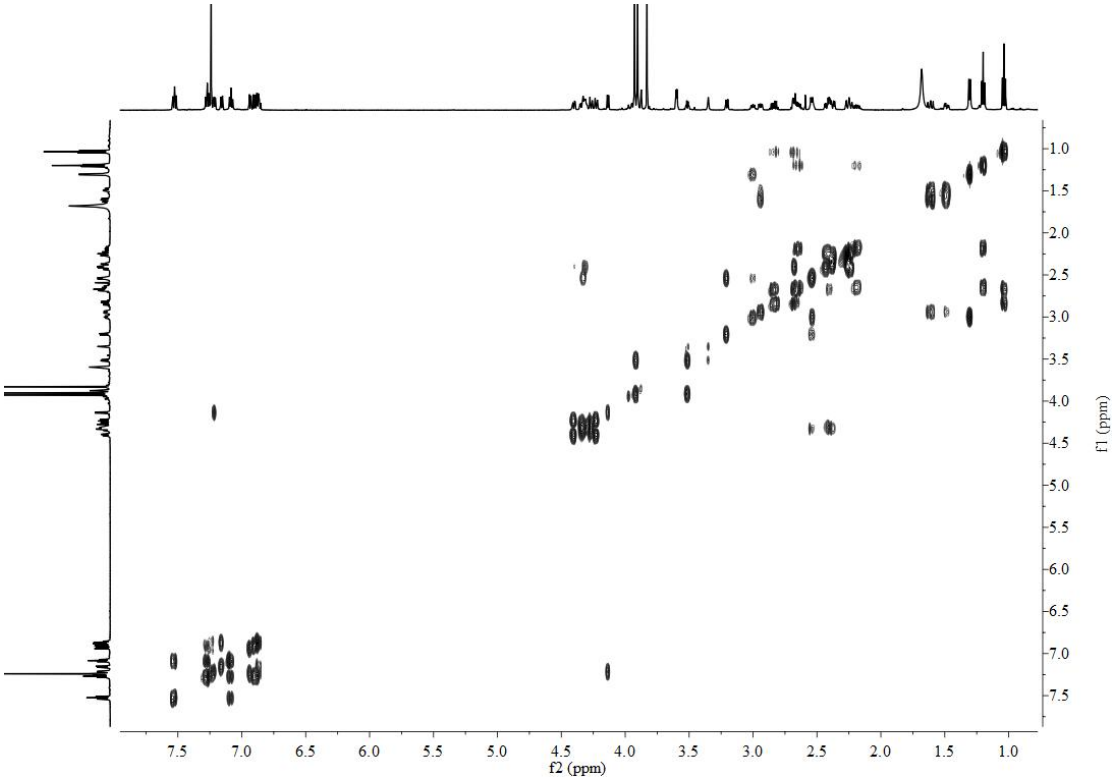

Fig. S45. ^{1}H-^{1}H COSY spectrum of **4** in $CDCl_3$

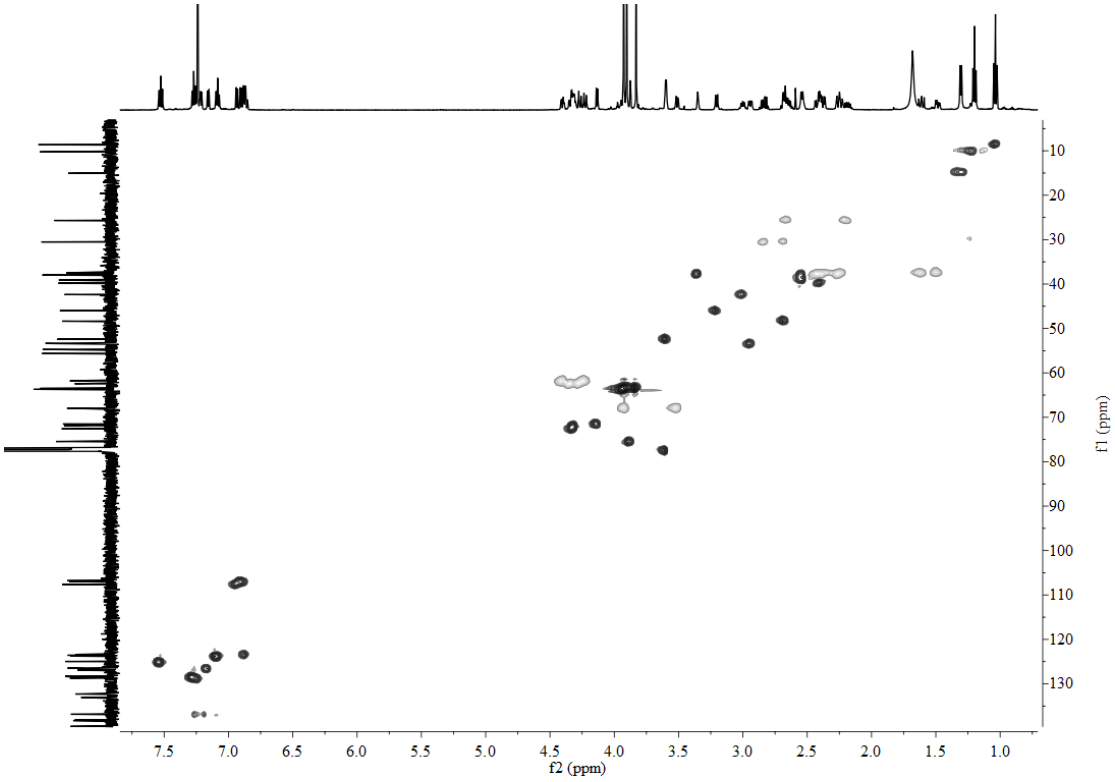

Fig. S46. HSQC spectrum of **4** in $CDCl_3$

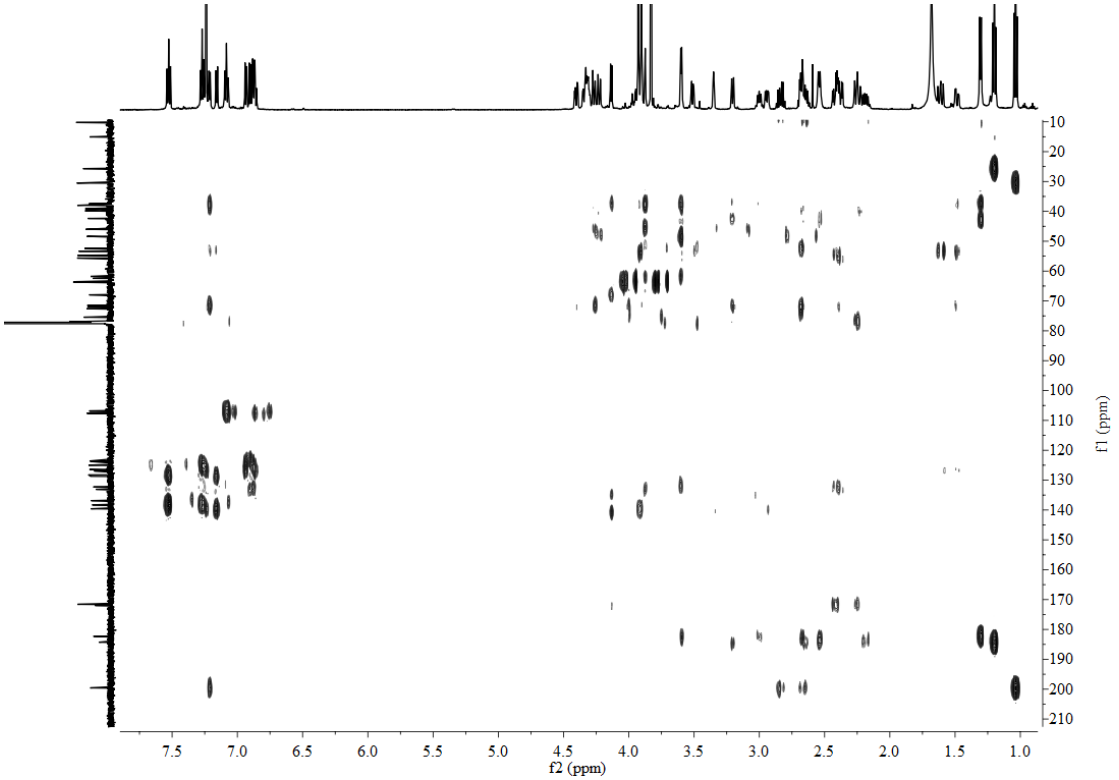

Fig. S47. HMBC spectrum of **4** in $CDCl_3$

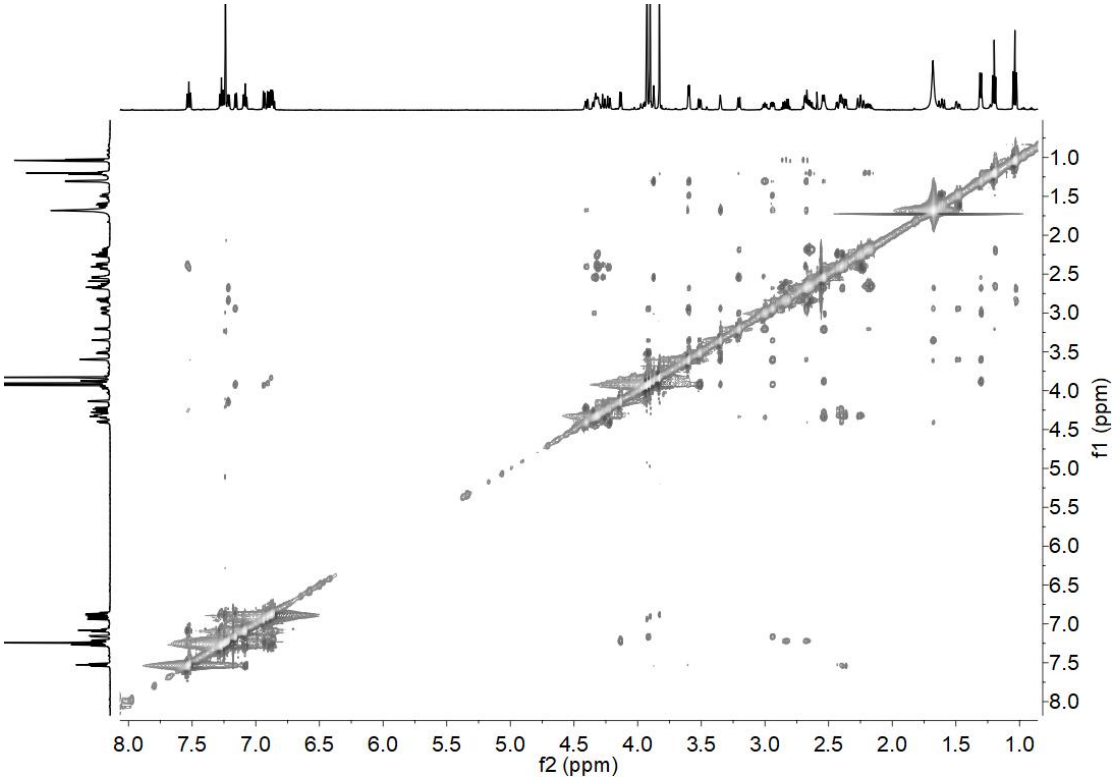

Fig. S48. NOESY spectrum of **4** in $CDCl_3$

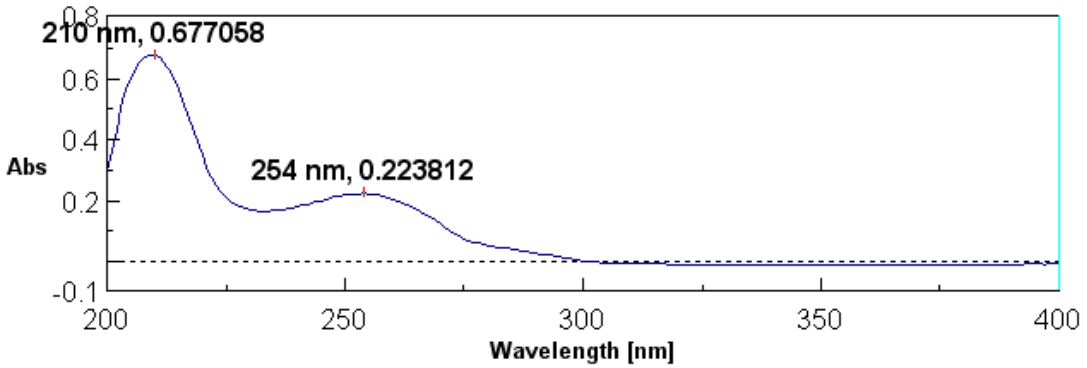

Fig. S49. UV spectrum of **5**

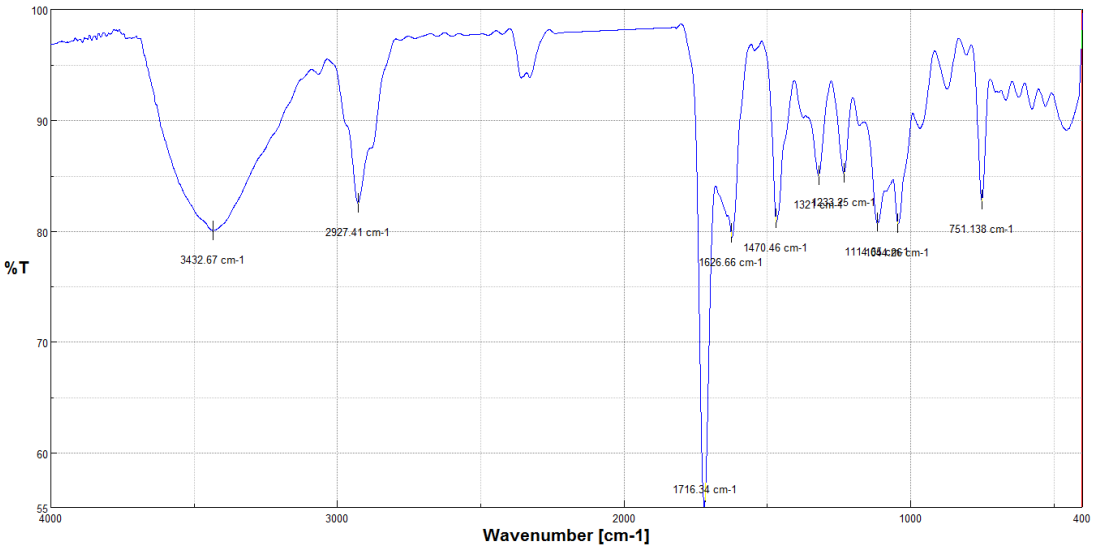

Fig. S50. IR (KBr disc) spectrum of **5**

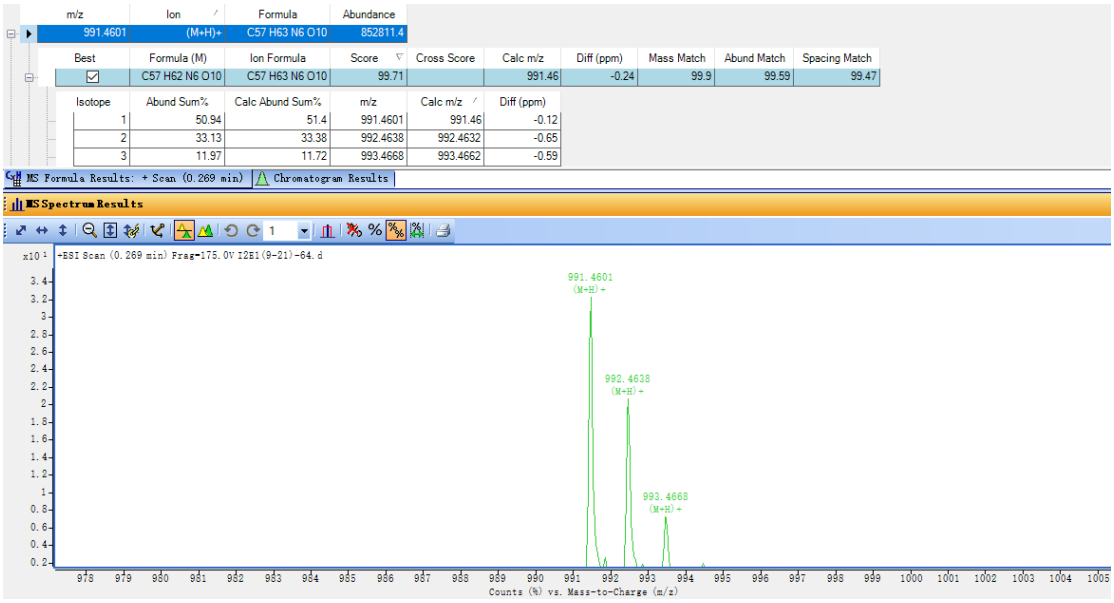

Fig. S51. HR-ESI-MS spectrum of **5**

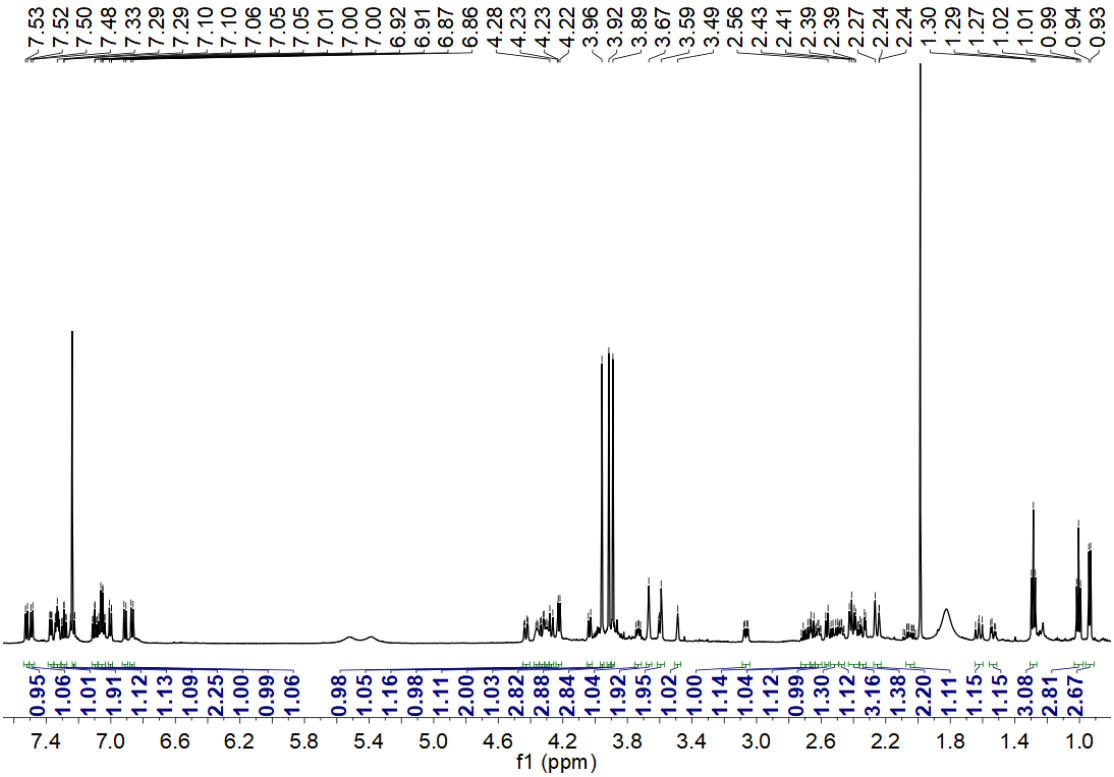

Fig. S52. ^{1}H NMR spectrum of **5** in $CDCl_3$

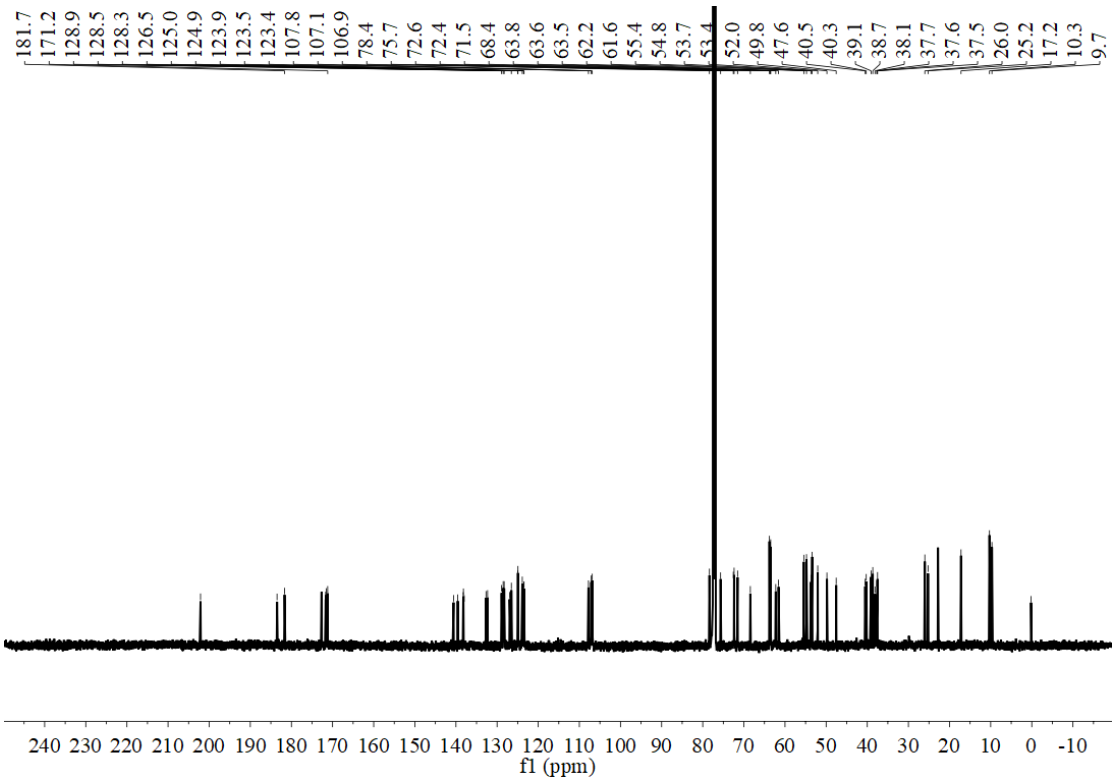

Fig. S53. ^{13}C NMR spectrum of **5** in $CDCl_3$

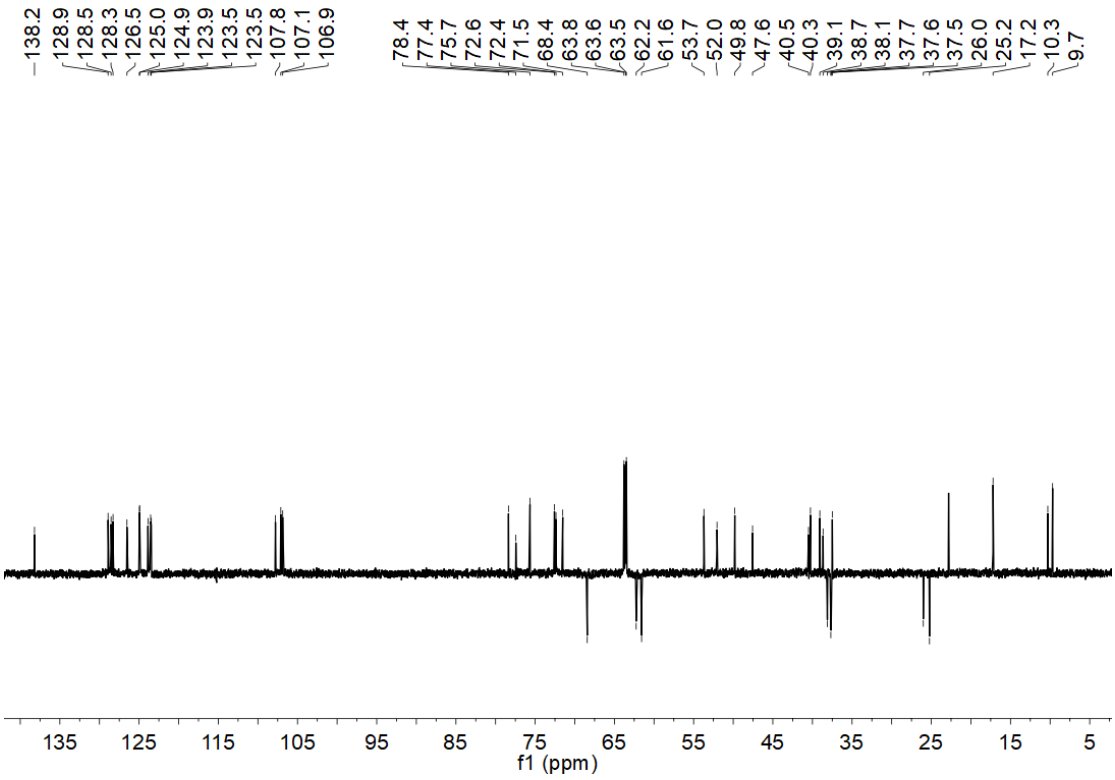

Fig. S54. DEPT-135 spectrum of **5** in $CDCl_3$

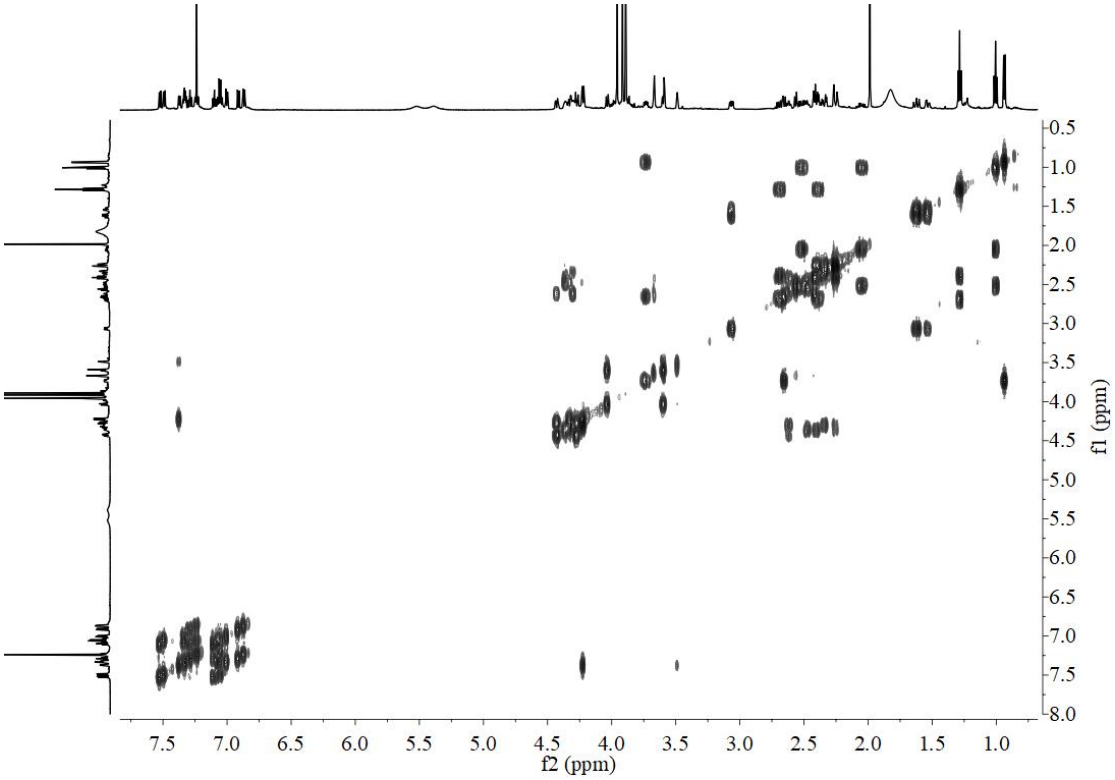

Fig. S55. ^{1}H-^{1}H COSY spectrum of **5** in $CDCl_3$

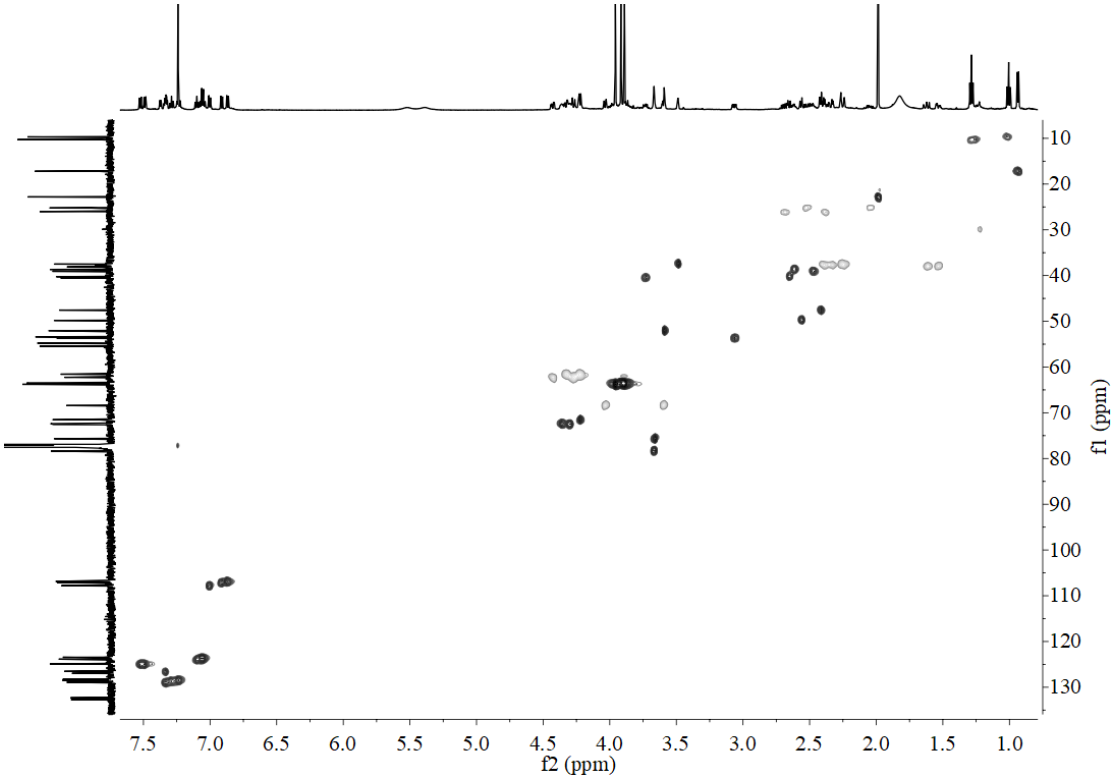

Fig. S56. HSQC spectrum of **5** in $CDCl_3$

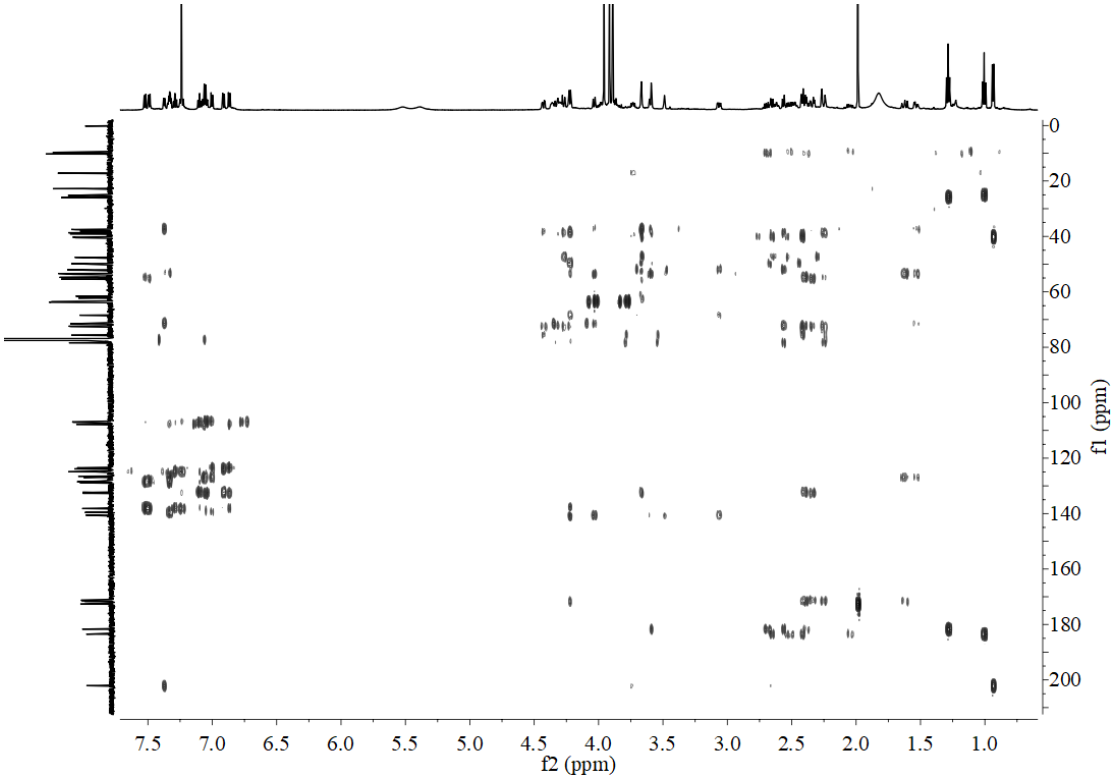

Fig. S57. HMBC spectrum of **5** in $CDCl_3$

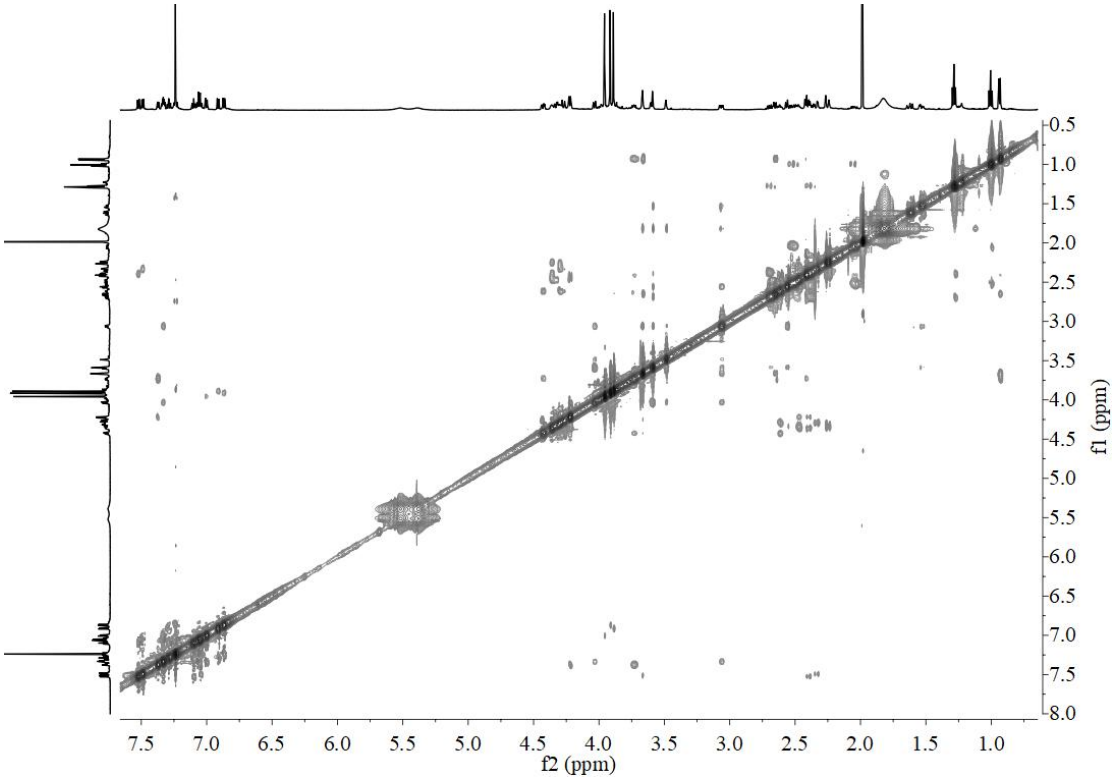

Fig. S58. NOESY spectrum of **5** in $CDCl_3$

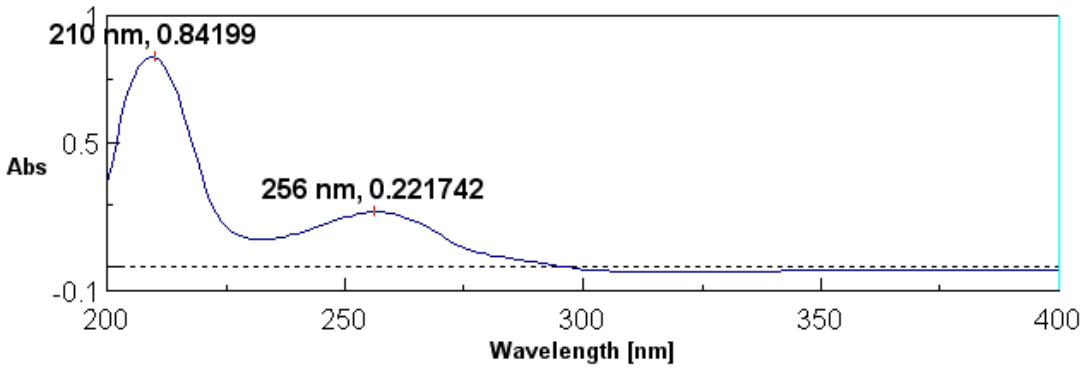

Fig. S59. UV spectrum of **6**

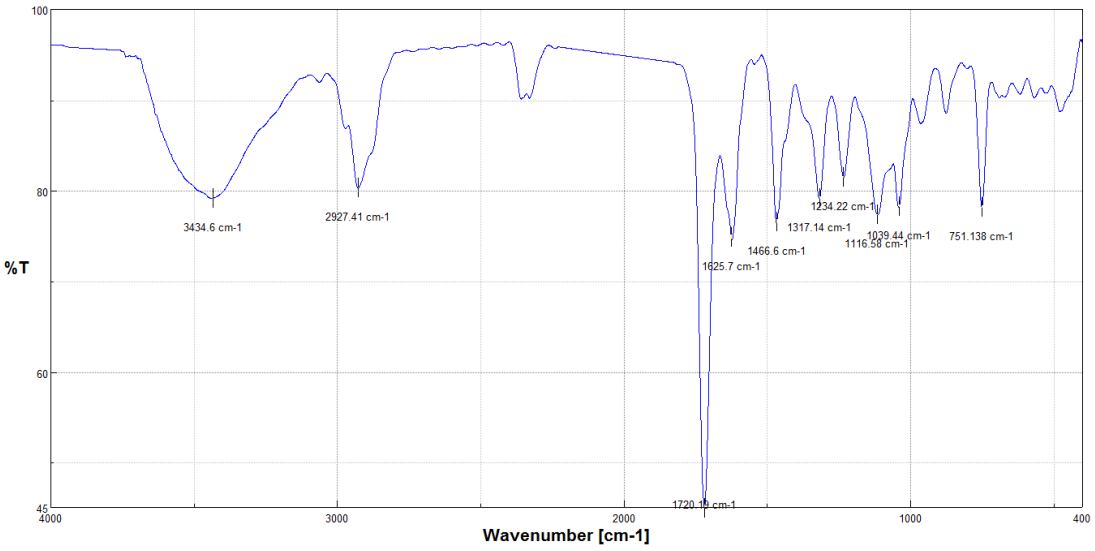

Fig. S60. IR (KBr disc) spectrum of **6**

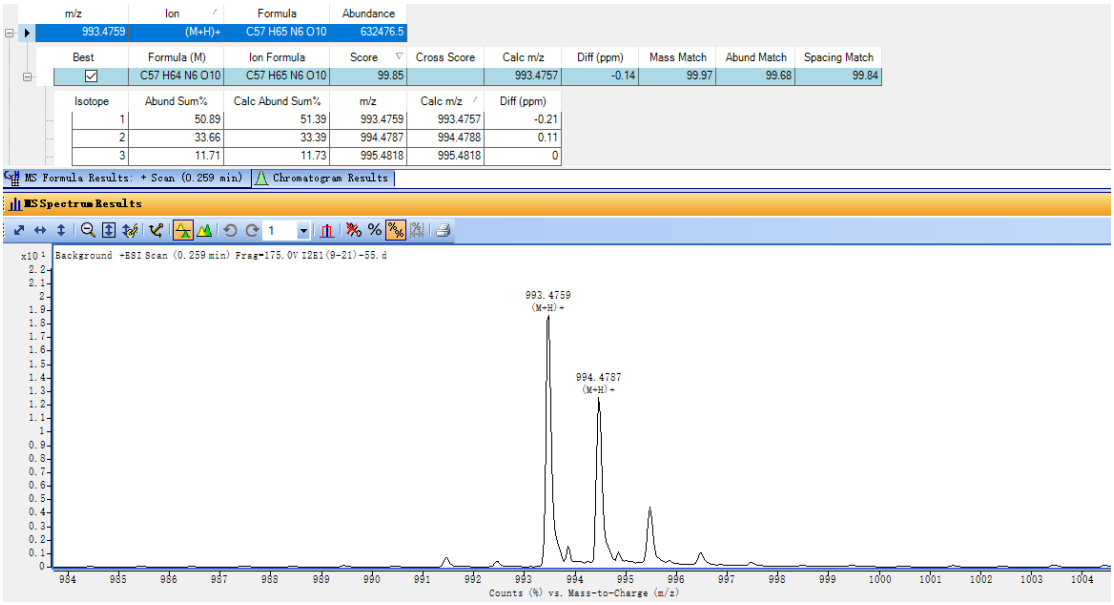

Fig. S61. HR-ESI-MS spectrum of **6**

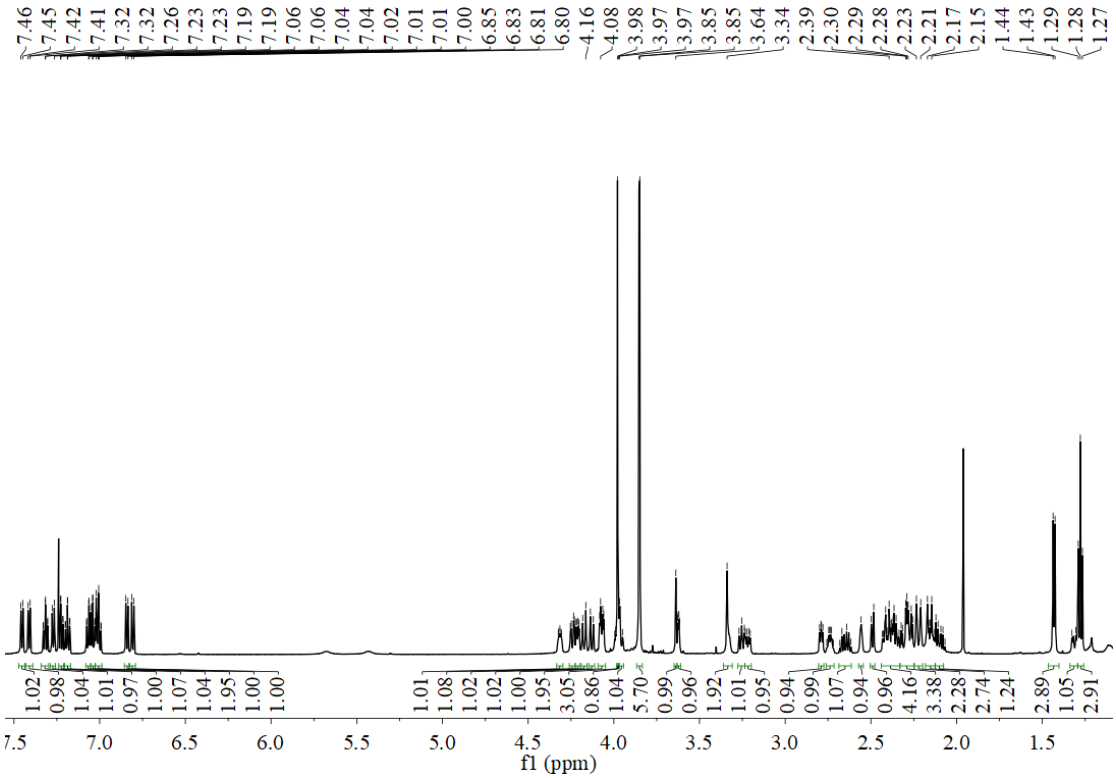

Fig. S62. ^{1}H NMR spectrum of **6** in $CDCl_3$

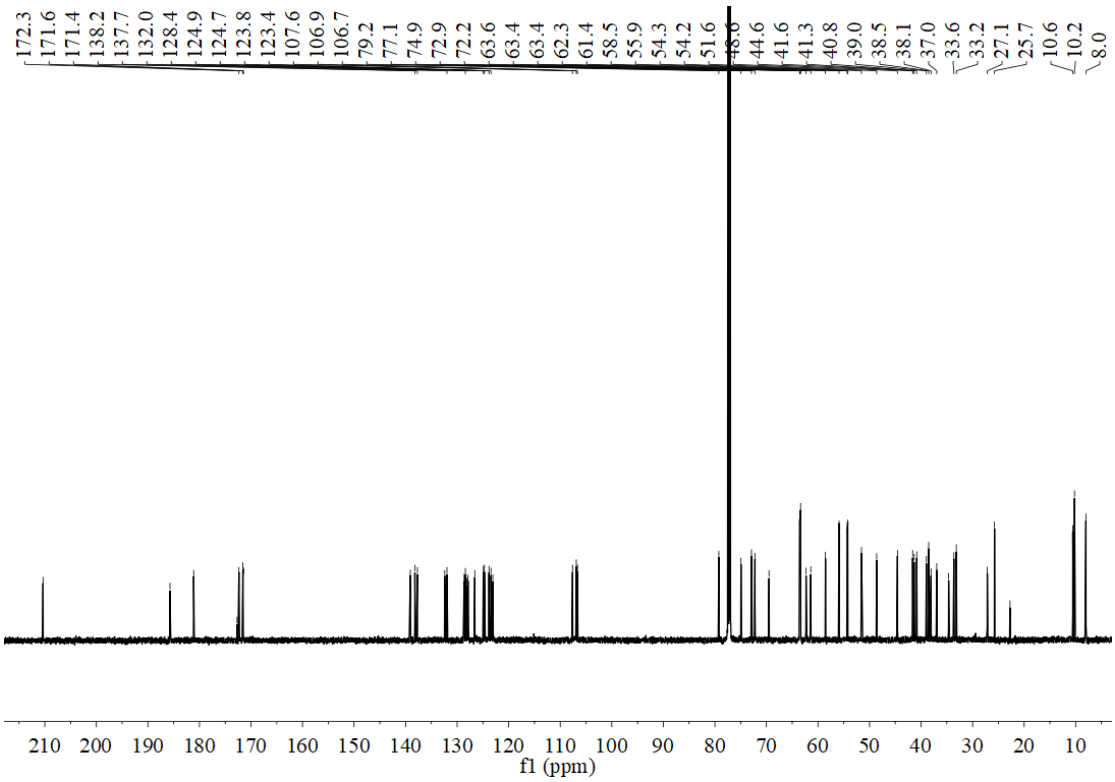

Fig. S63. ^{13}C NMR spectrum of **6** in $CDCl_3$

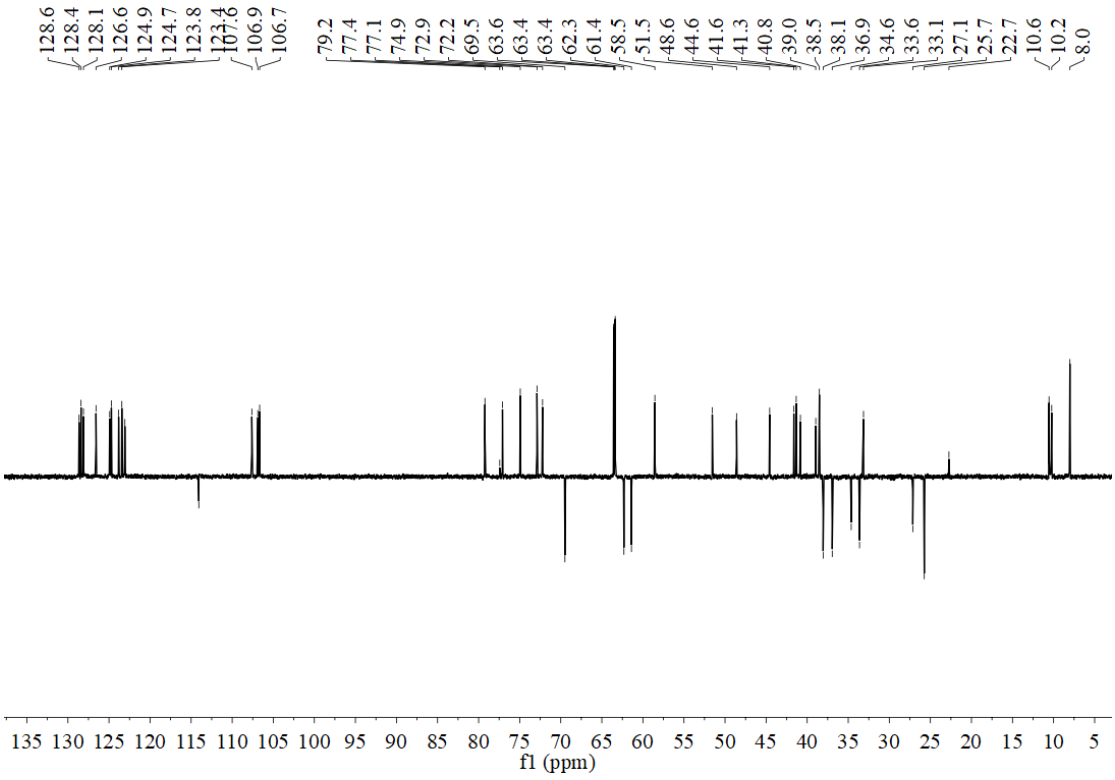

Fig. S64. DEPT-135 spectrum of **6** in $CDCl_3$

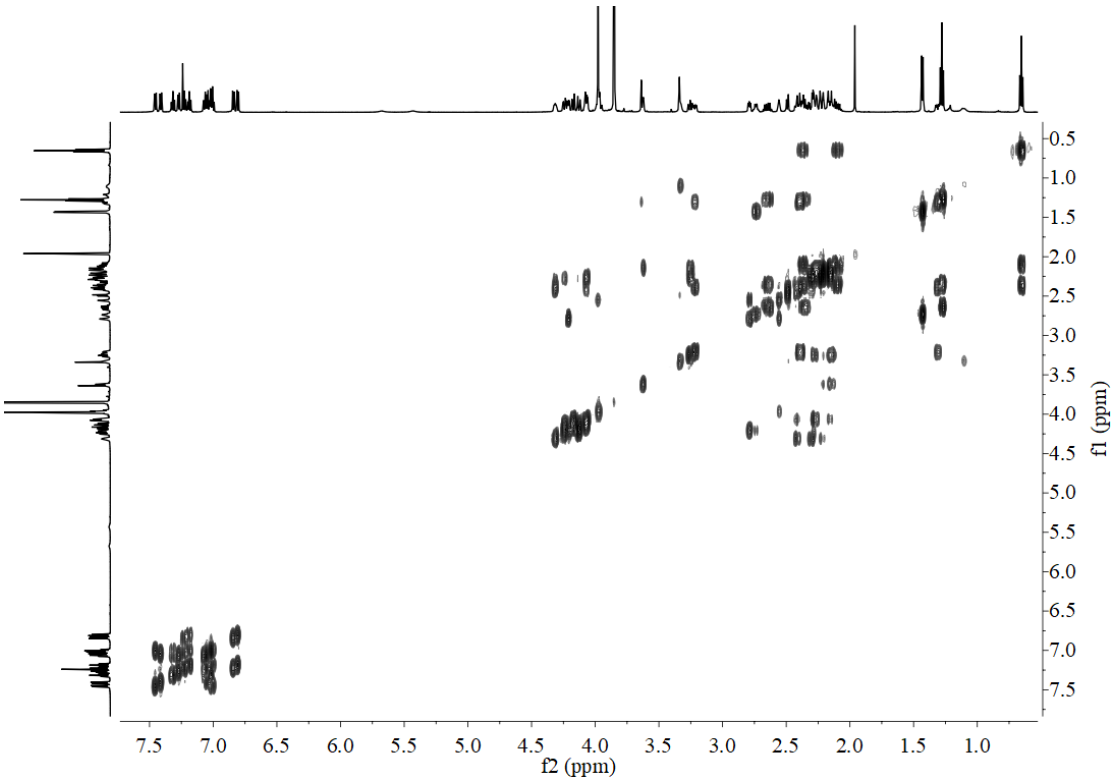

Fig. S65. ^{1}H-^{1}H COSY spectrum of **6** in $CDCl_3$

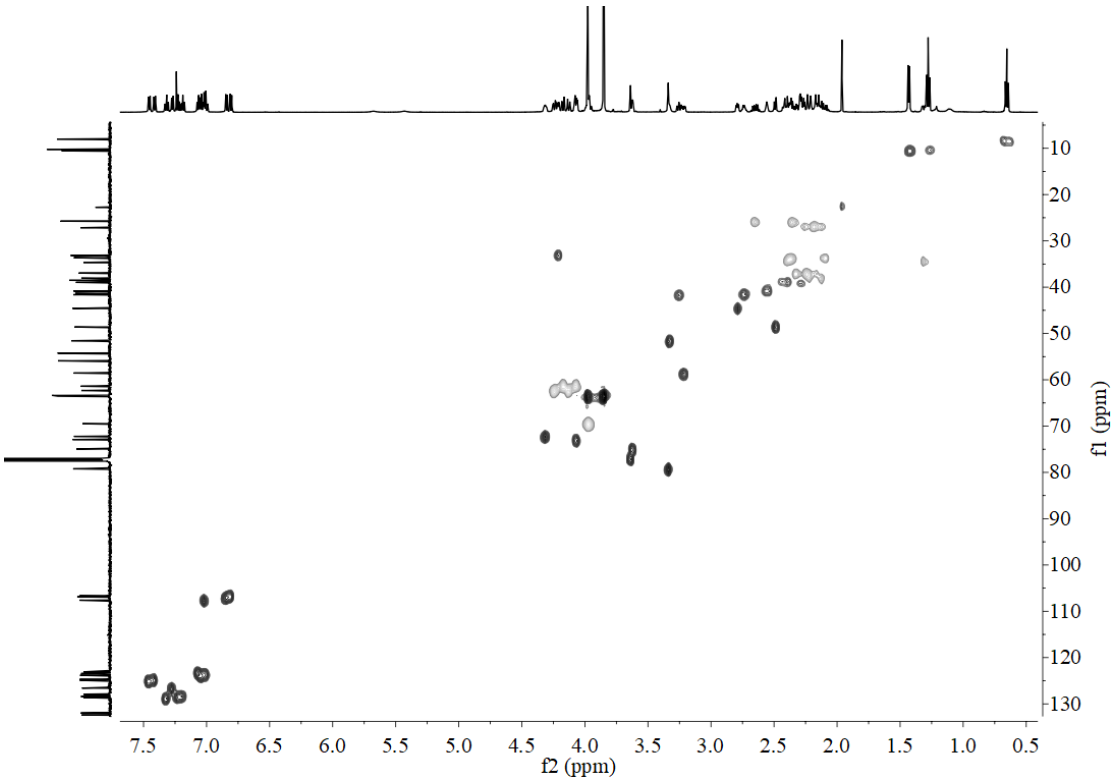

Fig. S66. HSQC spectrum of **6** in $CDCl_3$

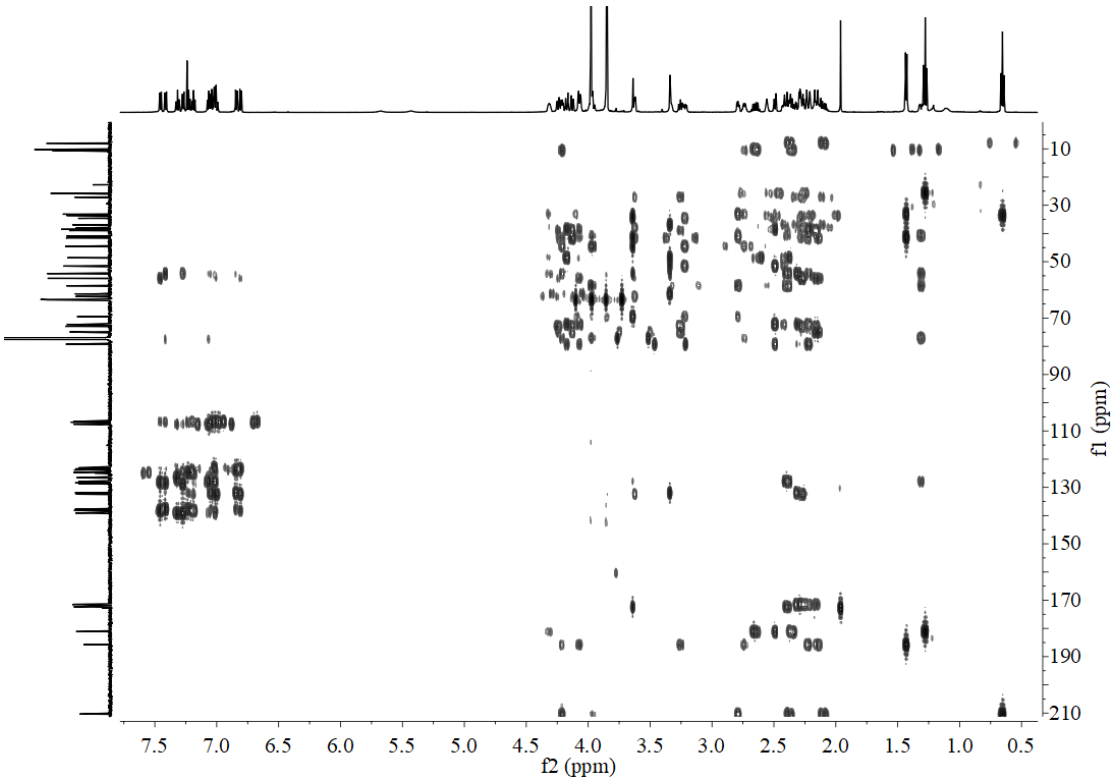

Fig. S67. HMBC spectrum of **6** in $CDCl_3$

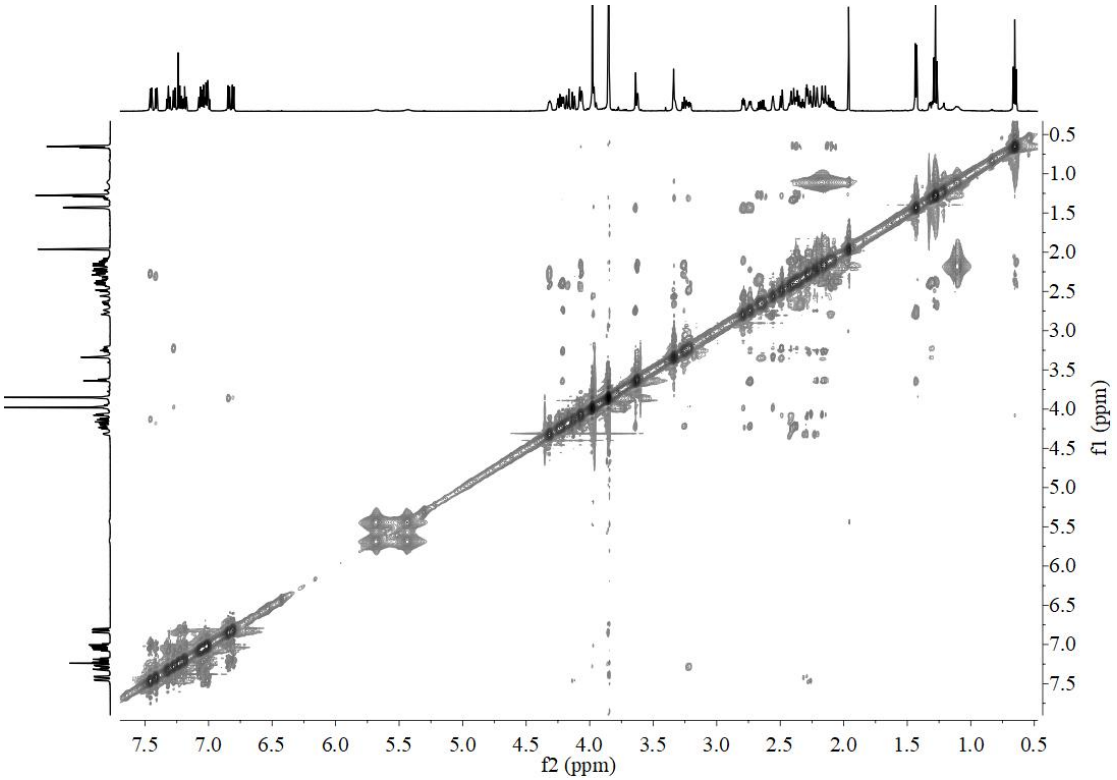

Fig. S68. NOESY spectrum of **6** in $CDCl_3$

10. 1D NMR spectra of 7–11 and synthetic 3.

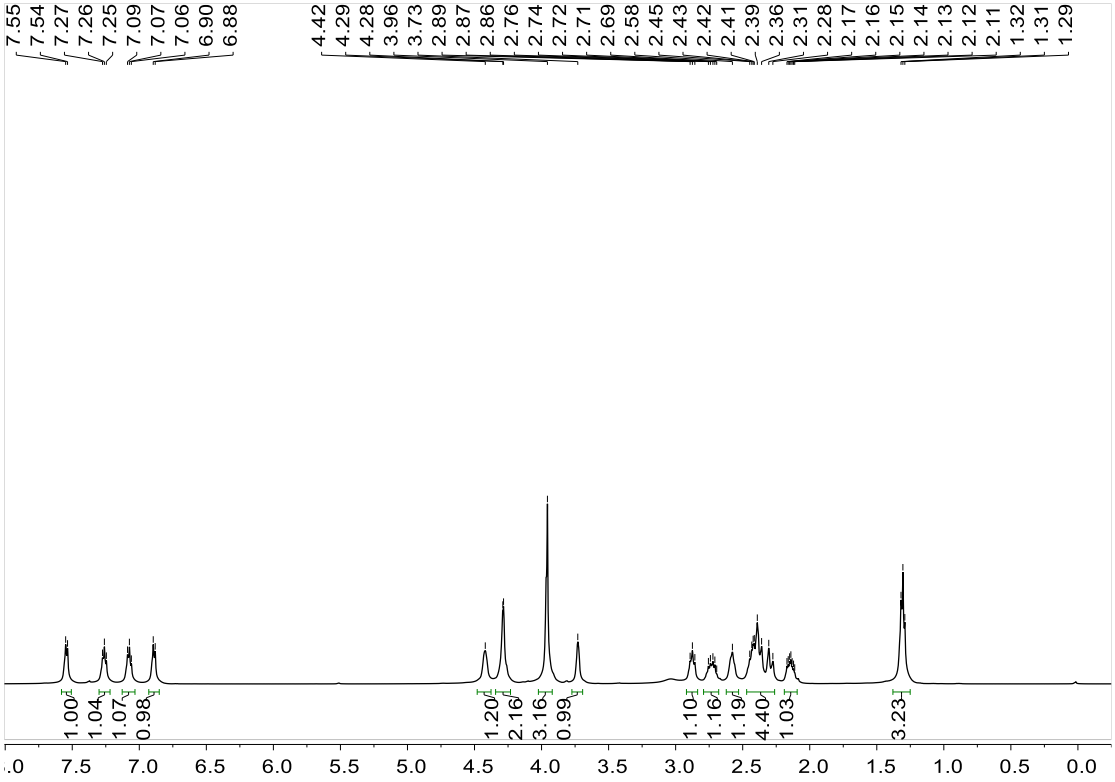

Fig. S69. ^{1}H NMR spectrum of **7** in $CDCl_3$

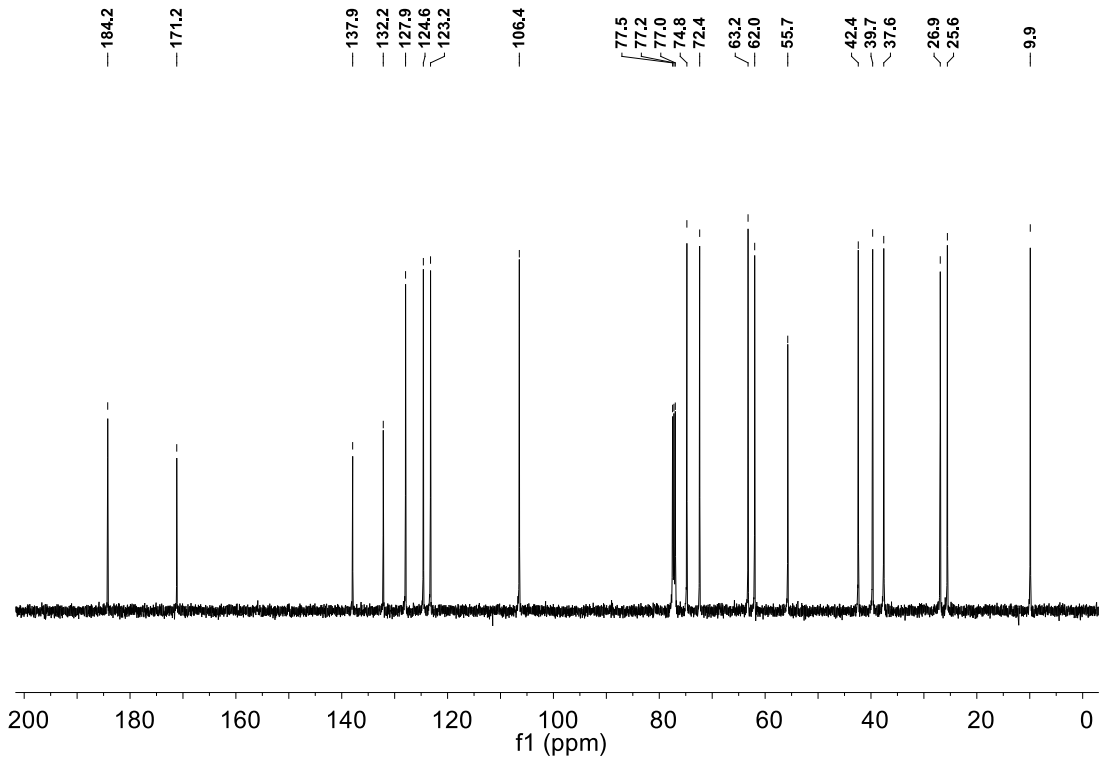

Fig. S70. ^{13}C NMR spectrum of **7** in $CDCl_3$

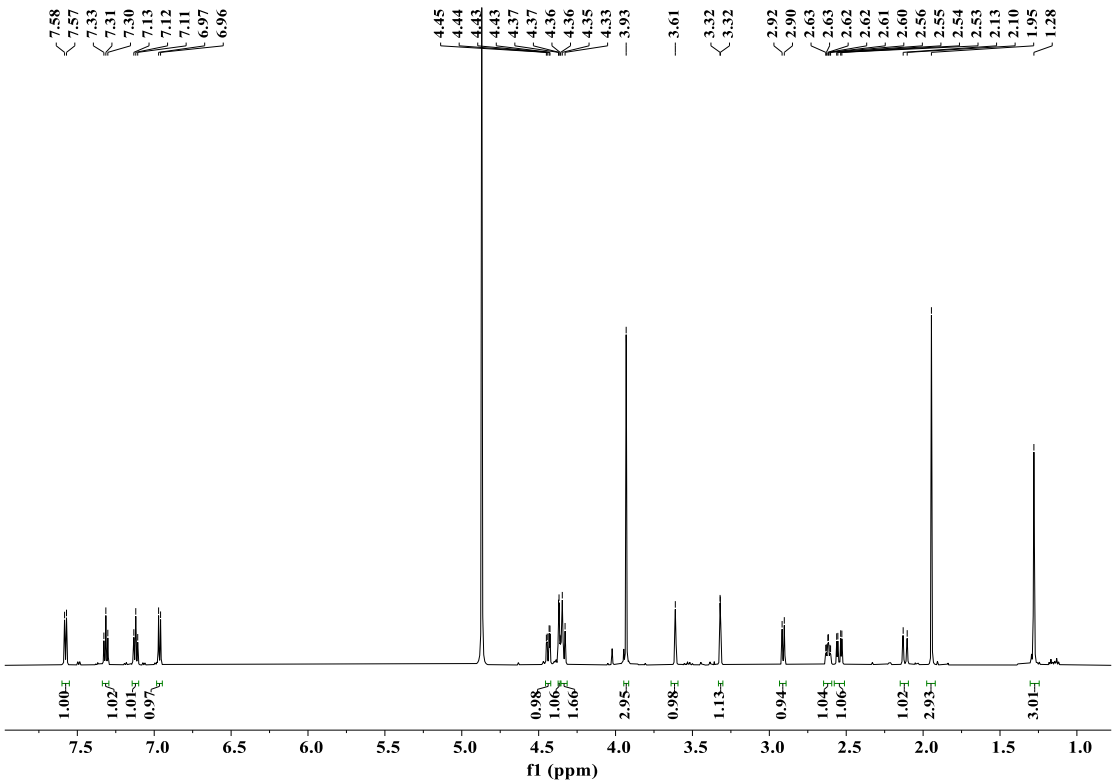

Fig. S71. ^{1}H NMR spectrum of **8** in CD_3OD

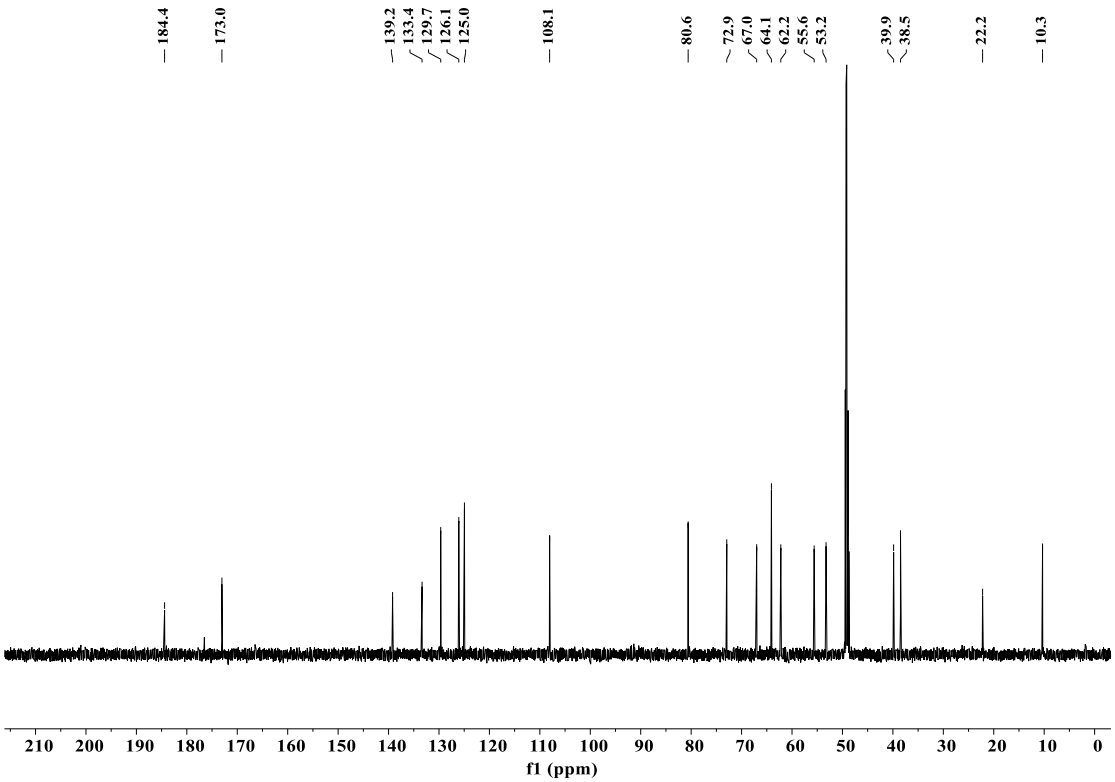

Fig. S72. ^{13}C NMR spectrum of **8** in CD_3OD

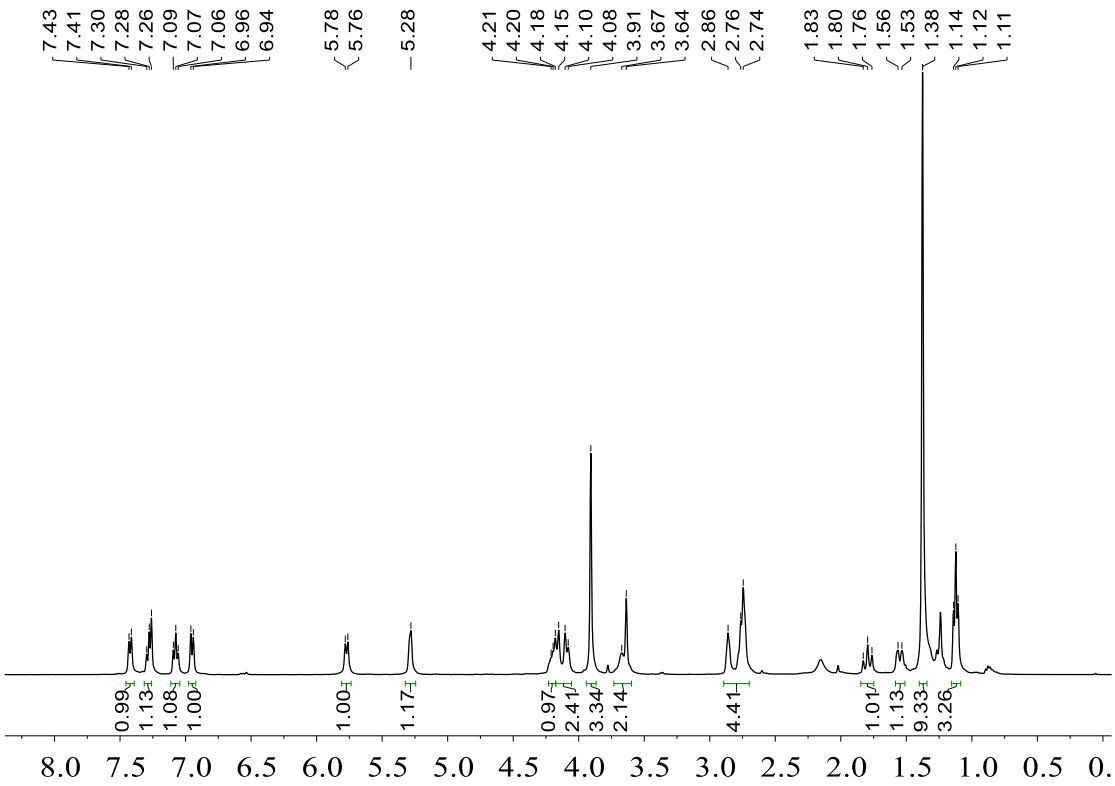

Fig. S73. ^{1}H NMR spectrum of **9** in $CDCl_3$

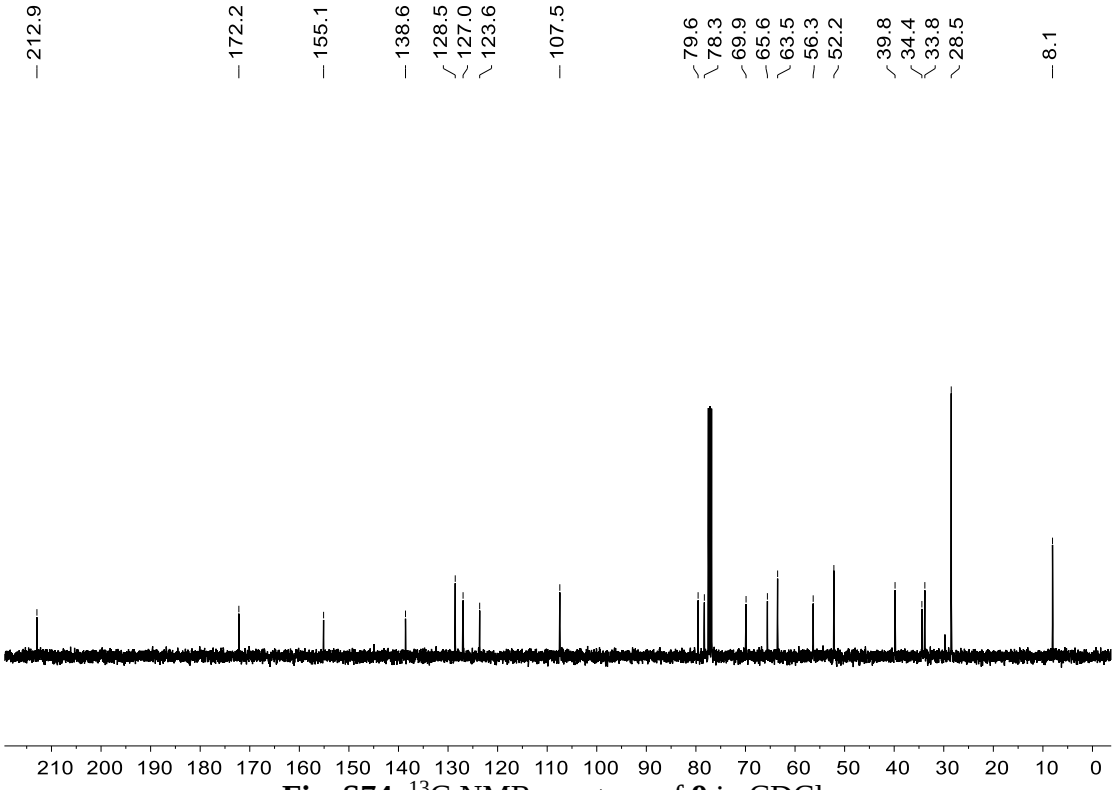

Fig. S74. ^{13}C NMR spectrumof **9** in $CDCl_3$

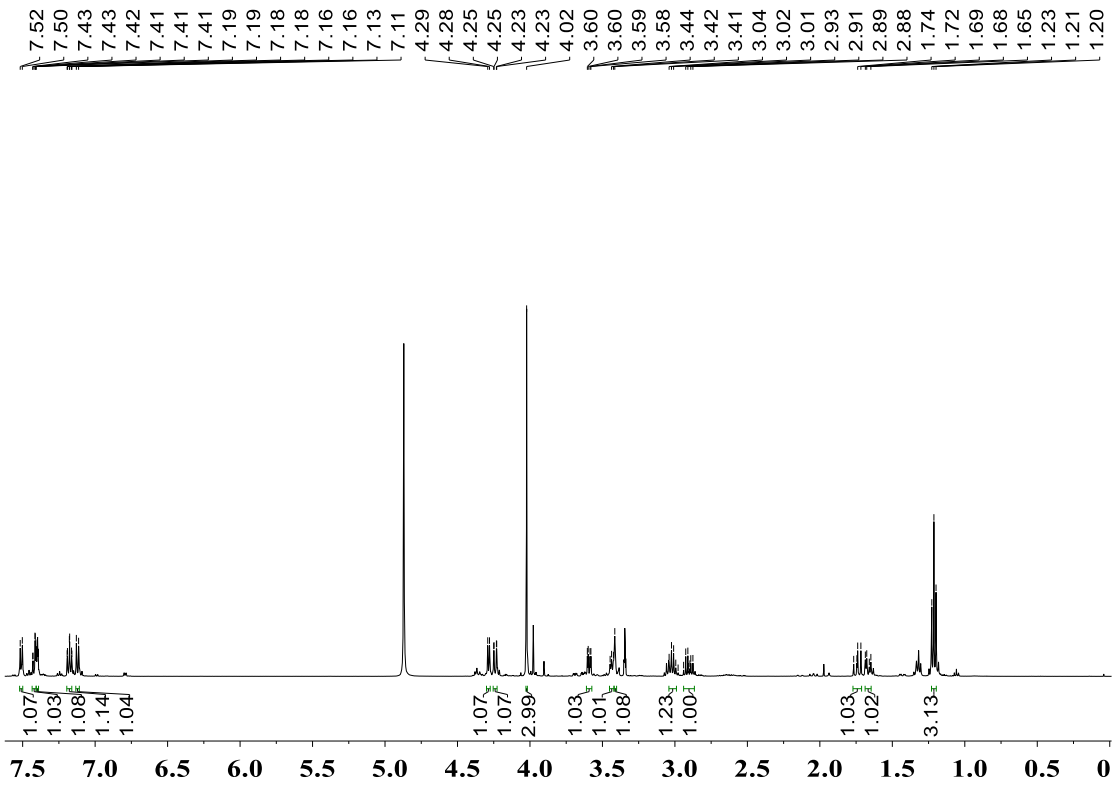

Fig. S75. ^{1}H NMR spectrum of **11** in CD_3OD

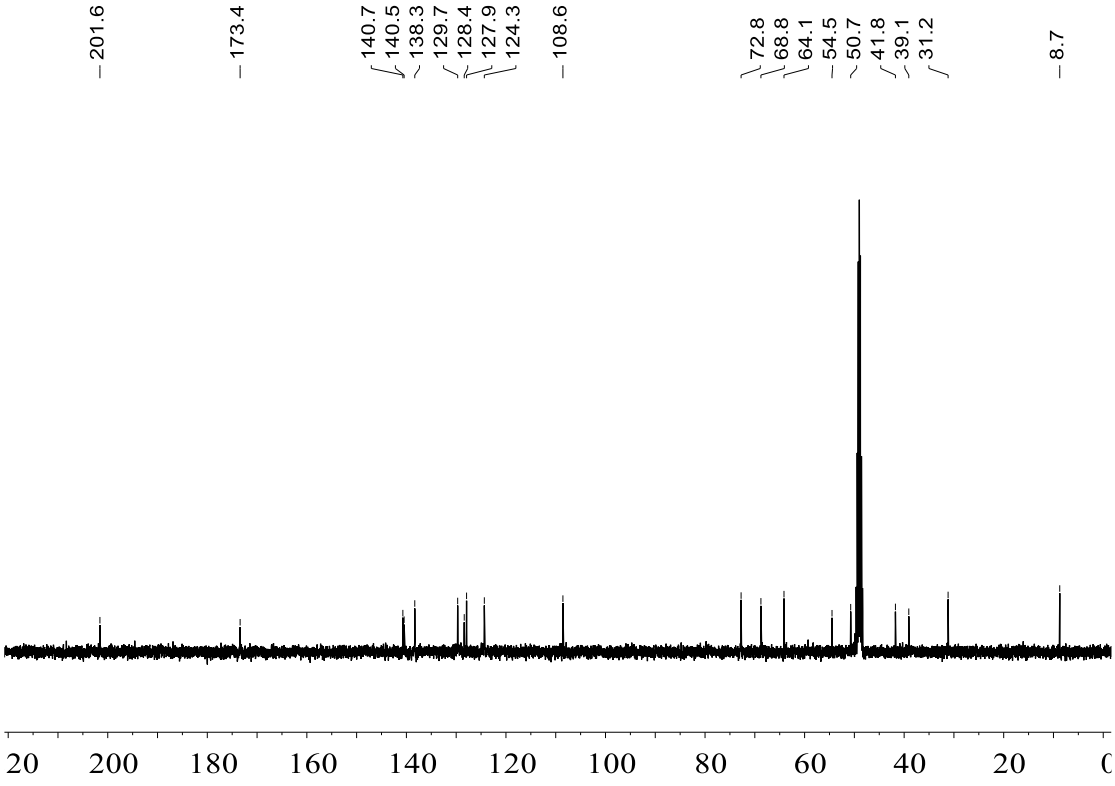

Fig. S76. ^{13}C NMR spectrum of **11** in CD_3OD

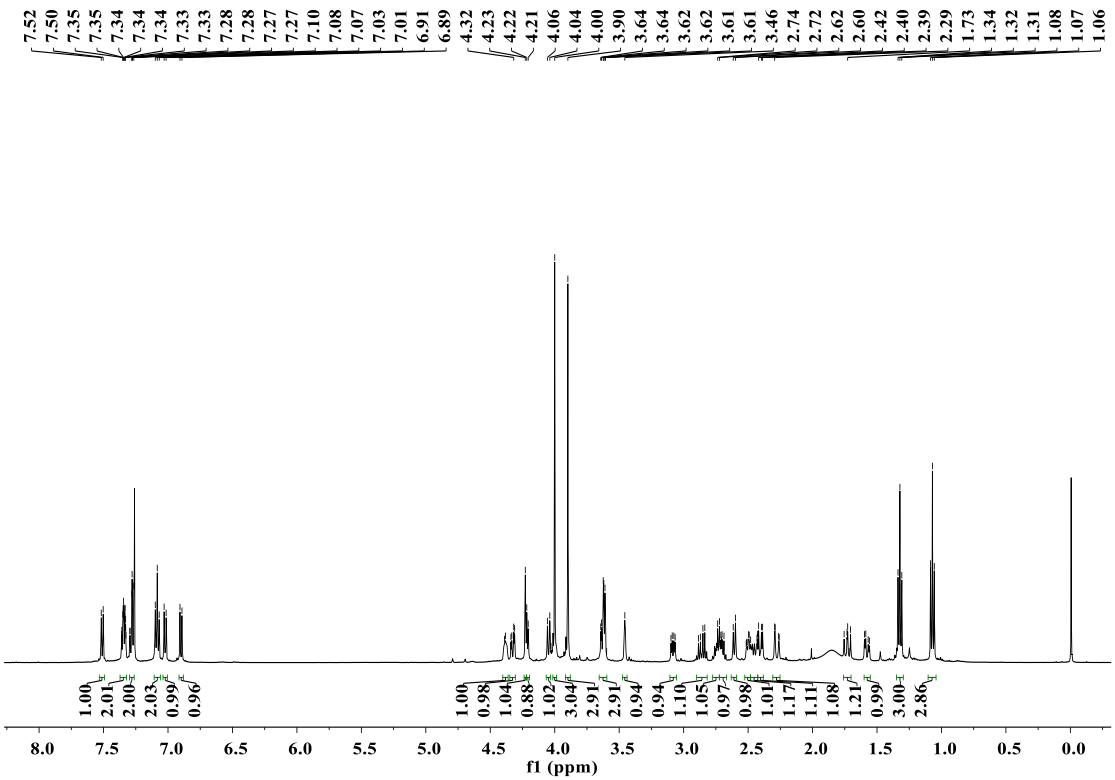

Fig. S77. ^{1}H NMR spectrum of synthetic **3** in $CDCl_3$

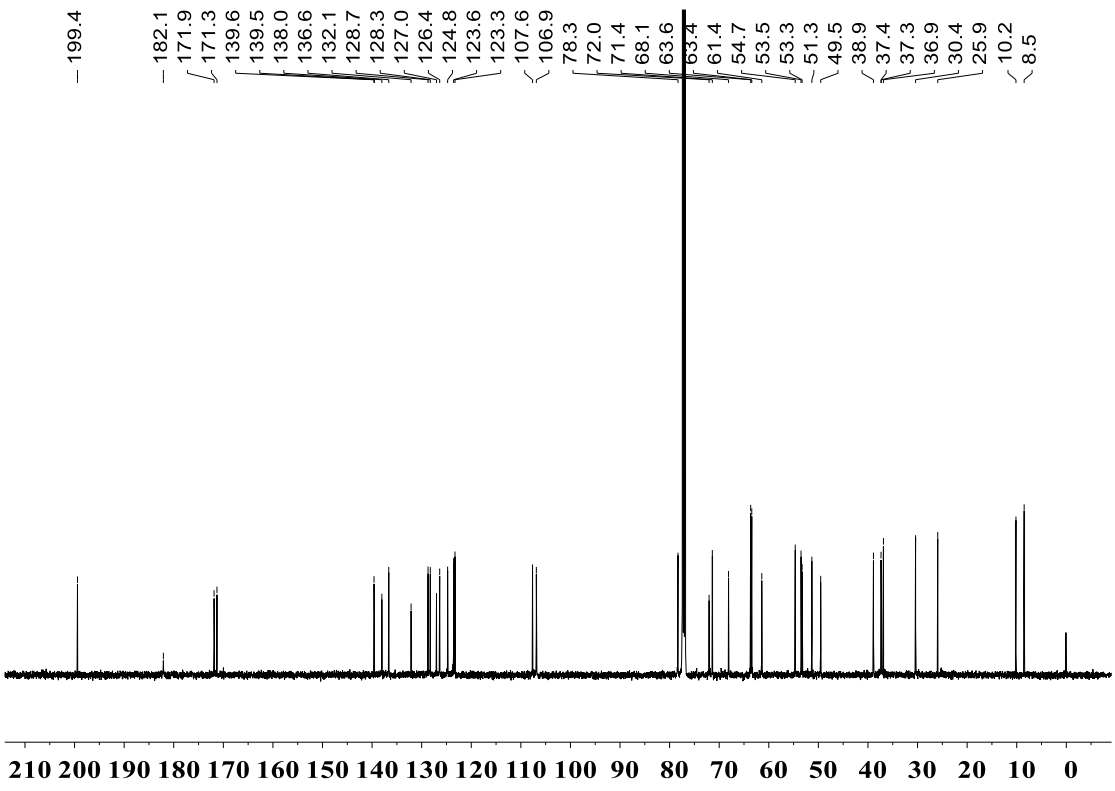

Fig. S78. ^{13}C NMR spectrum of synthetic **3** in $CDCl_3$

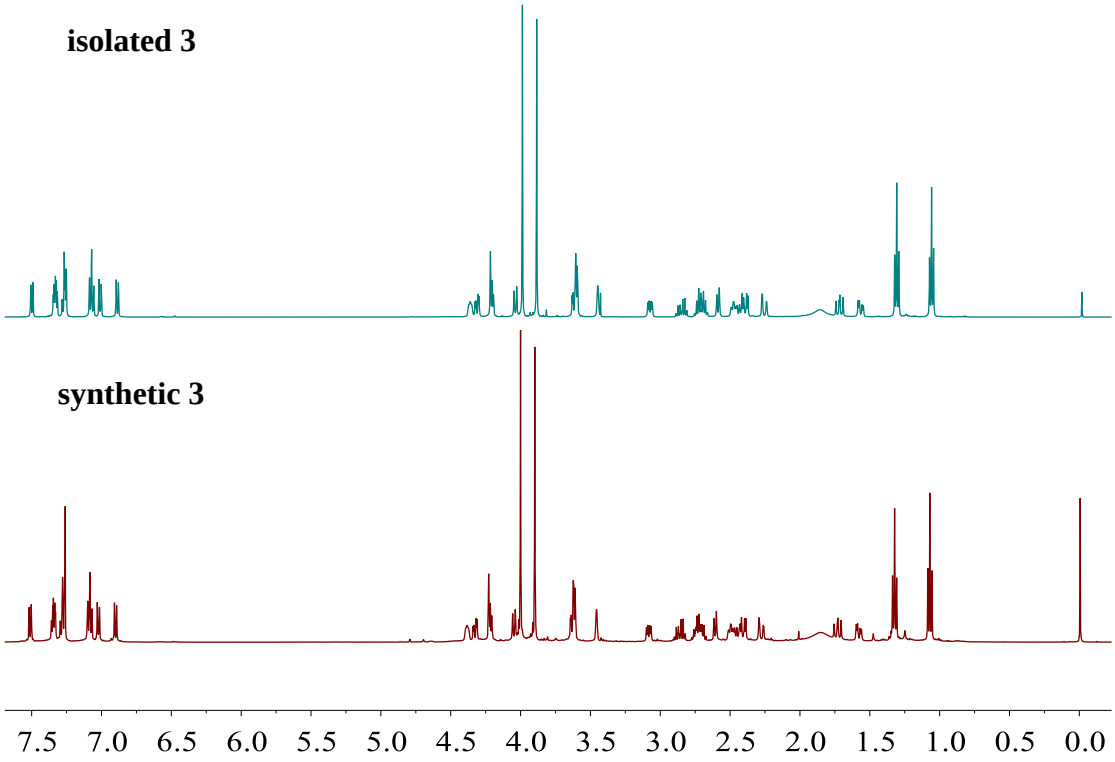

Figure S79. Comparison of ^{1}H NMR spectra of isolated and synthetic **3** in $CDCl_3$

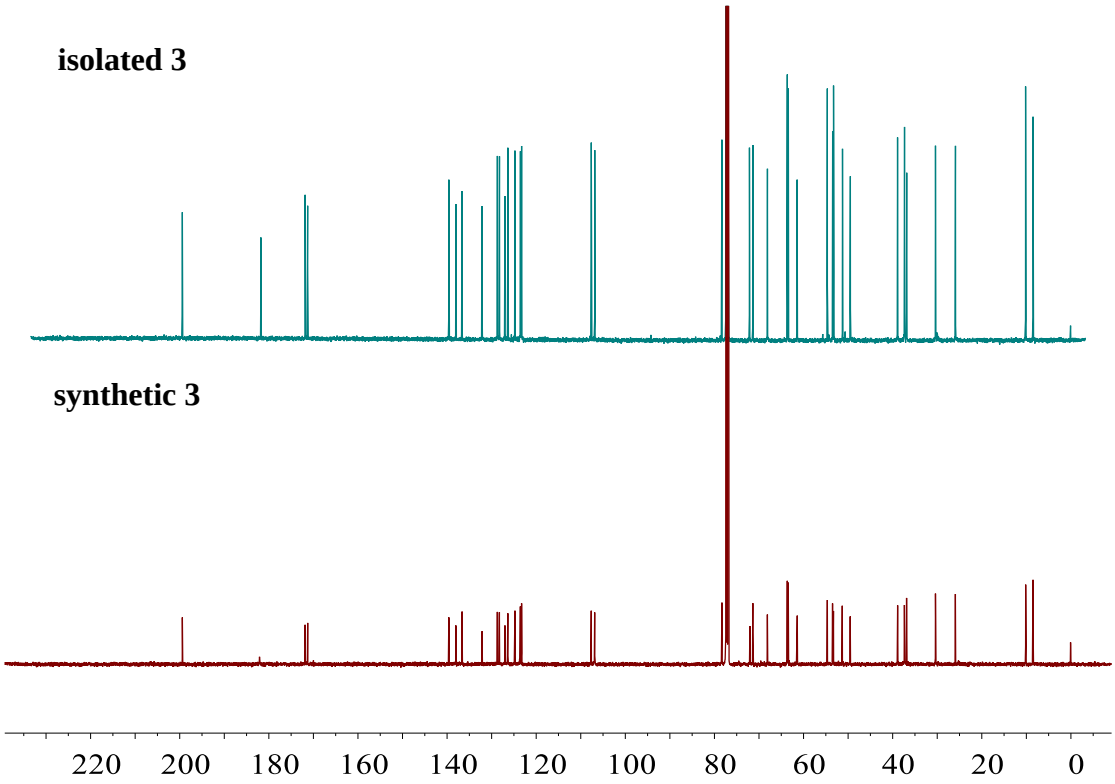

Figure S80. Comparison of ^{13}C NMR spectra of isolated and synthetic **3** in $CDCl_3$

Reference

[1] Gaussian 09, Revision E.01, M. J. Frisch, G. W. Trucks, H. B. Schlegel, G. E. Scuseria, M. A. Robb, J. R. Cheeseman, G. Scalmani, V. Barone, B. Mennucci, G. A. Petersson, H. Nakatsuji, M. Caricato, X. Li, H. P. Hratchian, A. F. Izmaylov, J. Bloino, G. Zheng, J. L. Sonnenberg, M. Hada, M. Ehara, K. Toyota, R. Fukuda, J. Hasegawa, M. Ishida, T. Nakajima, Y. Honda, O. Kitao, H. Nakai, T. Vreven, J. A. Montgomery, Jr., J. E. Peralta, F. Ogliaro, M. Bearpark, J. J. Heyd, E. Brothers, K. N. Kudin, V. N. Staroverov, T. Keith, R. Kobayashi, J. Normand, K. Raghavachari, A. Rendell, J. C. Burant, S. S. Iyengar, J. Tomasi, M. Cossi, N. Rega, J. M. Millam, M. Klene, J. E. Knox, J. B. Cross, V. Bakken, C. Adamo, J. Jaramillo, R. Gomperts, R. E. Stratmann, O. Yazyev, A. J. Austin, R. Cammi, C. Pomelli, J. W. Ochterski, R. L. Martin, K. Morokuma, V. G. Zakrzewski, G. A. Voth, P. Salvador, J. J. Dannenberg, S. Dapprich, A. D. Daniels, O. Farkas, J. B. Foresman, J. V. Ortiz, J. Cioslowski, and D. J. Fox, Gaussian, Inc., Wallingford CT, 2013.

[2] T. Bruhn, A. Schaumloffel, Y. Hemberger, G. Pescitelli. SpecDis version 1.71, Berlin, Germany, 2017. http:/specdis-software.jimdo.com.

[3] N. P. Li, J. S. Liu, J. W. Liu, et al, Bioorg Chem 107 (2021) 104624.

[4] P. Xie, L.J. Yan, H.L. Zhou, et al, Front. Pharmacol. 13 (2022) 717271.

[5] J.H. Gu, W. Zhang, W.Y. Cai, et al, Org. Chem. Front. 8(2021) 1918-1925.

[6] Y.R. Zheng, C.Y. Tian, C.L. Fan, et al, J. Ethnopharmacol. 267(2021) 113497.

[7] D. van der Helm, A. Groenewoud, E.S.M. de Jonge-Muller, et al, Sci. Rep. 8(2018) 16005.